Atmospheric Environment 43 (2009) 5138–5192

Contents lists available at ScienceDirect

Atmospheric Environment

journal homepage: www.elsevier.com/locate/atmosenv

# Atmospheric composition change: Climate–Chemistry interactions

I.S.A. Isaksen [a,b,*], C. Granier [c,d,e,f], G. Myhre [a,b], T.K. Berntsen [a,b], S.B. Dalsøren [a,b], M. Gauss [g], Z. Klimont [h], R. Benestad [g], P. Bousquet [i], W. Collins [j], T. Cox [k], V. Eyring [l], D. Fowler [m], S. Fuzzi [n], P. Jöckel [o], P. Laj [p,q], U. Lohmann [r], M. Maione [s], P. Monks [t], A.S.H. Prevot [u], F. Raes [v], A. Richter [w], B. Rognerud [a], M. Schulz [x], D. Shindell [y], D.S. Stevenson [z], T. Storelvmo [r], W.-C. Wang [aa], M. van Weele [bb], M. Wild [r], D. Wuebbles [cc]

[a] Department of Geosciences, University of Oslo, Oslo, Norway
[b] Center for International Climate and Environmental Research – Oslo (CICERO), Oslo, Norway
[c] Université Pierre et Marie Curie-Paris 6, UMR7620, Paris, France
[d] Service d'Aéronomie CNRS, UMR7620, Paris, France
[e] NOAA Earth System Research Laboratory, Chemical Sciences Division, Boulder, CO USA
[f] Cooperative Institute for Research in Environmental Sciences, University of Colorado, Boulder, CO, USA
[g] Norwegian Meteorological Institute, Oslo, Norway
[h] International Institute for Applied Systems Analysis, Laxenburg, Austria
[i] Service d'Aéronomie/Institut Pierre-Simon Laplace, Paris, France
[j] Hadley Centre, Met Office, Exeter, UK
[k] Centre for Atmospheric Science, University of Cambridge, Cambridge, UK
[l] Deutsches Zentrum für Luft- und Raumfahrt, Institut für Physik der Atmosphäre, Oberpfaffenhofen, 82234 Wessling, Germany
[m] Centre of Ecology and Hydrology, EH26 0QB Penicuik Midlothian, UK
[n] Instituto di Scienze dell'Amtosfera e del Clima - CNR, 40129 Bologna, Italy
[o] Max Planck Institute for Chemistry, Mainz, Germany
[p] Laboratoire de Météorologie Physique, Observatoire de Physique du Globe de Clermont Ferrand, Université Blaise Pascal - CNRS, 63177 Aubière, France
[q] Université Joseph Fourier - Grenoble 1 / CNRS, Laboratoire de Glaciologie et Géophysique de l'Environnement, 38400 St Martin d'Hères, France
[r] ETH, Inst Atmospher & Climate Sci, Zurich, Switzerland
[s] Universita' di Urbino, Istituto di Scienze Chimiche "F. Bruner", 61029 Urbino, Italy
[t] Department of Chemistry, University of Leicester, LE1 7RH Leicester, UK
[u] Laboratory of Atmospheric Chemistry, Paul Scherrer Institute, Villigen PSI, Switzerland
[v] Environment Institute, European Commission Joint Research Centre, Ispra, Italy
[w] Institute of Environmental Physics, University of Bremen, Bremen, Germany
[x] Laboratoire des Sciences du Climat et de l'Environnement, CEA/CNRS–LSCE, Gif-sur-Yvette, France
[y] NASA Goddard Institute for Space Studies, New York, New York, USA
[z] School of GeoSciences, University of Edinburgh, Edinburgh, UK
[aa] Suny Albany, Atmospher Sci Res Ctr, Albany, NY, USA
[bb] Section of Atmospheric Composition, Royal Netherlands Meteorological Institute, De Bilt, Netherlands
[cc] Department of Atmospheric Sciences, University of Illinois at Urbana-Champaign, Urbana, Illinois, USA

ARTICLE INFO

*Article history:*
Received 29 January 2009
Received in revised form
4 August 2009
Accepted 10 August 2009

*Keywords:*
Atmosphere climate chemistry
Feedbacks modelling

ABSTRACT

Chemically active climate compounds are either primary compounds like methane ($CH_4$), removed by oxidation in the atmosphere, or secondary compounds like ozone ($O_3$), sulfate and organic aerosols, both formed and removed in the atmosphere. Man-induced climate–chemistry interaction is a two-way process: Emissions of pollutants change the atmospheric composition contributing to climate change through the aforementioned climate components, and climate change, through changes in temperature, dynamics, the hydrological cycle, atmospheric stability, and biosphere-atmosphere interactions, affects the atmospheric composition and oxidation processes in the troposphere. Here we present progress in our understanding of processes of importance for climate–chemistry interactions, and their contributions to changes in atmospheric composition and climate forcing. A key factor is the oxidation potential involving compounds like $O_3$ and the hydroxyl radical (OH). Reported studies represent both current and

* Corresponding author. Department of Geosciences, University of Oslo, Oslo, Norway.
*E-mail address:* ivar.isaksen@geo.uio.no (I.S.A. Isaksen).

1352-2310/$ – see front matter 
doi:10.1016/j.atmosenv.2009.08.003

future changes. Reported results include new estimates of radiative forcing based on extensive model studies of chemically active climate compounds like $O_3$, and of particles inducing both direct and indirect effects. Through EU projects like ACCENT, QUANTIFY, and the AeroCom project, extensive studies on regional and sector-wise differences in the impact on atmospheric distribution are performed. Studies have shown that land-based emissions have a different effect on climate than ship and aircraft emissions, and different measures are needed to reduce the climate impact. Several areas where climate change can affect the tropospheric oxidation process and the chemical composition are identified. This can take place through enhanced stratospheric–tropospheric exchange of ozone, more frequent periods with stable conditions favoring pollution build up over industrial areas, enhanced temperature induced biogenic emissions, methane releases from permafrost thawing, and enhanced concentration through reduced biospheric uptake. During the last 5–10 years, new observational data have been made available and used for model validation and the study of atmospheric processes. Although there are significant uncertainties in the modeling of composition changes, access to new observational data has improved modeling capability. Emission scenarios for the coming decades have a large uncertainty range, in particular with respect to regional trends, leading to a significant uncertainty range in estimated regional composition changes and climate impact.



**Contents**

## 1. Introduction

The coupling between climate change and atmospheric composition results from the basic structure of the Earth-atmosphere climate system, and the fundamental processes within it. The composition of the atmosphere is determined by natural and human-related emissions, and the energy that flows into, out of, and within the atmosphere. The principal source of this energy is sunlight at ultraviolet (UV), visible, and near-infrared (NIR) wavelengths. This incoming energy is balanced at the top of the atmosphere by the outgoing emission of infrared (IR) radiation from the Earth's surface and from the atmosphere. The structure of the troposphere (with temperature generally decreasing with altitude) is largely determined by the energy absorbed at or near the Earth's surface, which leads to the evaporation of water and the presence of reflecting clouds. Through many interactions, the composition and chemistry of the atmosphere are inherently connected to the climate system. The importance of climate–chemistry interactions has been recognized for more than 20 years (Ramanathan et al., 1987).

Atmospheric composition influences climate by regulating the radiation budget. As shown in Fig. 1, clouds reflect incoming solar radiation (the albedo effect) and absorb outgoing surface thermal radiation, and reradiate at the local temperature (the greenhouse effect). It is well recognized that the thermal structure of the atmosphere is influenced by the presence of small amounts of $H_2O$, $CO_2$, $CH_4$, $O_3$, and aerosols. The main radiative effect of the gases is through the greenhouse effect, while aerosols may either heat or cool the surface, depending on their optical properties, which affect the solar and thermal radiation.

Compounds like methane, ozone, and different types of secondary particles (sulfate, organic particles and nitrate) are active chemical compounds in the troposphere; they also have important radiative effects on climate. These compounds are either emitted directly into the atmosphere (methane, primary particles), or

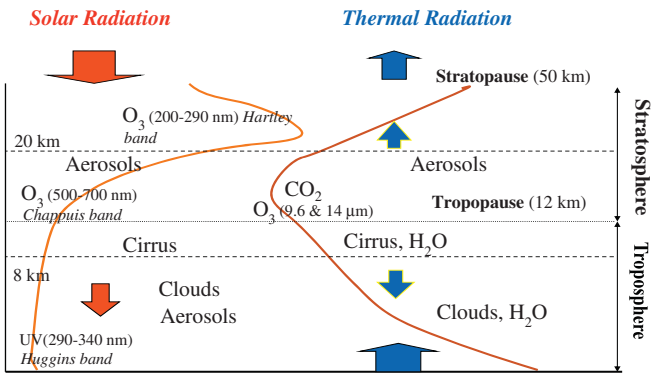


**Fig. 1.** Atmospheric radiatively-important gases, aerosols and clouds. For illustrative purpose, the mid-latitude, annual vertical distributions of $O_3$ (in orange) and temperature (in brown) are taken from IPCC/TEAP (2005).

formed in the atmosphere (ozone, secondary particles). They are either strongly controlled by chemical oxidation in the atmosphere (e.g., methane and ozone), removed through cloud and precipitation processes (primary and secondary particles), or deposited on the Earth's surface (ozone, particles). Note that the effects on climate from $O_3$ and secondary particles are non-uniform and will be more difficult to assess than those of the well-mixed greenhouse gases (methane). For example, changes in absolute $O_3$ densities in the lower stratosphere and upper troposphere have been demonstrated to lead to pronounced impact on surface temperature (Wang and Sze, 1980; Lacis et al., 1990).

Pollutants such as CO, VOC, $NO_x$ and $SO_2$, which by themselves are negligible greenhouse compounds, have an important indirect effect on climate by altering the abundances of radiatively active gases such as $O_3$ and $CH_4$. Furthermore, they act as precursors for sulfate and secondary organic particles. Oxidation in the troposphere, driven by solar UV photo dissociation, result in the formation of the hydroxyl radical (OH), the key oxidant in the troposphere. The hydroxyl radical initiates a large number of chemical reactions affecting the climatically important compounds such as ozone, methane, and secondary particles.

Although the potential importance of the coupling between climate change and atmospheric chemistry has been recognized for some time, it is only recently that it has been possible to capture the full complexity of the most important interactions. Observations and theory go hand in hand towards understanding this complexity. An important example is the emerging evidence that key interactions can occur through atmosphere-biosphere interactions (Fowler et al., 2009), affecting biogenic emissions, ozone deposition, uptake and removal of particles in clouds.

New observations, in particular from satellite platforms, provide data to verify models and to diagnose the chemical and physical processes, which are important for understanding chemical distributions and processes involved, as well as their long time trends and sensitivity to climate change.

Tropospheric climate–chemistry interactions deal to a largely with chemical processes and compounds that show large inhomogeneous global distribution and trends, mainly initiated by inhomogeneous distribution of precursor emissions. There have been extensive studies of climate impact from specific sectors with large spatial variations in emissions and composition changes such as air and ship traffic during the past 3–5 years (Sausen et al., 2005; Eyring et al., 2005a,b; Eyring et al., 2007a; Dalsøren et al., 2007). The potential impact from such sectors is discussed.

There are significant differences in the temporal changes of human-related emissions and natural emissions as well as in their geographical distribution. Human-related emissions are characterized by different responses worldwide to regulations and to different growth rates in energy use, in transportation systems, and in industrial behavior. European and U.S. emissions of pollutants generally show reductions from regulatory actions over the last 2 to 3 decades, while emissions in regions like Southeast Asia, and in other developing countries show large increases during recent years. Similarly, certain industrial sectors such as aircraft and shipping show large increases, with potential for further large increases in the future (see Chapter 3). Natural emissions of key climate precursors ($NO_x$, CO, biogenic VOCs and sulfur compounds) are characterized with large year-to-year variations (e.g., biomass burning).

In addition, there is a strong potential for large changes in the emission and deposition of these compounds resulting from future climate change (e.g., due to changes in surface temperature, moisture, atmospheric stability and biogenic activity). Such climate responses have the potential to affect global chemistry. Although there are a few recent examples indicating possible strong feedback from climate change (Zeng and Pyle, 2003; Collins et al., 2003; Sitch et al., 2007; Solberg et al., 2008), further studies are needed to reveal the full extent of this impact.

This synthesis is based on studies following the Working Group I Fourth Assessment Report of the IPCC (IPCC, 2007). ACCENT activities, and activities obtained in other EU financed projects have initiated some of the results described. The IPCC report describes progress in understanding of the human and natural drivers of climate change, climate processes and attribution, observed climate changes and estimates of projected future changes. We will especially focus on developments of significance for climate–chemistry interactions that have appeared after the writing of the IPCC report, with reference to newly published research results. We will, however, also include earlier work where we find it necessary, to give a more comprehensive picture of the scientific development.

## 2. Key interactions in the climate–chemistry system

The physical climate is a major determinant of the atmospheric concentration for all chemically active species, including key climate compounds like $CH_4$, $O_3$ and secondary aerosol compounds like sulfate and organic aerosols. This applies both locally (more important for short-lived species, e.g., ozone, aerosols) and globally (more important for long-lived species, e.g., methane). The physical state of the atmosphere varies considerably with location, in particular with altitude and latitude. Physical climate exerts its influence in many ways, e.g., by affecting natural emissions, photolysis rates, chemical reactions, transport and mixing, and deposition processes. When considering climate–chemistry interactions in the atmosphere, it is not only important to study the emissions and distribution of the climate compounds, but also to consider the chemical processes and the distribution of the compounds determining the tropospheric oxidation.

An overview of important climate–chemistry interactions is given in Fig. 2 for the chemical active climate compounds $O_3$, $CH_4$, and particles (sulfate, secondary organic aerosols (SOA)) and discussed in Chapter 7.

The role of climate for atmospheric chemistry can be demonstrated by considering its influence on the hydroxyl radical (OH). OH is the major component for the overall oxidising capacity of the troposphere. The primary source of OH is the reaction of excited state oxygen atoms, and it is formed from ozone photolysis, and reaction with water vapour:

$$O_3 + h\nu \rightarrow O(^1D) + O_2 (\lambda < 320\,\text{nm}) \quad \text{(R1)}$$

$$O(^1D) + H_2O \rightarrow 2OH \quad \text{(R2)}$$

Water vapour concentrations are assumed to increase in a warming climate, thus increasing the rate of reaction R2, which contributes to ozone loss as it competes with the stabilization of $O(^1D)$ to the ground-state oxygen atom that would return ozone. On the other hand, higher temperatures also cause larger emissions of isoprene, an important ozone precursor, and reduce the stability of PAN, thus releasing $NO_x$, which catalyzes ozone production. Model studies indicate that the result of these temperature responses would be an increase in summertime ozone over polluted areas and a reduction of background ozone (Jacob and Winner, 2009). The same publication also summarizes possible effects of temperature increase on particle formation, with sulphate aerosols likely to increase in a warming climate related to faster $SO_2$ oxidation (Aw and Kleeman, 2003; Dawson et al., 2007; Kleeman, 2007), while nitrate particles and organic semi-volatile components are reduced as they shift from the particle phase to the gas phase (Sheehan and Bowman, 2001; Tsigaridis and Kanakidou, 2007).

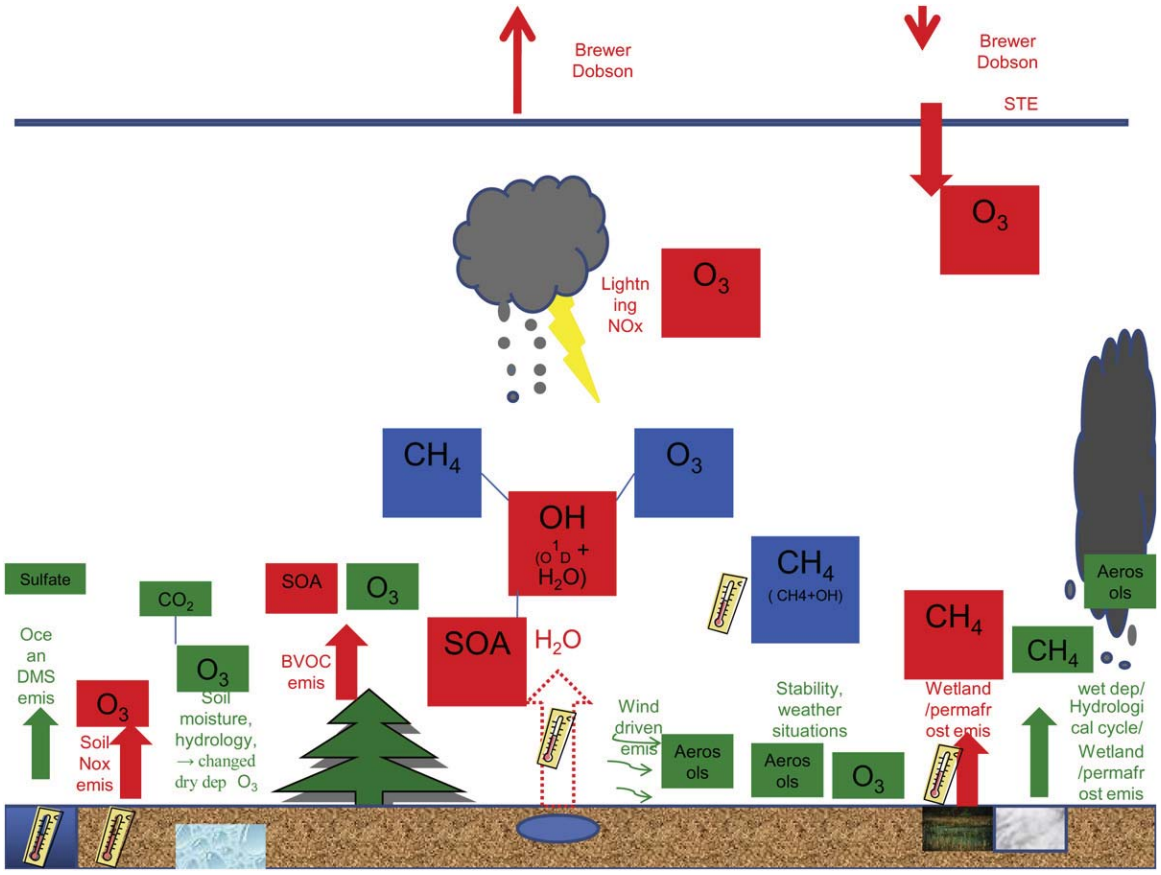


**Fig. 2.** Important climate–chemistry interactions in the troposphere. The colour denotes the sign of the effects, blue represents a decrease, red an increase and for green the effect or sign is uncertain or regionally very variable. The sizes of the boxes indicate the importance of the changes for the respective component. The boxes are also placed vertically approximately where the effects are most pronounced.

### 2.1. Observing chemistry–climate interactions

Direct observation of chemistry–climate interactions is extremely challenging. Composition change is often caused by non-climate factors such as anthropogenic emission trends, while multiple forcing agents have caused climate change in recent decades. This makes it difficult to attribute trends to particular gaseous or aerosol species. The hemispheric asymmetry of observed temperature trends and characteristics of the regional spatial structure of temperature changes have been used however to indirectly estimate the effects of Northern Hemisphere sulfate aerosols (Santer et al., 1996; Kaufmann and Stern, 2002; Stott et al., 2006).

Some effects of climate change on chemistry are observed during short-term climate anomalies periods. For example, as expected from the atmospheric increase in sulfate particles, global temperatures decreased significantly during the years following the 1991 eruption of Mt. Pinatubo. Observations show that tropospheric water vapor decreased after the eruption (Soden et al., 2002), in agreement with the response seen in climate models. Additionally, methane emissions from wetlands were reduced during this time (Walter et al., 2001). Observations provide additional evidence for climate-sensitive emissions: Satellite measurements show inter-annual variations in formaldehyde distributions that appear to be tied to changes in biogenic isoprene emissions (Palmer et al., 2006). Ice core records show that emissions of mineral dust can also change dramatically with climate change, at least over glacial-interglacial transitions (Delmonte et al., 2004). Large inter-annual variations in biomass burning have also been observed (van der Werf et al., 2006), some of which have been related to climate (such as anomalies following a large ENSO event).

The influence of composition changes on climate has been estimated using a variety of observations. Changes in the Earth's outgoing energy have been observed at precisely the wavelengths where $CO_2$, methane and ozone absorb long-wave radiation, demonstrating their impact in the enhancement of the greenhouse effect (Harries et al., 2001). Recently, satellite data have been used to estimate the clear-sky radiative forcing from upper tropospheric ozone over the oceans at $0.48 \pm 0.14\ W\ m^{-2}$ (Worden et al., 2008) (note that this is a total forcing value, not the anthropogenic portion). For aerosols, satellite-based estimates of the direct all-sky forcing at the top of the atmosphere (TOA) have yielded values of $-0.35$ to $-0.9\ W\ m^{-2}$ (Chung et al., 2005; Bellouin et al., 2005; Quaas et al., 2008), with uncertainty ranges that do not overlap, emphasizing the large uncertainties resulting from the use of satellite measurements of optical attenuation to infer aerosol forcing. Such estimates require assumptions about factors such as aerosol composition, shape, scattering properties, and location relative to clouds. Satellite data have also been used to estimate radiative forcing due to indirect effect of aerosols on cloud albedo (the first indirect effect), yielding a value of $-0.2 \pm 0.1\ W\ m^{-2}$ (Quaas et al., 2008), substantially lower than that seen in most forward model calculations.

Although there are limitations to forcing estimate from ozone and aerosols using satellite observations, such data usually have better global coverage than traditional data from ground based and aircraft observations. One limitation with satellite data is that

forcing is based on the total abundance of the species rather than on the anthropogenic contribution. Additionally, satellite data are generally limited in spatial coverage, and tend to lack sufficient coverage at high latitudes. Furthermore, radiative forcing, while a useful metric, does not describe fully the climate response to ozone and aerosols, especially at regional scales. Finally, the information obtained by satellites is not sufficient to characterize the effects of aerosols.

At smaller spatial scales, much more detailed measurements are available, giving more precise estimates of aerosol radiative effects. For example, absorbing aerosols can substantially perturb both total organic aerosols and surface radiative fluxes (Satheesh and Ramanathan, 2000). Aerosols can also have a strong warming effect by enhancing cloudiness at high latitudes during seasons with little sunlight (Garrett and Zhao, 2006; Lubin and Vogelmann, 2006) (see Section 6.4.2). Model studies have provided indirect confirmation of the ability of aerosols to modulate local temperatures and precipitation based on comparison of climate observations with simulations with and without observed absorbing aerosols (Menon et al., 2002). These data provide valuable information about chemistry–climate interactions on regional scales.

### 2.2. Modeling chemistry–climate interactions

A range of numerical models is developed to investigate connections between atmospheric chemistry and the climate system. Past changes in atmospheric composition and climate, and projections of the future state of the atmosphere under various scenarios use such models to understand observations. The following discussion is restricted to models at the global scale.

Chemistry-Transport Models (CTMs) are three-dimensional models of atmospheric composition driven by meteorological data. The use of re-analyzed data makes it possible to simulate the real evolution of the atmosphere; output from such models can then be usefully compared to observational data, for example for model validation. Extensive model validation was performed through the ACCENT project inter-comparisons both for gas phase compounds and for particles (Shindell et al., 2006; Schulz et al., 2006). CTMs that additionally assimilate atmospheric composition data, for example from surface stations, sondes or satellites, are used to simulate "Chemical Weather". These models can provide short-term forecasts of the atmospheric composition, for example air quality forecasts, and can be used in flight route planning during aircraft observation campaigns. Assimilation of atmospheric data is extensively used for estimating emissions of compounds like CO and $CH_4$ (Butler et al., 2005; Bousquet et al., 2006; Bergamaschi et al., 2007; Pison et al., 2009).

Alternatively, climate models provide meteorological data – such models are called Chemistry–Climate Models (CCMs). CCMs include different degrees of coupling between the climate and chemistry components.

A CCM simulates the physical state of the atmosphere (dynamics and thermodynamics), largely determined by the flows of energy through the atmosphere and across its lower boundary with the Earth's surface. The chemistry model simulates the chemical state of the atmosphere, integrating the emissions, transport, mixing, physical and chemical transformation, and deposition of key atmospheric components (trace gases and aerosols). All these processes are linked to the physical state of the atmosphere, which to a varying degree is parameterized in the models. Transport and mixing are determined by wind fields and by atmospheric stability. Chemical and photochemical reaction rates are functions of many physical variables, such as levels of ultraviolet radiation, pressure and temperature. Dry deposition to the Earth's surface is controlled by boundary layer turbulence and the surface properties, and the rate of natural emissions of several important species is strongly linked to the physical climate.

While the physical climate strongly influences the chemical climate, as outlined above, there are also influences of the chemical climate on the physical climate in this coupled system. Transmission of radiation through the atmosphere depends on the distribution of radiatively active gases and aerosols. In the stratosphere, where large quantities of UV radiation are absorbed mainly by ozone, significant local heating, and reduced penetration into the troposphere occur. Parameterizations of stratospheric interactions in a CCM remain a major research area since the high complexity of CCMs requires a systematic evaluation of the results of the simulations as well as a quantification of uncertainties in the model results. This effort is part of the Chemistry–Climate Model Validation Activity (CCMVal) of the SPARC (Stratospheric Processes and their Role in Climate Programme) (Eyring et al., 2005a,b; 2006; 2007b).

Aerosol–cloud interactions represent an area with potential for strong interactions in the climate system. Aerosols determine the cloud radiative properties and thus the radiative heating/cooling, and participate in the precipitation process. Fig. 3 illustrates the processes linking aerosols, clouds and climate. Although considerable progress has been made in recent years to include parameterization of aerosol–cloud droplet interaction and explicit microphysics for cloud water/ice content in GCMs, inadequate understanding of the processes contributes to significant uncertainties in model simulated future climate changes. The individual components shown in Fig. 3 are currently being developed, but there is still a lack of consistent and accurate parameterization for and their implementation into GCMs is being actively pursued (IPCC, 2007). Further discussions of the interactions are presented in more detail in Sections 5.2–5.4.

Tropospheric composition also interacts with the physical climate system via radiatively active trace gases and aerosols. In typical "state-of-the-art" climate modeling (IPCC-AR4), changes in tropospheric composition are calculated offline and then imposed

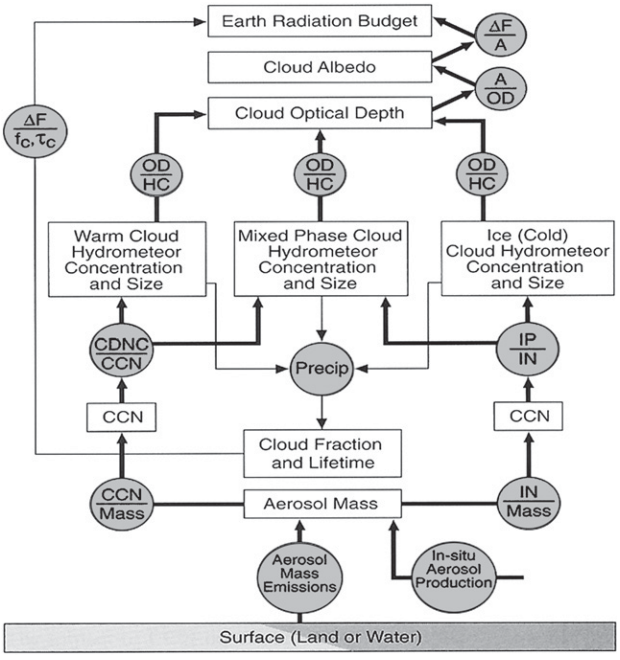


**Fig. 3.** Flow chart showing the processes linking aerosol emissions/production, cloud condensation nuclei (CCN), cloud droplet number concentration (CDNC), ice nuclei (IN), ice particles (IP), optical depth (OD), hydrometeor (HC), albedo (A), cloud fraction (fc), cloud optical depth (τc) and radiative forcing (ΔF) (Adopted from IPCC, 2001).

on the climate, rather than being allowed to develop interactively. Fully coupled CCMs are not yet widely used in studies of tropospheric composition.

### 2.3. Scale issues

Anthropogenic activity has altered the chemical composition of the atmosphere on local, regional, and global scales. As of today, no single model is capable of reproducing a sufficiently wide range of spatial and temporal scales to address all issues related to air pollution and climate change.

Due to computational requirements, there is a limit to the resolution of global models, which currently is 0.5 or 1 degree. On the other hand, in local and regional models it is difficult to account for processes that occur on the global scale, i.e. outside the modeled domain, but which affect the regional to local scales within the model domain. A well-known example is long-range transport of air pollutants, with intercontinental transport of pollutants and changes in background concentrations.

Most model results reviewed in this report are taken from global models, as a number of global models now have sufficient resolution to cover regional variability as well. However, global scale models have obvious limitations in representing climate–chemistry interactions occurring on local scales, such as the impact of particle emissions or formation of clouds and precipitation.

Fig. 4 compares typical spatial and temporal scales of common atmospheric processes with different types of models. For example, deep convection occurs on a spatial scale of a few kilometers and during a few minutes to hours. Global circulation, such as exchange between the Northern and Southern Hemispheres, occurs on timescales of several months (troposphere) to years (middle and upper atmosphere). Typical wind speeds of the respective processes are used to relate spatial scales to temporal scales. The figure also shows typical focus areas of today's model systems. For example, global climate models cover the entire globe, i.e. tens of thousands of kilometers, and are run for up to several decades to centuries to investigate long-term changes. Urban scale models cover much smaller domains through which pollutants are mixed over a much shorter time scale. In order to address all relevant spatial and temporal scales it is necessary to use advanced parameterizations or a modeling system consisting of a hierarchy of models of different scales that are nested into each other. In nesting approaches, particular attention has to be given to the way models communicate information to each other.

One-way nesting accounts only for influences from the larger to the smaller scale, the flow of information going from the coarse model to the finer-scale model, while in two-way nesting, feedback processes from the high resolution to the coarse resolution domain are also considered. The small-scale model uses output from the large-scale model as boundary condition, while the large-scale model uses a combination of output from the small-scale model to define distributions within the domain covered by the small-scale model. For instance at the boundaries of the smaller-scale model, the larger scale model can provide temporally and spatially varying ozone and particulate matter, which are species that have a sufficiently long lifetime to be transported over the smaller-scale model domain. In two-way nesting, the larger scale model may replace or assimilate species distributions from the smaller-scale model in the grid boxes where a higher resolution is desirable. Depending on the kind of model (e.g., chemical transport model or numerical weather prediction model) the output to be exchanged includes chemical species or meteorological parameters or both. One drawback is that inconsistencies with the principal equations may emerge after the distributions calculated by the large-scale model are updated using output from the small-scale model. This is because after each time step in the large-scale model the species distributions and meteorological parameters are calculated from the principal equations, and any change due to input from another model will induce inconsistencies. Currently available nesting techniques can thus lead to problems such as artificial variability in large-scale models that originates from the calculations of small-scale models, but cannot be resolved in the large-scale models. Although coordination of research among model groups focusing on different scales is well underway (e.g., Moussiopoulos and Isaksen, 2006), there is still a long way to go until scale interactions are fully understood and adequately represented.

### 2.4. Upper tropospheric processes

Temperatures in the tropical upper troposphere have increased with about 0.65 K since the 1970s (Allen and Sherwood, 2008), essentially at what is expected from climate models based on observed surface temperature trends. Other analyses suggest that the change in the tropopause height could be a better indication of climate change than the vertical temperature profile (Sausen and Santer, 2003; Santer et al., 2003a; Santer et al., 2003b). In particular, changes affecting $O_3$ is important since $O_3$ contributes to chemical changes and affects the temperature distribution in the upper

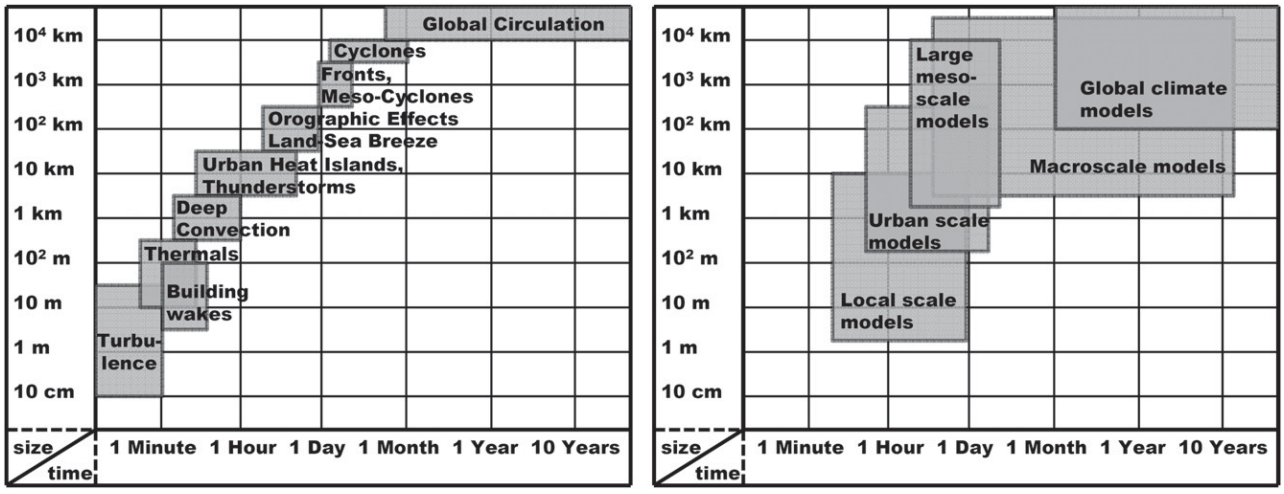


**Fig. 4.** Characteristic spatial scales versus characteristic timescales. Left panel: common atmospheric phenomena. Right panel: atmospheric models covering different spatial and temporal scales. See text for more details.

equatorial troposphere/lower stratosphere (Ramaswamy and Bowen, 1994; Cariolle and Morcrette, 2006). Recent model studies (Hoor et al., 2009) demonstrated that emission from different sectors (Hoor et al., 2009) has highly different effect on the height distribution of ozone perturbation in the troposphere, which is important as indicated in Fig. 1. Measurements from satellites and other platforms during recent years have improved the understanding of processes in the upper troposphere and lower stratosphere (e.g., Pan et al., 2007; Strahan et al., 2007).

The ability to represent dynamical processes, in particular convection, is critical for the calculation of the transport of chemical compounds from the boundary layer to the upper troposphere of short-lived compounds like $NO_x$ and $SO_2$, and for the downward transported compounds destroyed at the Earths surface like ozone. Such processes can also bring insoluble organic trace gases to higher altitudes to produce new particles (Kulmala et al., 2006). Currently in global models, this results in large differences in estimates of transport and chemistry. Furthermore, there are limitations in our ability to model stratospheric-tropospheric exchanges (e.g., transport of ozone from the stratosphere to the troposphere), and chemical source gases emitted at the Earths surface and water vapor to the stratosphere.

Because of the importance of $NO_x$ changes to ozone, its distribution and changes in the upper troposphere can be relevant to climate. Models have generally underestimated the amount of $NO_x$ in the upper troposphere compared with observations (Schultz, et al., 1999; Penner et al., 1998). In a more recent analysis (Brunner et al., 2005) based on global model studies in the UTLS region comparisons were made with observations from two measurement campaigns. A number of processes affect UTLS $NO_x$, including in situ production from lightning, emissions from aircraft, convection, stratospheric intrusions, and photochemical recycling from long-lived gases, especially peroxyacetyl nitrate (PAN) and nitric acid ($HNO_3$). Brunner et al. (2005) concluded that it is difficult to reproduce the observed distribution and variations, and that adopted emissions were critical for the modeled results.

Observations have shown that there are specific processes that are significant for the upper tropospheric chemistry. Acetone influences levels of the hydroxyl radical in the upper troposphere (Kotamarthi et al., 1999; Folkins and Chatfield, 2000). Model studies have demonstrated that upper tropospheric OH distribution and changes are sensitive to model assumptions (Shindell et al., 2006; Hoor et al., 2009). Furthermore, new particle formation is active in the upper troposphere (Young et al., 2007; Benson et al., 2008). Emissions from aviation, of sulfur compounds along with small amounts of soot and hydrocarbons, will contribute to the formation of new particles. Once released at cruise altitudes within the upper troposphere and lower stratosphere, these species interact with the background atmosphere and undergo complex processes, resulting in the formation of contrails. Aged contrails may have effects on upper tropospheric cirrus clouds – and these effects may exert spatially inhomogeneous radiative impacts on climate.

The occurrence of wild fires can be affected by climate change. Fires generate updrafts that efficiently transport pollutants into the upper troposphere, a process generally referred to as pyro-convection. Several studies show that this can have a significant impact on the chemical composition in that altitude region (e.g., Damoah et al., 2006; Turquety et al., 2007).

## 3. Trends in emissions of chemical species and in chemically active greenhouse compounds

Understanding of the past developments in emissions of pollutants and greenhouse gases and the driving forces behind the changes in strength of specific sources of radiatively active chemical compounds is crucial for understanding and modeling of the changing atmosphere as well as for the development of future policies. While the role and historical trends of specific compounds are discussed in the companion paper (Monks et al., 2009), this paper focuses on projections of future emissions.

The growth in the emissions of pollutants associated with the growth of industry, transport and agriculture started at the end of the 19th century, and accelerated strongly after the Second World War. While anthropogenic emissions of $SO_2$, $NO_x$, CH4, and $CO_2$ merely doubled in the first 50 years of the 20th century, the next doubling took only about half as long followed by another doubling in the last quarter of the century (Olivier et al., 2003, Lefohn et al., 1999; Stern, 2005; Smith et al., 2004). During the 20th century, emissions of black carbon (BC) doubled and primary particulate organic carbon (OC) increased by about 40% (Bond et al., 2007). The largest sources of BC and OC include solid fuel combustion in the residential sector and open biomass burning. Recent year's growth in diesel consumption in transportation caused rapid increase in BC emissions. In the last decades of the 20th century, a slowdown or even stabilization of global emissions of primary air pollutants has been observed. As discussed in more detail in the companion paper (Monks et al., 2009), this is due to the effect of air pollution legislation introduced in the OECD countries starting in the early 1980s. The current increase, owing to unprecedented growth rates of Asian economies, primarily China and India, is not expected to continue.

### 3.1. Future emissions

#### 3.1.1. Driving forces

The most important factors determining future emission levels are activity, level of technology development, and penetration of abatement measures. Activity changes are strongly linked to economic, population, and energy growth, but they are also dependent on the geo-political situation, trade agreements, level of subsidies, labour costs, etc. While production technology improvements (with respect to emission levels) are also related to economic growth, a far more important factor is environmental legislation. The latter can be a key factor in determining the penetration of abatement measures and consequently the apparent emission factors. Comparison of historical per-capita $NO_x$ emissions in the United States and Europe shows a strong relationship to per-capita income: for example, income above $5,000 in the U.S. led to a strong increase in car ownership. Recently, several developing countries reached such income levels and face a rapid increase in traffic-related emissions and worsening of air quality, especially in mega-cities. Societal acceptance of measures to improve local air quality has also grown with increasing economic wealth. Therefore, there will be limits to growth in air pollutant emissions in the future (Klimont and Streets, 2007). Transportation is one of the fastest growing sectors, but, owing to ever stricter legislation, its emissions have been growing at a much slower pace or even declined in some industrialized countries. A similar development is expected also in Asia, where many countries either already implement comparable emission limits or prepare respective policies.

Traditionally, national legislation drives the installation of control technology, but in some regions, international (regional or global) agreements have become the key drivers. Examples include the Kyoto Protocol, UNECE CLRTAP (United Nations Economic Commission for Europe Convention on Long-Range Trans-boundary Air Pollution) Protocols, and EU Directives. At the national level, the economic projections are frequently updated, as are some key activity factors, e.g., population and energy use. Regional or global projections of drivers are updated less frequently, and such work is often driven by policy needs, e.g., the global SRES scenarios (Special

Report on Emissions Scenarios) (Nakicenovic et al., 2000) developed as part of the IPCC (Intergovernmental Panel on Climate Change) reports, EU energy or agricultural projections, and the work of international agencies such as IEA (International Energy Agency), OECD (Organization for Economic Cooperation and Development), and FAO (United Nations Food and Agriculture Organization).

An example of the impact of already committed legislation on $NO_x$ emission estimates for the SRES scenarios compared to the original SRES scenario results (Nakicenovic et al., 2000) is demonstrated in Fig. 5.

One additional aspect of environmental legislation to be taken into account is the actual level of compliance. For projections, it is assumed that the technical abatement measures will be implemented in a timely manner to comply with the law. As far as performance of the equipment is concerned, approaches vary between studies: some assume that emission factors equal emission standards, while others make explicit assumptions about the probability of failure, e.g., the percentage of 'smokers' among the vehicle population. The latter assumptions most often rely on the experience with existing equipment that might not necessarily be representative for the new and future technologies. For a good understanding of the projections, it is of utmost importance to state these assumptions explicitly. There is also a strong interdependence among different air pollutant species, such that many species can be mitigated at the same time by certain kinds of environmental policies, i.e., ambitious $CO_2$ reduction targets will result also in significant overall reduction of air pollutants. On the other hand, some specific reduction technologies include a 'pollution penalty', i.e., increase in emissions of other compounds, e.g., slight increase in fuel consumption when particle traps are installed in vehicles will lead to increase of several pollutants.

### 3.1.2. Global and regional future emission inventories

There are a number of key studies and papers that provide important information on future emission levels, globally and in certain world regions and countries. The IPCC SRES scenarios (Nakicenovic et al., 2000) reflect a large, global, long-term effort. Although the SRES scenarios assume improvements in production technology, they do not include some of the expected changes in the future penetration of abatement measures (the impacts of recent legislation); they do not include either some of the aerosols and PM species and are available only for aggregated regions rather than countries.

There are a number of global projections that have been published in the peer-reviewed literature. For example, Streets et al. (2004) developed a forecast of future BC and OC emissions, drawing on SRES activity data and incorporating the evolution of production and control technology, specifically for non-industrial sectors. Cofala et al. (2007) developed global projections for air pollutants, BC, OC, and methane up to 2030. A longer-term projection (up to 2100) for BC and OC also taking into account $CO_2$ abatement options and policies was prepared by Rao et al. (2005); the activity data are based on the SRES scenarios. The Royal Society Report (2008) assessed possible future changes in global and regional ozone concentrations in 2050 and 2100, given changes in socioeconomic factors (Riahi et al., 2006), trends in emissions of precursor gases as well as climate change projections. As part of its Clean Air Interstate Rule (CAIR), the U.S. EPA has developed near-term emission forecasts of $SO_2$ and $NO_x$ (http://www.epa.gov/cair).

Several regional projections are also available. For Europe, the GAINS model (Amann et al., 2004; http://gains.iiasa.ac.at) includes projections of air pollutants and greenhouse gases up to 2030, developed in consultation with national experts (Amann et al., 2008; Kupiainen and Klimont, 2007) and the EMEP database (http://www.emep.int) contains official projections (up to 2020) for several European countries (Vestreng et al., 2006). For Asia, several studies looked at particular pollutants (e.g., $SO_2$, $NO_x$) but recently more integrated work has been also published, e.g., the Japanese Regional Emission Inventory in Asia (REAS) (Ohara et al., 2007) presenting emissions for several pollutants for the period 1980–2020. The GAINS-Asia model has also been updated, superseding previous versions and published projections based on RAINS-Asia (Klimont et al., 2009).

The SRES scenarios are widely used in the evaluation of the future distribution of atmospheric compounds. In the framework of ACCENT and AEROCOM, two other scenarios of the evolution of the emissions of air pollutants ($SO_2$, $NO_x$, CO, BC, OC) and methane have been developed (e.g., Dentener et al., 2005; Dentener et al., 2006b; Cofala et al., 2007). The Current Legislation scenario (CLE) is based primarily on national expectations of economic and energy growth and present (end of 2002) emission control legislation. The Maximum Feasible Reduction (MFR) scenario assumes a full implementation of all available current emission reduction technologies. All these scenarios suggest a decrease of most emissions in OECD countries, but large changes in Asia.

In spite of recently introduced environmental legislation specifically targeting transport sector in urban areas as well as power plant sector, the emissions have continued to grow in Asia: the contribution of Asian emissions to the global emissions of $SO_2$

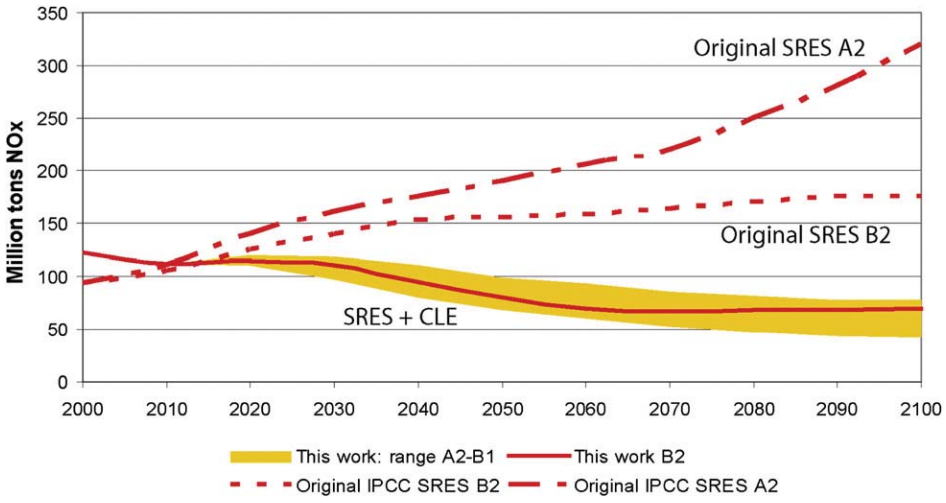


**Fig. 5.** Change in $NO_x$ future emissions resulting from traffic emissions limits, compared with the original SRES scenarios B2 and A2.

and $NO_x$ increased from about 30 and 20 percent in the beginning of the 90's to 50 and 35 percent in 2005, respectively (Cofala et al., 2007). Early inventories and projections suffered from poor data availability, were too optimistic about the pace of introduction and efficiency of environmental legislation, and underestimated the economic growth, and several authors reassessed their previous emission estimates for Asia for several pollutants, e.g., Streets et al. (2006a), Ohara et al. (2007), Zhang et al. (2007), Klimont et al. (2009). Fig. 6 shows the evolution of the emissions of $SO_2$, $NO_x$ and BC in Asia. It can be seen from this figure that the SRES A2 scenarios show much higher emissions and seem to underestimate the impact of the current legislation, especially for $SO_2$, while for $NO_x$ also growth in transport demand was underestimated in the SRES A2 scenario. MFR scenarios suggest a large technical potential for emission reduction after 2010 except BC where majority of emissions originate from domestic combustion and end-of-pipe measures are estimated to have only limited applicability within considered time horizon.

Fig. 7 illustrates the estimated changes in emissions of $SO_2$ and $NO_x$ between 2000 and 2030 for a baseline scenario comparable to the IIASA-CLE scenario (Cofala et al., 2007), the basis for the scenarios s used in the ACCENT model comparisons (Stevenson et al., 2006). The largest changes occur in the same areas, with China and India showing a strong increase and Europe, North America, and Japan a decline in emissions (Akimoto, 2003).

Major uncertainties in emission inventories are associated with inadequate knowledge of open biomass burning (forest fires, agriculture waste burning), biofuel use (heating and cooking), artisanal industry, residential combustion of coal, and agricultural production systems. Due to a lack of comprehensive activity data, there is a tendency to underestimate the emissions of these pollutants. Uncertainties in inventories will vary by region, source, pollutant and inventory year. Uncertainty estimates for all world regions are not available.

Uncertainties for individual pollutants differ also with the level of experience of compiling an inventory, with reduced uncertainties obtained over time. $SO_2$ inventories have a long history in Europe and North America and are considered relatively reliable in those regions. Due to the short experience in compiling PM, BC, and OC inventories and the lack of data on the distribution of technology types in key regions, these are even more uncertain. BC and OC inventories have uncertainty ranges of −25% to a factor of two (higher for open burning) (Bond et al., 2004). Typical reported ranges of uncertainty estimates for Europe are: $SO_2$: ±5%, $NO_x$: ±14%, NMVOC: 10–39% and CO: ±32% (EMEP, 2006). The TRACE-P inventory (Streets et al., 2003) estimated uncertainties in Asian emissions that ranged from ±16% for $SO_2$ and ±37% for $NO_x$ to more than a factor of four for BC and OC. Within Asia, there was wide variation among countries and regions, with emission uncertainties in Japan being similar to those in Europe, and emissions in South Asia having high uncertainty.

### 3.1.3. *Future inventories from different sectors*

The relative importance of different sectors for global anthropogenic emissions in 2000 is presented in Fig. 8 (gaseous species) and Fig. 9 (BC). The estimates are based on the GAINS model calculations and for historical years are broadly consistent with the EDGAR FT2000 (van Aardenne et al., 2005) and Bond et al. (2004). The contributions shown in these figures can be markedly different, however, for individual countries and regions and they exclude international shipping and air traffic. The figures also show changes in the source structure in the CLE and MFR scenarios for 2030. The change in size of the pie charts symbolizes[1] change (increase or decrease) in emissions compared to the year 2000.

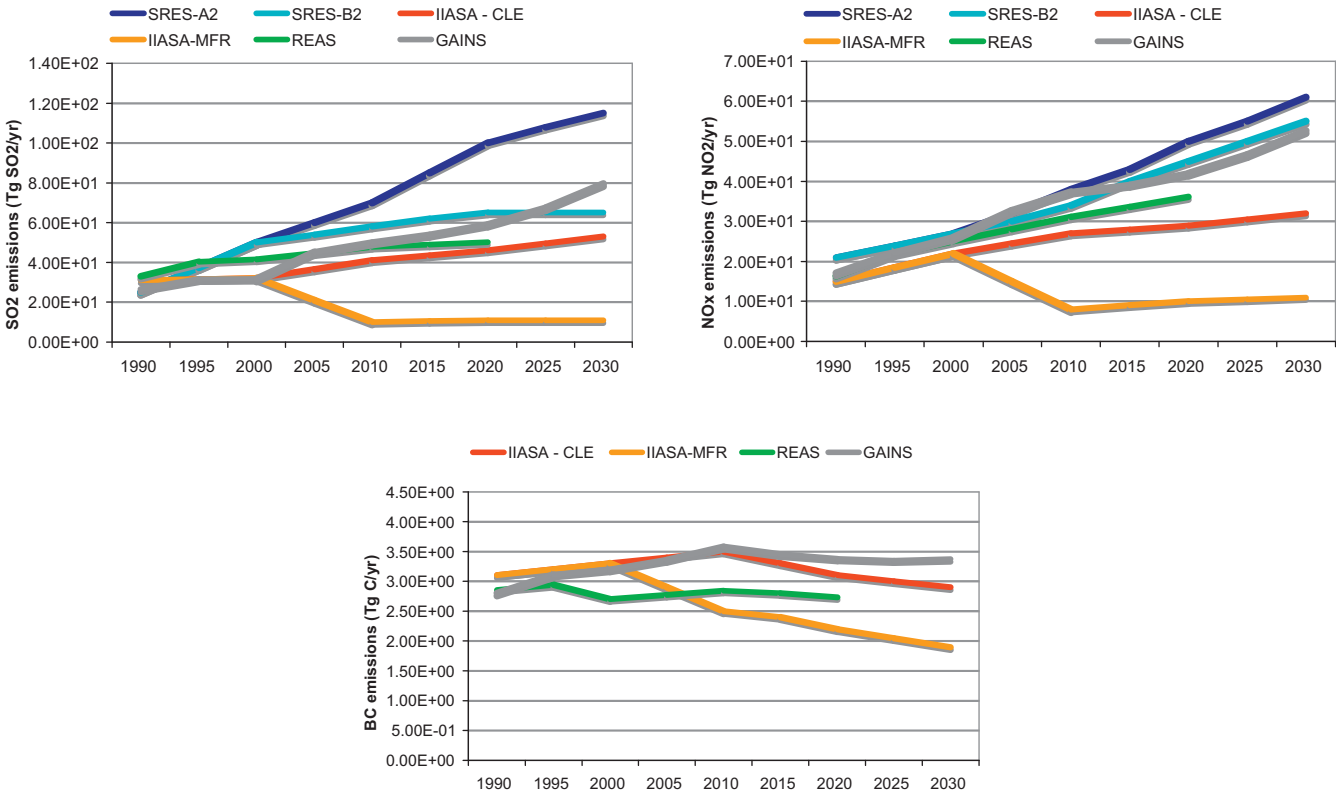


**Fig. 6.** Evolution of the emissions of $SO_2$ (left), $NO_x$ (right) and BC (bottom) from different inventories for the 1990–2030 period; Source: SRES (Nakicenovic et al., 2000), IIASA (Cofala et al., 2007), REAS (Ohara et al, 2007), GAINS (Klimont et al., 2009).

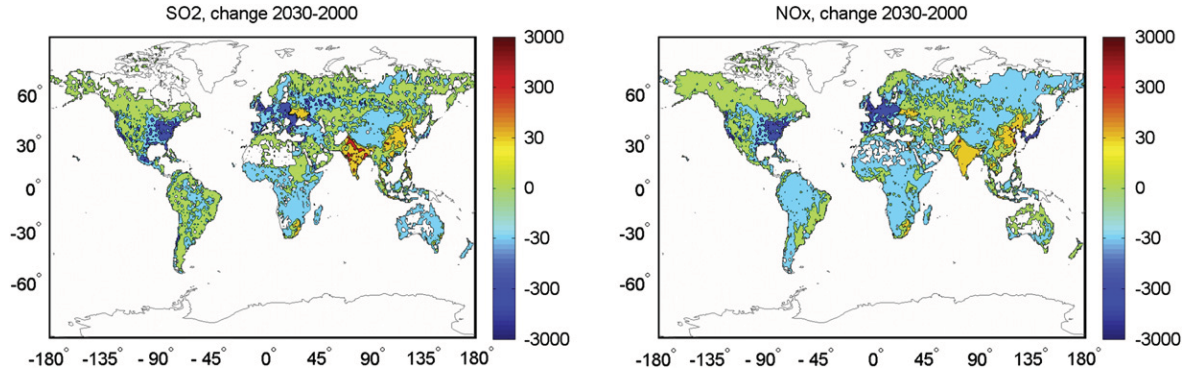


**Fig. 7.** Change in emissions of $SO_2$ (left) and $NO_x$ (right) in the 2000–2030 period. Units are ng cm$^{-2}$ s$^{-1}$. Source: GAINS model results, gridding courtesy of Tami Bond.

Industrial combustion sources (including power plants) dominate emissions of $SO_2$, $NO_x$, and $CO_2$ in nearly all scenarios, except for 2000 for $NO_x$ where the penetration of reduction measures in transport sector was still relatively low in several world regions leading to high emissions from this sector. It changes in the future when relative contribution of emissions from transport declines from over 50 percent in 2000 to about 40 percent in 2030. For $CO_2$ and $SO_2$, the industrial combustion share increases by few percentage points from about 63 and 74 to 69 and 79 percent, respectively.

Emissions of methane (Fig. 8) are dominated by agriculture, waste, and production and transmission of natural gas (the latter two included in "Industrial processes"). Growing demand for gas leads also to increase in share of the latter sector in future emissions; only in the MFR scenario effective control of losses reduces its importance and makes agriculture even a more prominent source.

Primary source of emissions of BC is combustion of solid fuels, mostly biomass, in the domestic sector (Fig. 9) representing over 60 percent of BC. Transport plays also an important role, especially for BC due to diesel emissions, representing nearly 20% of total. Relatively high share of industrial combustion in total emissions is associated with assumptions of high emission factors for small industrial boilers (stokers) and furnaces used in the developing countries.

## 4. Distribution and changes of chemical active greenhouse gases and their precursors

Models and observations represent powerful tools to understand past and current behavior of atmospheric constituents. Observations by satellites, which have a global scale is of particular importance for understanding large-scale distributions and trends. Also, since we are considering chemical active greenhouse compounds with significant spatial and temporal variations, more limited scale observations represented by surface and sonde observations are necessary for understanding chemical processes and their impact on the distribution. Prediction of future changes due to emission changes and climate initiated atmospheric changes (temperatures, dynamics, humidity, biospheric response), can only be made if we have reasonable understanding of past and present conditions. We need to know the non-linear responses in composition from emission changes caused by human activities, and the behavior of the chemical active greenhouse gases ($CH_4$, $O_3$, particles). Such knowledge helps us distinguish natural variability from human-induced changes.

The number of observations available for global comparisons have increased manifold during the last decade and include satellite, airborne and surface observations (Richter et al., 2004; Levelt et al., 2006; Schoeberl et al., 2007; Oltmans et al., 2006). A large number of model/measurement comparisons have been performed, which clearly show that model performance and our understanding of processes have improved (Isaksen et al., 2005; Textor et al., 2006; Kinne et al., 2006; Schulz et al., 2006; Hoor et al., 2009). Models are also important for improving our understanding of compounds with low spatial and temporal coverage in the observations.

Future changes in the chemically active greenhouse gases and particles are to a large extent dependent on the emission scenarios adopted, which are based on assumptions of population growth, technology development, implementation of environmental measures to reduce emissions and economical growth. It is interesting to note that growth in emissions since the turn of the century from several sectors (e.g., air traffic, ship transport) have exceeded predictions made only a few years ago significantly. Scenarios commonly used in model predictions are the IPCC SRES scenarios, the EDGAR and RETRO databases, and scenarios from the QUANTIFY project for the transport sector, and particular databases or scenarios for specific sectors like ship transport and regions like South-East Asia. Unfortunately, there are not yet any common accepted databases or scenarios for future adaption. A discussion of future emission scenarios is given in Chapter 3.

### *4.1. Observations and analysis of greenhouse gases and their precursors*

#### *4.1.1. Satellite observations*

Satellite observations during the last decade of chemically active compounds like ozone, methane, CO and $NO_2$ have proven to be particularly valuable for the validation of global chemical transport models (CTMs), and for increasing our knowledge of key chemical and physical processes in the troposphere. This improves our capability to reproduce and assess the impact of man induced emission changes (Richter et al., 2004; Levelt et al., 2006; Schoeberl et al., 2007). Such studies include the identification of key source regions, the quantification of sources strengths, and the assessment of changes and trends over past decades. The first extended satellite data set of observed tropospheric composition came from the TOMS instrument (Krueger, 1989), which was designed to observe total ozone column but can be used to retrieve tropospheric ozone columns.

The Global Ozone Monitoring Experiment GOME (Burrows et al., 1999) was the first satellite instrument having enough spectral resolution to observe ozone as well as some of its precursors ($NO_2$, HCHO). These measurements were continued and extended with the SCIAMACHY instrument (Bovensmann et al., 1999) which has

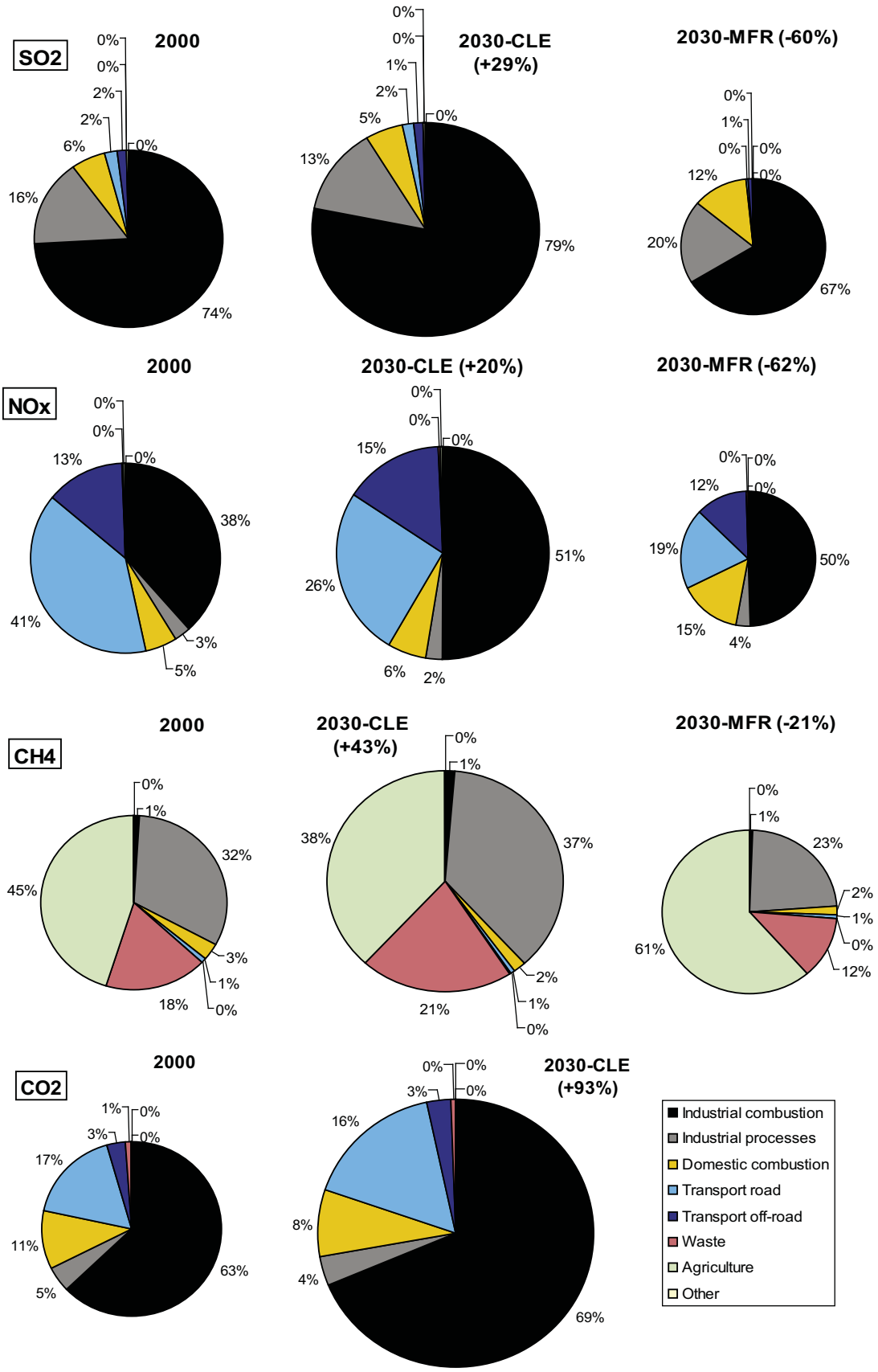


**Fig. 8.** Source sector contribution to the global emissions of selected aerosols and greenhouse gasses; Source: GAINS model.

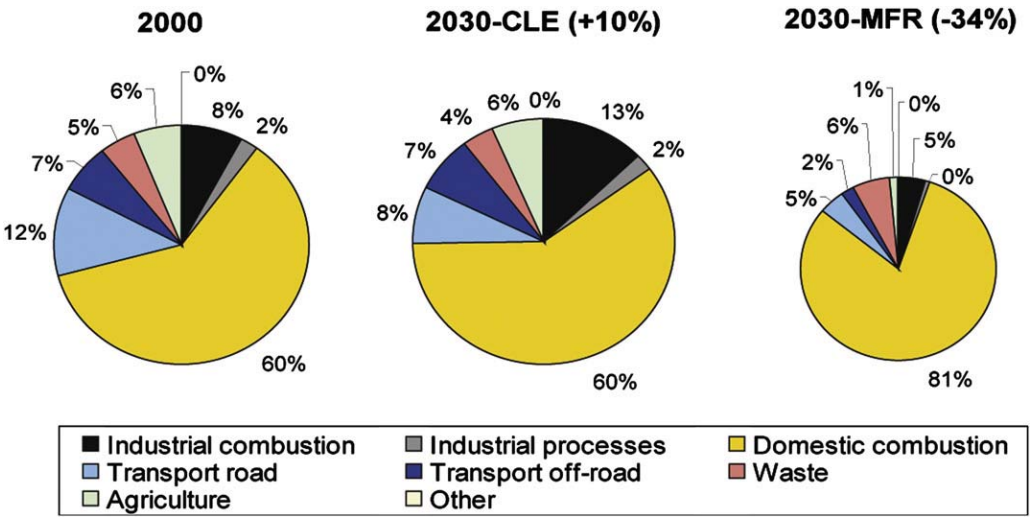


**Fig. 9.** Source sector contribution to the global anthropogenic (excluding forest fires and savannah burning) emissions of BC; Source: GAINS model.

a better spatial resolution and near-infrared (NIR) observing capability, allowing CO, $CH_4$, and $CO_2$ observations. More recently, the OMI instrument (Levelt et al., 2006) on the AURA platform and the GOME-2 (Callies et al., 2000) on MetOp add to the UV/visible data record, with a high spatial resolution and improved coverage. Using measurements in the IR spectral region, the MOPITT instrument (Drummond and Mand, 1996) has been observing CO in the upper and middle troposphere since its launch in December 1999. A number of other tropospheric species including $O_3$ and several hydrocarbons can also be observed in the upper troposphere by the ACE instrument in solar occultation and in nadir from the TES and IASI instruments. While the IR nadir observations provide some degree of vertical information, they usually have low sensitivity to the lowermost troposphere. However, they greatly extend the list of observable species (Clerbaux et al., 2009 and reference therein), and allowing for night-time measurements. All of these datasets are extremely useful in evaluating the modeling capabilities of CTMs. In the next sections, some examples are given for CO, methane and HCHO. Further discussion, on recent advances in space borne observations of atmospheric composition and their applications, is given in the paper by Laj et al. (2009).

*4.1.1.1. Methane.* Methane ($CH_4$) concentrations in the atmosphere have increased by at least 2.5-fold during the agro-industrial era (the past 3 centuries) from about 700 ppb, as derived from ice cores, up to a global average concentration of about 1770 ppb in 2005 based on present-day surface monitoring networks. Satellite observations of methane ($CH_4$) columns have become possible with the measurements of the SCIAMACHY instrument (Buchwitz et al., 2005; Frankenberg et al., 2006). The measurements show the hemispheric gradient, the seasonality and hot spots over rice paddies and tropical rain forests. Overall the agreement between satellite measured and modeled $CH_4$ fields is good but there is indication of a significant underestimation of methane emissions from tropical rain forests (Buchwitz et al., 2005; Frankenberg et al., 2005; Houweling et al., 2006), as seen in Fig. 10. A recent re-analysis of the satellite data using improved spectroscopic data reduced the difference (Frankenberg et al. 2008).

*4.1.1.2. Nitrogen dioxide ($NO_2$).* Tropospheric $NO_2$ columns have been derived from measurements of several UV/vis satellite instruments starting with GOME in 1995. As the lifetime of $NO_2$ in the lower troposphere is short, most of the $NO_2$ is observed close to the sources and satellite measurements have been used to derive $NO_x$ emissions, both globally and for specific sources (Beirle et al., 2004; Konovalov et al., 2006; Martin et al., 2004; Muller and Stavrakou, 2005; Richter et al., 2004). Although models represent patterns of observed distributions, there are discrepancies that can be linked to inaccuracies in missions. An example of such discrepancies can be attributed to the de-noxification of power plant exhausts during summer in the Eastern US following emissions regulations (Kim et al., 2006) (Fig. 11). Changes in $NO_x$

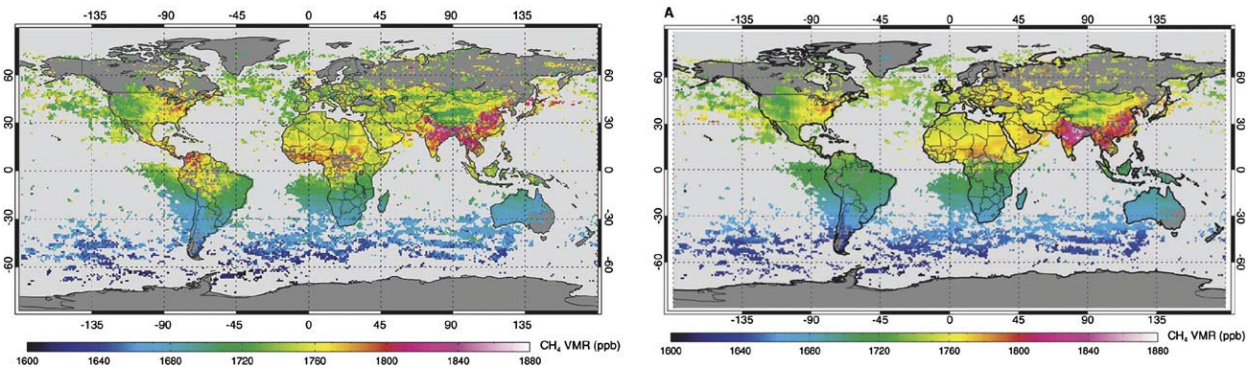


**Fig. 10.** SCIAMACHY measurements of column-averaged methane mixing ratios in ppb (left) and TM3 model results of column averaged $CH_4$ mixing ratios (right), averaged for the time period August -November 2003 (Frankenberg et al. (2005)).

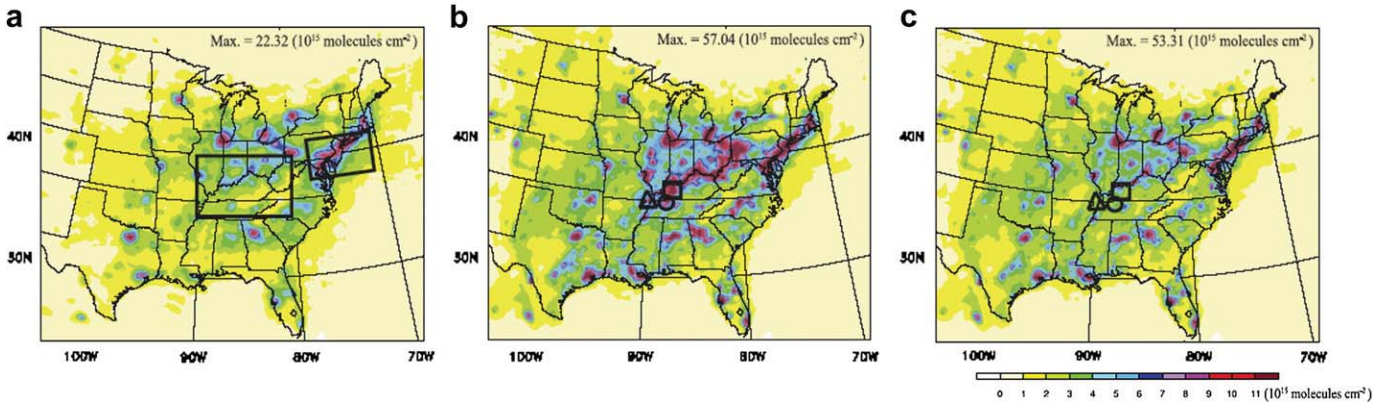


**Fig. 11.** Spatial distribution of $NO_2$ columns time averaged over June–August 2004 from (a) SCIAMACHY satellite observations, (b) WRF-Chem reference emission case runs, and (c) WRF-Chem updated emission case runs. From (Kim et al., 2006).

emissions are particularly large in parts of China, as seen from satellite observations (Richter et al., 2005).

Comparisons of satellite $NO_2$ measurements with model results indicate a possible underestimation of microbial sources of $NO_x$ (Bertram et al., 2005; Jaegle et al., 2004; Wang et al., 2007). Furthermore, lightning $NO_x$ emissions derived from satellite measurements are at the low end of other estimates (Beirle et al., 2006; Boersma et al., 2005; Martin et al., 2007) with potential implications for ozone production.

*4.1.1.3. Formaldehyde (HCOH).* Satellite measurements reveal large concentrations of HCHO over ecosystems emitting isoprene and terpenes, in particular over tropical rain forests (Chance et al., 2000; Wittrock et al., 2006). The seasonal and inter-annual cycle has been compared to models and good agreement was found in many regions (De Smedt et al., 2008; Palmer et al., 2003) (see also Fig. 12) The observations have also been used to estimate emissions of isoprene and other VOCs (Abbot et al., 2003; Fu et al., 2007; Stavrakou et al., 2008). Satellite observations show enhanced formaldehyde distribution over regions affected by biomass burning. Parallel inversion of HCHO and glyoxal (CHOCHO) has confirmed previous HCHO emission estimates but indicated a large missing biogenic source for glyoxal, which must be secondary to explain the satellite observations (Stavrakou et al., 2009a,b).

*4.1.1.4. Carbon monoxide (CO).* Comparisons of satellite CO observations from the MOPITT satellite instrument with models reveal substantial differences (Fig. 13). There is a large underestimate in models of the Northern Hemisphere springtime maximum in CO. A similar bias is seen in comparison with surface observations at Northern middle and high latitudes (Shindell et al., 2006), suggesting that the discrepancy cannot be attributed purely to biases in the satellite retrievals. Although all models show this bias, there is nonetheless a large range of CO values in the various models. Simulated CO is correlated with OH in the models (Fig. 4.6). Some models produce OH fields inconsistent with observational constraints on OH, but even those models whose OH values are in accord with observation-based estimates are biased in CO, suggesting an underestimate in current emission inventories of CO or its hydrocarbon precursors. Indeed, in a recent study Pison et al. (2009), developed a data assimilation system and applied it to infer CO emissions (for 2004), and came up with significant higher global emissions than currently used, indicating that underestimated CO is a result of too low emissions. However, the large spread in methane lifetimes in the models (a factor of two; Fig. 14) indicates that there are also substantial uncertainties in our understanding of the present-day oxidation capacity of the troposphere.

*4.1.2. Trends at surface stations*

*4.1.2.1. Ozone.* Chemical transport models indicate that 60–85% of the present ozone burden in the troposphere results from chemical production in the troposphere. (Fusco and Logan, 2003; Lelieveld and Dentener, 2000). Comparisons of present ozone concentrations with values at a few stations in the Northern Hemisphere making continuous measurements in the late 19th century and early 20th century suggest that surface ozone approximately doubled over the last century (Vingarzan, 2004). For the last two to three decades the global picture obtained from observations is not uniform. In general, the increases are larger from the 70s to mid- 80s than in recent years with a more mixed picture. Fig. 15 shows ozone background trends at northern hemispheric mid-latitude stations at the western coasts of the United States and Europe as well as the high-altitude site Jungfraujoch. At the low altitude station, the background conditions were carefully selected (Parrish et al., 2008). Ozone concentrations have consistently increased at some background stations in Europe and the US since the 1950s. European stations show an increase until the year 2000 from when on the concentrations remained constant. At the west coast of the US the ozone concentrations are still increasing in air coming from the marine boundary layer. For northern hemisphere mid-latitude stations observations are determined by trends in emission in the source regions. The increase in the 1990s is likely to be affected by large changes in stratospheric ozone concentrations (Isaksen et al., 2005; Ordóñez et al., 2007). Large increases in emissions in Asia and from ocean going ship during the last 10 years can probably explain some of the increases at the west coasts of the US and Europe (ship emissions) (Dalsøren et al., 2009a; Dalsøren et al., 2009b).

Stations in different areas of the world might show different trends. Observations in the eastern Mediterranean over a 7 year time period (1997 to 2004) show a significant decline in surface ozone of 3.1%/year, reflecting the influence of transport from continental Europe with declining emissions of ozone precursors (Gerasopoulos et al., 2005). Observations from Northern Canada and the South Pole show a decline both at the surface and in the free troposphere (Logan, 1998; Vingarzan, 2004; Oltmans et al., 2006). This might be linked to decreased ozone flux from the stratosphere (Oltmans et al., 2006), or it could be a result of solar fluxes penetrating to the troposphere where enhanced fluxes seem to reduce ozone in pristine background areas (Isaksen et al., 2005). Observational record from other areas in the Southern Hemisphere is sparse with no clear trends (Vingarzan, 2004; Oltmans et al., 2006). On the other hand, ship-borne measurements in the Atlantic by Lelieveld et al. (2004) for the period 1979 to 2002 show significant regional increases, with increasing fossil fuel and biofuel use in Africa as the main source of this trend.

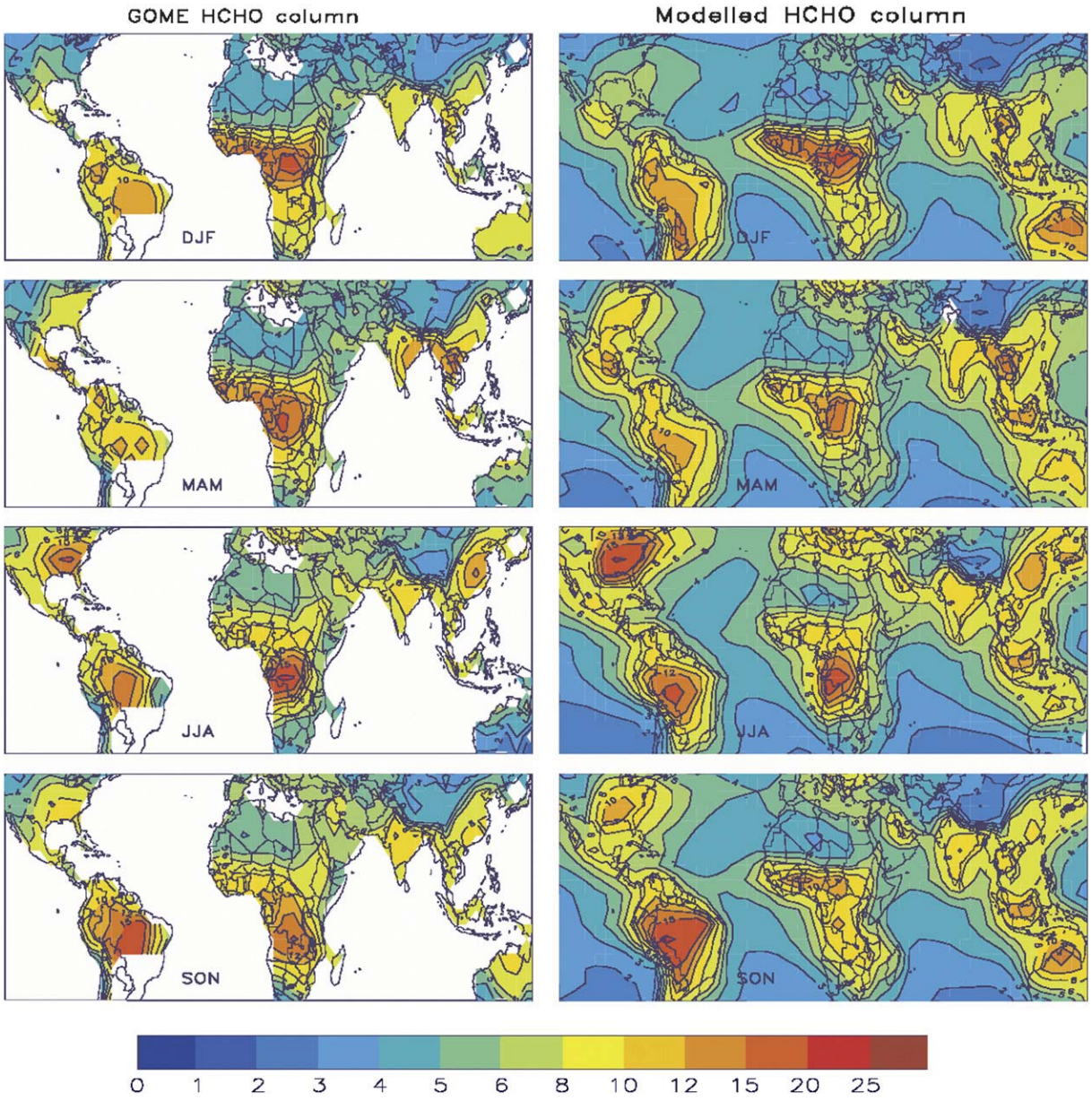


**Fig. 12.** Seasonally averaged HCHO columns retrieved from GOME in 2000 (left panels) and calculated columns using the GFEDv1 biomass burning inventory and biogenic emissions from the MEGAN model using ECMWF meteorology (right panels). Units are $10^{15}$ molecules $cm^{-2}$. From (Stavrakou et al., 2008).

Ozone increases since preindustrial time are reproduced by models (Berntsen et al., 1997; Wang and Jacob, 1998; Stevenson et al., 1998; Mickley et al., 1999; Hauglustaine and Brasseur, 2001; Shindell et al., 2003; Wong et al., 2004; Lamarque et al., 2005; Gauss et al., 2006), using current and pre-industrial emissions, although models tend to overestimate ozone for the pre-industrial period.

As part of the EU RETRO project (ECHAM5-MOZ, LMDz-INCA) model studies of the long-term trends for the last 40 years of the 20eth century were performed. In addition, time slice studies for specific years were performed (OsloCTM2 and p-TOMCAT). All models gave significant tropospheric ozone burden increases during the time period studied. The mean year-2000 tropospheric lifetime calculated by these models are in good agreement with the multi-model mean estimate of $22.3 \pm 2.0$ days of Stevenson et al. (2006). Other model studies investigating shorter time periods, (Karlsdóttir et al., 2000; Lelieveld and Dentener, 2000;Granier et al., 2003; Jonson et al., 2006) were able to reproduce some of the observed ozone trends.

Fusco and Logan (2003) made a thorough estimate of tropospheric ozone distribution and trends. They concluded that surface emissions of $NO_x$ have had the largest effect in the lower troposphere at northern mid-latitudes since 1970. The large emission increase and efficient outflow from Asia makes China responsible for 30% of the increase at mid latitudes. Methane levels could explain 25% of the global ozone trends. Although reduced stratospheric ozone lead to a 30% decrease in cross-tropopause flux giving significant decreased ozone in the upper and middle troposphere, little impact on surface ozone was found in the summer and fall.

*4.1.2.2. Methane monitoring.* Pre-anthropogenic methane levels of about 700 ppb constrain the current ratio of global natural

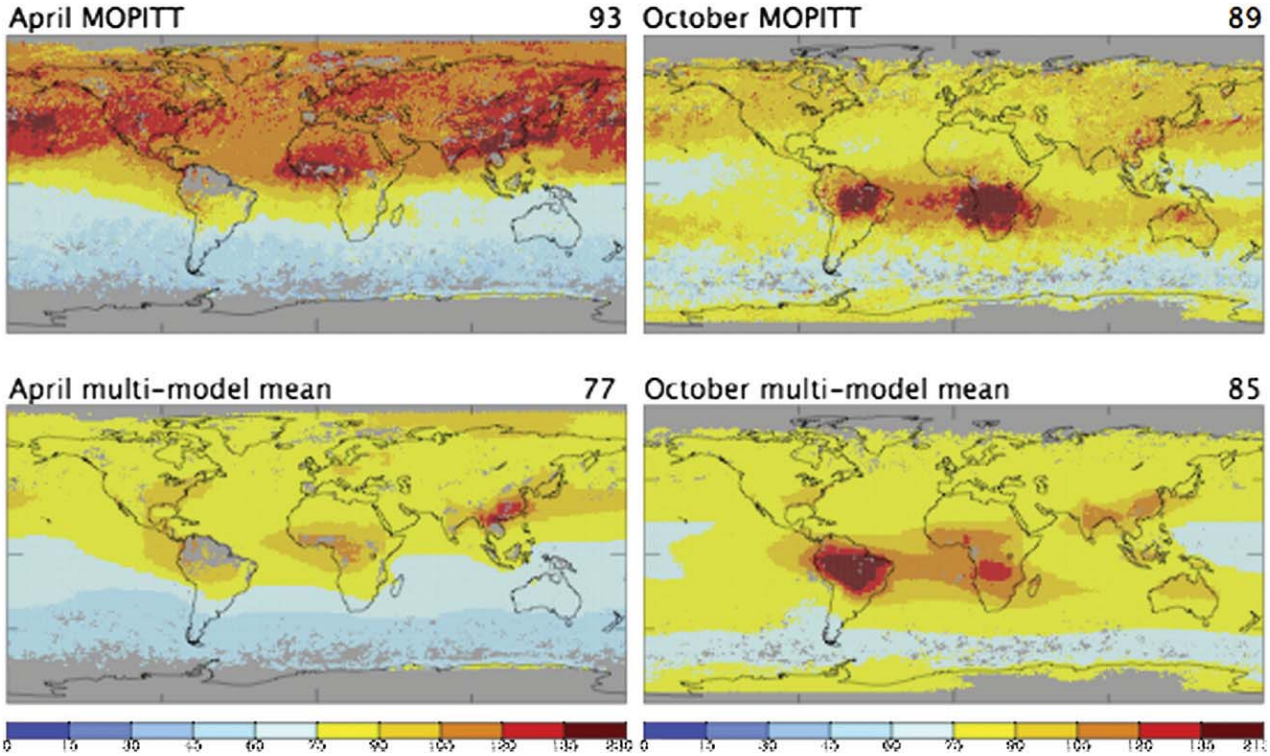


**Fig. 13.** MOPITT observations and multi-model distributions of CO (ppbv). The top row shows MOPITT observations in 2000 for April (left) and October (right) for the 500 hPa retrieval level. The bottom row shows the equivalent fields from a multi-model ensemble average (26 models participating in the ACCENT modeling project) sampled with the MOPITT averaging kernel and a priori CO profiles. Values in the upper right corner are the global mean area-weighted CO (ppbv). Grey areas indicate no data. Reprinted from Shindell et al. (2006).

(28–42%) to anthropogenic (58–72%) emissions to about 1:2. This implies that the present-day anthropogenic emissions exceed 300 Tg $yr^{-1}$ compared to total emission of 500–600 Tg $yr^{-1}$. Wetlands dominate the natural methane emissions and hydrology changes driven by meteorological variability, climate change (e.g., thawing permafrost), and/or anthropogenic activities (e.g., drainage, deforestation) may have induced significant changes. However, even the sign of such changes is still unknown. While higher arctic temperatures are assumed to increase high-latitude emissions, tropical wetland areas are likely diminishing by rapid

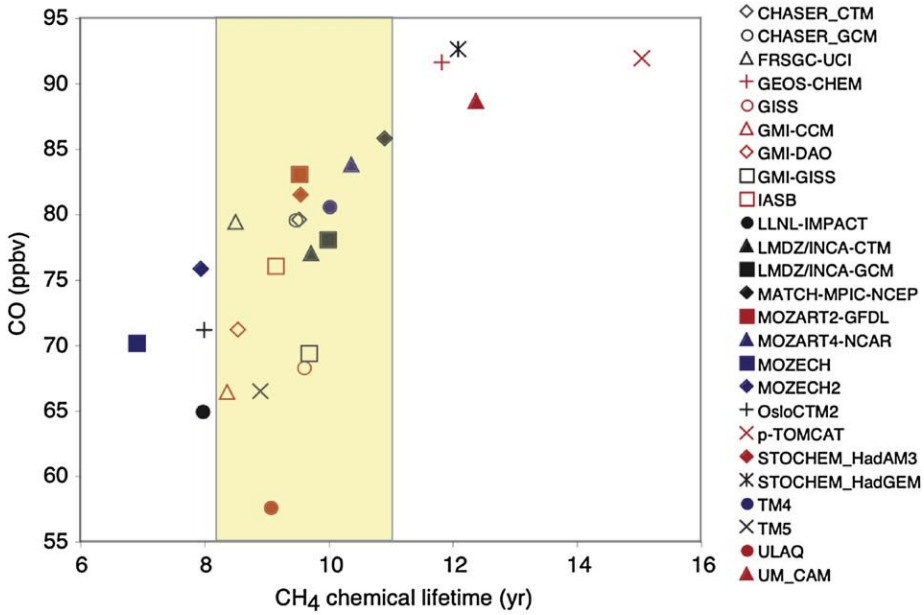


**Fig. 14.** Annual average methane chemical lifetime versus CO in the broad 500 hPa MOPITT retrieval level. Methane lifetime is inversely proportional to OH; all models used the same prescribed methane values, with only a very small deviation due to temperature differences between models. The shaded area indicates the IPCC-TAR lifetime derived from observations and modeling. Reprinted from Shindell et al. (2006).

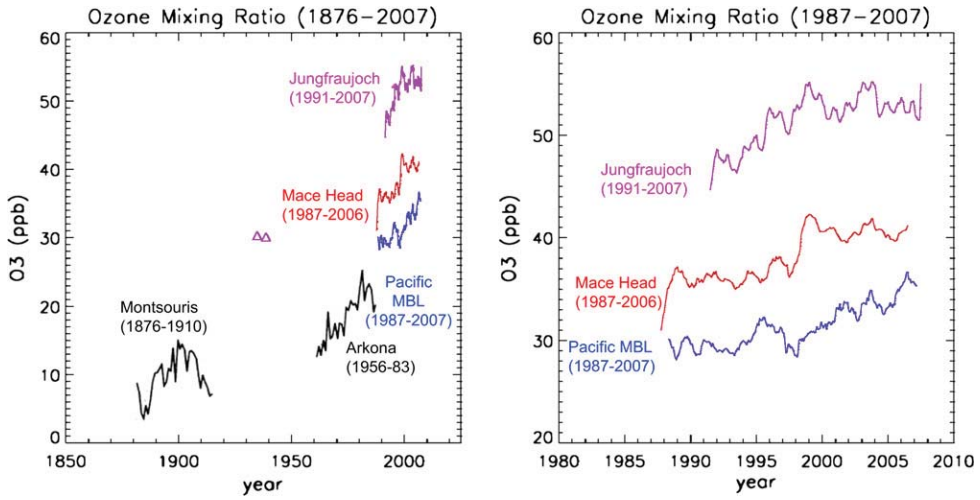


**Fig. 15.** Observed surface ozone at different Northern Hemispheric surface stations.

land use change. Significant progress is being made in process understanding, e.g., in relation to northern peat lands (Wania, 2007) and gas ebullition from northern lakes (Walter et al., 2006a,b). Based on pre-anthropogenic methane levels and fractionation present-day total natural emissions are likely to exceed 200 Tg $yr^{-1}$. New estimates on methane soil consumption amount to 28 (9–47) Tg $yr^{-1}$ (Curry, 2007).

Global methane monitoring networks include the in situ networks of NOAA-GMD and ALE-GAGE-AGAGE, and the NDACC FTIR network. The longest records currently span about 25 years. Fig. 16 shows the NOAA GMD surface measurements from 1984 until 2007, and the yearly variability in changes in global methane. The long-term methane growth rate has decreased markedly since the early 1990s, with periods of nearly constant global concentration levels as is seen during the first years of the 21st century. The possible causes of this leveling off are subject of intense scientific debate. On top of the declining trend anomalous events such as in 1991–1993 (ascribed to the Pinatubo eruption) and 1997–1998 (ascribed to an exceptional El Nino) have caused fluctuations in the annual growth rate in response to annual emission anomalies of the order of 10 to 20 Tg.

Atmospheric inversion is a powerful tool to convert atmospheric measurements into estimates of surface emissions. Estimating surface emissions using atmospheric measurements in combination with a CTM and prior estimates of sources and sinks is an efficient approach. This top–down approach is increasingly used also for reactive trace gases (Hein et al., 1997; Petron et al., 2004; Bousquet et al., 2005; 2006; Chen and Prinn, 2006). Using an inversion model, Bousquet et al. (2006) analyzed the large atmospheric variations of the growth rate of methane in terms of surface emissions. They found that natural wetlands are largely dominating the inter-annual variability over the 1984–2003 period. Emissions due to biomass burning have an impact on inter-annual variability only during the strong El Niño of 1997–1998. The study of Bousquet et al. (2006) has shown that inverse modeling represent a useful supplement to other estimates of methane emissions that can reduce uncertainties associated with methane trend studies.

*4.1.2.3. Carbon monoxide (CO).* CO plays a key role for tropospheric oxidation since the reaction with OH represents the main loss of OH. Studies has shown that since 1980 there has been large regional differences in the emission trends, and some regions like Europe succeeded in implementing efficient abatement measures (Monks et al., 2009; Olivier et al., 2003; EPA, 2003; EMEP, 2004; Dalsøren et al., 2007). Northern Hemisphere (NH) CO observations indicate an increase of about 1% $year^{-1}$ from the 1950s until the late 1980s, which are consistent with increased emissions (Novelli et al., 2003). Methane oxidation represents an important source of CO, particularly in unpolluted regions, and is likely to have contributed to the observed increase. There were no evident trends for the only available station in the Southern Hemisphere (SH). The recent regional reduction in emissions seems to be a likely explanation for measured CO decreases in the U.S. and Europe (EPA, 2003; EMEP, 2004). Anomalous declines in global concentrations were found for the period 1991–1993 and are likely explained by an OH increase after the eruption from Mt Piantubo in 1991 (Novelli et al., 1998). Large enhancements were observed due to unusually large emissions from vegetation fires during the 1997–1998 ENSO period.

*4.1.2.4. OH distribution and trend.* Long-term trends in global OH will have a significant impact on methane lifetime and thereby on the global methane trend. Changes in global OH will to a large extent be determined by the ratio of global $NO_x$ to CO emissions (Dalsøren and Isaksen, 2006), with enhanced NO emissions leading to enhanced OH, while enhanced emissions of CO as the main controller of OH, leading to reduced global OH.

Common to all model based studies is an overall high uncertainty in estimating OH trends. There are numerous studies of recent global OH changes. Lelieveld et al. (2002) conclude a 60% increase of the overall oxidation capacity during the last century. In contrast to this, Lamarque et al. (2005) found an overall decrease of the OH burden by 8% from 1890 to 1990. Dalsøren and Isaksen (2006) investigated the changes of OH (as well as the changes in the lifetime of methane) from 1990 to 2001 emission changes with a chemistry-transport model (Oslo CTM2) and found an average OH increase of 0.08%$year^{-1}$ over this time period.

Measurement campaigns with newly developed techniques to directly measure OH provide important insight into the chemical mechanisms more or less representative for a specific region or chemical regime (e.g., Kleffmann et al., 2005; Berresheim et al., 2003; Smith et al., 2006; Emmerson et al., 2007; Bloss et al., 2007; Lelieveld et al., 2008). The most widely used 'tracer of opportunity' to determine global OH is the purely man made methyl chloroform (MCF, 1,1,1-trichloroethane). It is not quite clear how long MCF can still be measured, since it is currently fading out

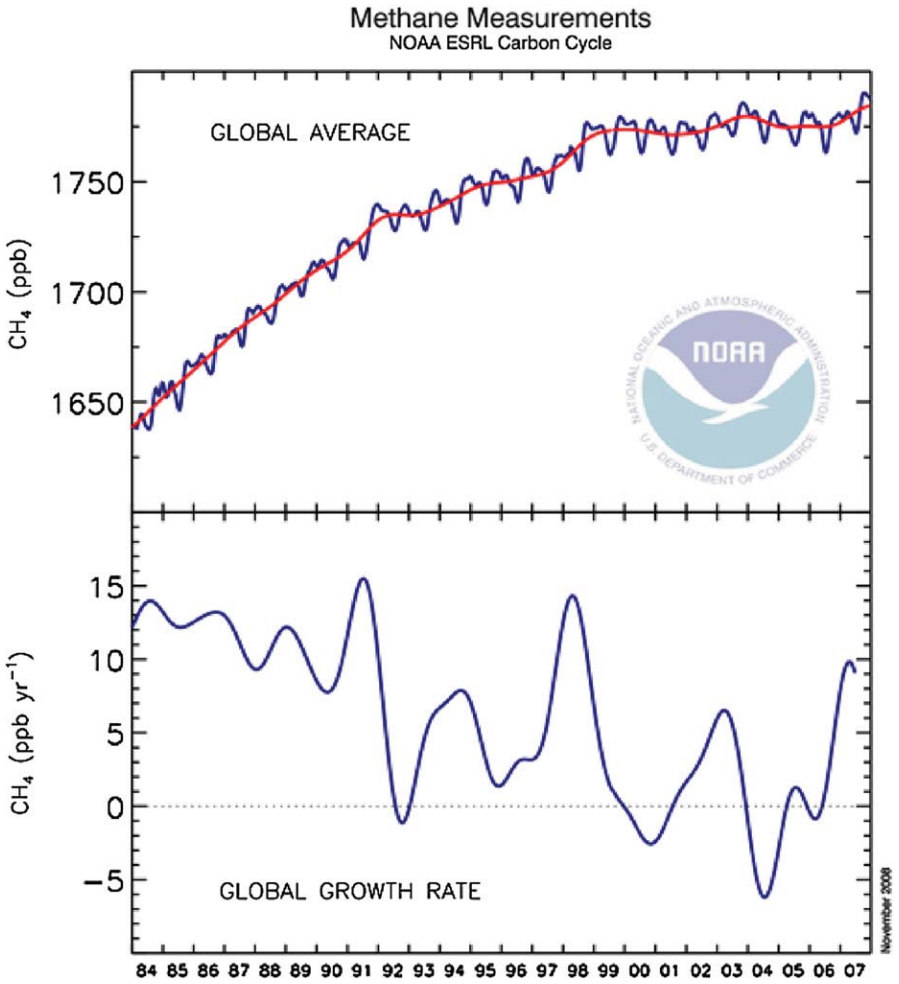


**Fig. 16.** Global methane time series from the NOAA ESRL network.

rapidly after being banned by the Montreal protocol. Note that different oxidation processes in the atmosphere could affect the OH distribution significantly. For instance: It has been shown by Cariolle et al. (2008) that simulated OH is significantly affected, when the results from a recent laboratory study by Butkovskaya et al. (2007) are included, which show that a small fraction of the $NO + HO_2$ yields $HNO_3$.

### 4.2. Modeling future changes

The relatively short atmospheric lifetime of chemically active compounds like $O_3$ and secondary aerosols, and pronounced spatial variability of their impact, make it necessary to consider carefully differences in regional development in future emission scenarios. The Atmospheric Composition Change European Network of Excellence (ACCENT) PhotoComp inter-comparison (Dentener et al., 2006b; Dentener et al., 2006c; Stevenson et al., 2006; Shindell et al., 2006) is the most comprehensive study, which evaluates the role of emissions and climate change until 2030. These papers describe results from up to 26 different global models that participated in the ACCENT study.

#### 4.2.1. Tropospheric ozone

In the ACCENT study of ozone changes in 2030 three emissions scenarios was selected to illustrate possible impact of emission changes (climate change not included): An upper estimate was the original IPCC SRES A2 scenario (Nakicenovic et al., 2000), a central case the IPCC B2 + IIASA-CLE (current legislation) scenario (hereinafter B2 + CLE), whilst a lower case was the IPCC B2 + IIASA MFR (maximum feasible reduction) scenario (Dentener et al., 2005; Cofala et al., 2007; hereinafter B2 + MFR). The scenarios represent the range of possible anthropogenic emissions in the near future. In an additional ACCENT PhotoComp experiment the potential impact of climate change on $O_3$ by 2030 was studied, using a subset of 10 models.

A summary of the results for tropospheric ozone from the ACCENT PhotoComp study is given in Stevenson et al. (2006). It is shown that the evolution of anthropogenic emissions has a strong impact on tropospheric ozone in 2030. Under the high growth, unregulated A2 scenario, tropospheric ozone increases significantly at northern mid latitudes with peak changes over SE Asia, where annual tropospheric column (ATC) increases approach 10 DU (1 DU = $2.67 \times 10^{16}$ molecules $cm^{-2}$) (>20% increases over year 2000). On the other hand, under the highly regulated B2 + MFR (Maximum Feasible Reduction) scenario, ATC is reduced by 3–4 DU over much of the continental Northern Hemisphere. The central scenario, with B2 socioeconomics and full implementation of year 2000 legislation (B2 + CLE), shows increases with ATC peaking at 5 DU over S. Asia.

Emission changes could have significant impact on surface ozone, with large regional variations. Seasonal mean changes in surface $O_3$ between 2000 and 2030 for June, July, August (JJA) from the ACCENT study are shown in Fig. 17. June, July, August is generally the maximum surface $O_3$ season at polluted northern mid-latitudes,

whereas at other locations ozone reaches a maximum in different seasons. In particular, decreases in surface ozone up to 25 ppb can be achieved under the B2 + MFR emission scenario while ozone is predicted to increase by up to 25 ppb in some regions in the A2 emission scenario. The effects of climate change in 2030, while uncertain, are small, compared to potential effects of emission changes. The ACCENT modeling studies show that $O_3$ in 2030 depends in particular $NO_x$ emissions, but also $CH_4$, CO and NMVOC. Therefore, 2030 $O_3$ levels are largely determined by emission control.

In a recent study organized by the Royal Society (Royal Society, 2008) several new model simulations were performed to evaluate the relative roles of changes in emissions and changes in climate slightly further into the future (2050) when the effects of climate change on $O_3$ should be larger and more easily detected. Fig. 18 shows the change in seasonal mean surface $O_3$ projected under the new 2050 B2 + CLE emissions scenario, relative to the year 2000. Most regions show reduced or near constant $O_3$ concentrations by 2050 due to lower future emissions, with improved air quality over much of the developed world. Over the North-East US in the summer, $O_3$ is reduced by up to 15 ppb. There are also substantial reductions over Europe and Japan. Ozone is generally reduced across most of the Northern Hemisphere mid-latitudes by about 5 ppb. One exception is during northern winter, when reduced $NO_x$ emissions result in higher $O_3$ levels over Europe and North America. This is due to the reduced titration of $O_3$ by NO. In some parts of Asia and Africa where there is very little current legislation in place and where significant economic growth is projected, increases in $O_3$ of up to 3 ppb are expected.

Fig. 19 summarizes global annual mean surface $O_3$ values for the various scenarios and time horizons considered in the Royal Society study (Royal Society, 2008), the ACCENT PhotoComp study (Dentener et al., 2006b; Stevenson et al., 2006), and from the IPCC Third Assessment Report (Prather et al., 2003). The B + CLE and, in particular, the B2 + MFR scenarios represent relatively successful futures in terms of emissions control policies. The A2 scenario represents a policy fail situation which demonstrates that background $O_3$ levels will increase through the next century if $NO_x$, $CH_4$, CO and NMVOC emissions rise (Prather et al., 2003) and control legislation is not implemented. This is illustrated by the potential range of $O_3$ values in 2100 given in Fig. 19 and represents the response of surface $O_3$ to the full range of IPCC SRES scenarios, as estimated by Prather et al. (2003). The high end of this range represents scenarios with very high emissions of $O_3$ precursors, such as A2 and A1FI. Conversely, the low end represents the more optimistic SRES scenarios, such as B1 and A1 T. Note that the IPCC considered each scenario equally likely.

There have been several recent regional modeling studies which considered future $O_3$ levels over Europe (Langner et al., 2005, Szopa et al., 2006, Van Loon et al., 2006, Vautard et al., 2006), over N. America (Hogrefe et al., 2004, Tagaris et al., 2007; Wu et al., 2008a), and over E. Asia (Yamaji et al., 2008). The regional studies together with the global model results presented above which provide regional information albeit on a coarse horizontal resolution (~200 km), demonstrate that future changes in surface $O_3$ will be spatially heterogeneous, with different drivers in different regions and seasons.

Several studies show that enhanced hemispheric background $O_3$ in the coming decades will potentially offset efforts to improve regional air quality via reductions in ozone precursor emissions (Collins et al., 2000; Bergin et al., 2005; Dentener et al., 2005; Derwent et al., 2006; Keating et al., 2004; Solberg et al., 2005; Szopa et al., 2006; Yienger et al., 2000). Control of emissions on a global scale is needed.

#### 4.2.2. *Projections of OH and $CH_4$*

Over a long time horizon (a period of several decades) methane trends might be strongly affected by changes in the OH distribution. In a coupled climate–chemistry model simulation, Stevenson et al. (2005) found that the expected increase in temperature will increase humidity and result therefore in an increased OH abundance in 2030. The increasing oxidation from enhanced OH will increase aerosol formation and concentration, leading to dominantly negative climate–chemistry feedbacks (less $O_3$, more OH, a shorter $CH_4$ lifetime, and more aerosols). This is also in

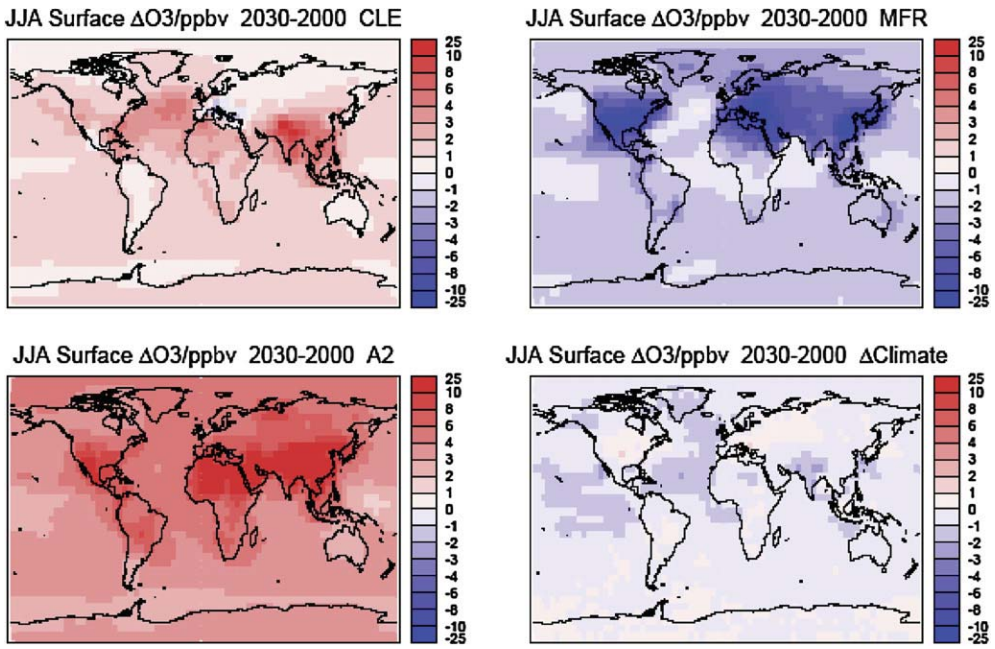


**Fig. 17.** The mean change in surface $O_3$ (ppb) between 2000–2030 for the period June-July-August (JJA) from the ACCENT PhotoComp study (Dentener et al., 2006a; Stevenson et al., 2006). The top left panel shows the mean change in surface $O_3$ under the B2 + CLE scenario; the top right panel under the B2 + MFR scenario; and the bottom left under the A2 scenario. The bottom right panel shows the mean change in surface $O_3$ due to climate change. The results presented are the ensemble mean of 26 models.

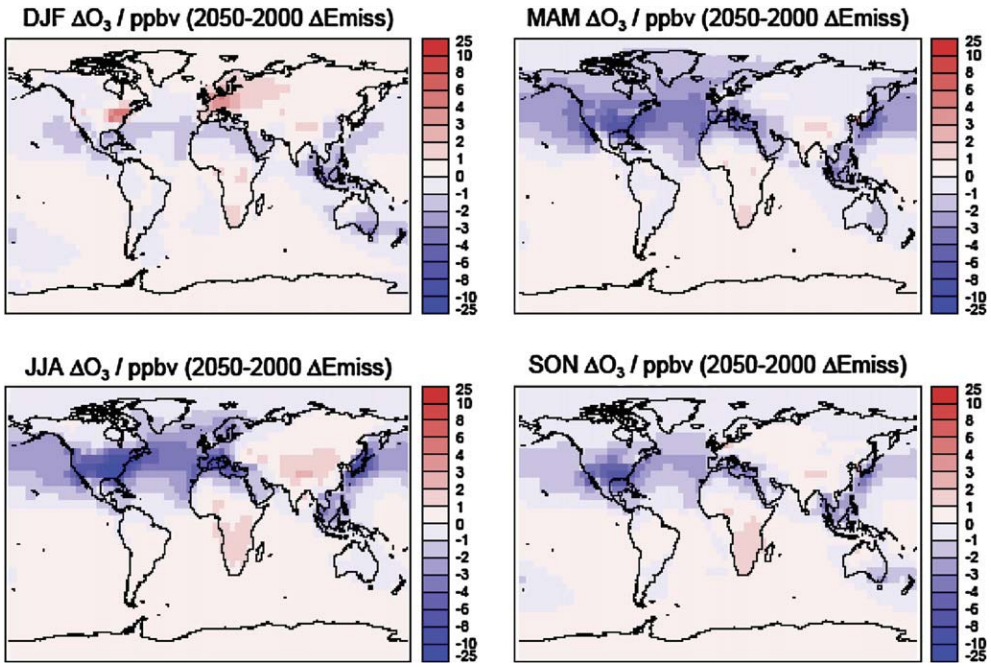


**Fig. 18.** Projected change in surface $O_3$ for the four seasons between 2000 and 2050 due to changes in emissions following the IIASA B2 + CLE 2050 scenario. Top left panel: changes in surface $O_3$ for December, January, February (DJF). Top right panel: March, April, May (MAM). Bottom left: June, July, August (JJA). Bottom right: September, October, November (SON). The results presented are the ensemble mean of 5 models (Royal Society, 2008).

accordance with the CCM study of Lamarque et al. (2005), predicting a warmer and moister climate with a higher OH abundance under reduced aerosol (precursor) emissions. Note that production of secondary organic aerosols by ozone, which is not included, could alter these results. However, since $O_3$ is driving the production of secondary biogenic volatile organics it is unclear what the overall effect will be.

Future projections of $CH_4$ depend on the evolution of its sources and sinks. Estimates of anthropogenic $CH_4$ sources are available for a range of future scenarios (Nakicenovic et al., 2000). $CH_4$ has also significant natural sources. Some of these (in particular, wetlands) are strongly linked to climate change (Gedney et al., 2004; Shindell et al., 2004).

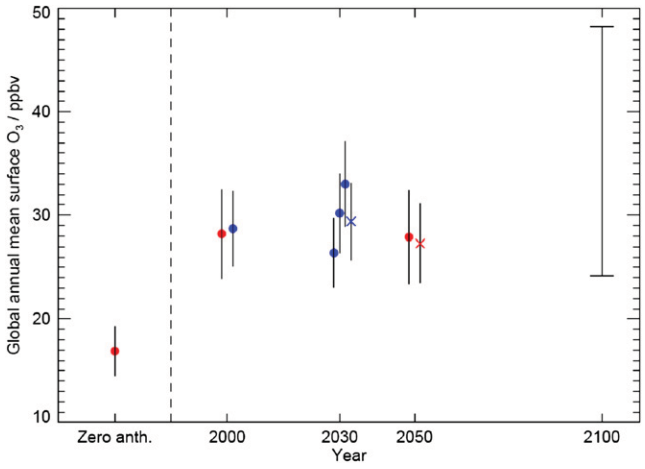


**Fig. 19.** Multi-model global annual mean surface ozone (ppb) for various scenarios from Royal Society (2008); (red symbols) and the ACCENT PhotoComp study (blue symbols). The bars indicate inter-model standard deviations. The three blue dots for 2030 are the B2 + MFR (lowest value), B2 + CLE and A2 (highest value) scenarios. The crosses are model results simulated with a future climate, as well as a future emissions scenario (the 2030 emissions scenario is the central one: B2 + CLE). These show a small negative impact of climate change on global annual mean surface $O_3$ (see Section 5.2.2). All other model simulations used a year 2000 climate. The bar shown for 2100 is the estimated range of $O_3$ responses to the full range of SRES scenarios, as reported by Prather et al. (2003) (from Royal Society, 2008; their Fig. 5.5).

A study by Stevenson et al. (2005) for the period 1990–2030 following the B2 + CLE emissions scenario, with the climate forced by the IS92a scenario showed a $CH_4$ growth to 2088 ppb in 2030 when climate change was not considered, but only a growth to 2012 ppb when it was included. Dentener et al. (2005) additionally report that using the same modeling set-up, $CH_4$ levels in 2030 were 1760 ppb for the B2 + MFR scenario (unchanged from 2000). These values, together with the A2 value from IPCC TAR (2163 ppb), were used as boundary conditions in the ACCENT PhotoComp 2030 scenarios (Stevenson et al., 2006). Stevenson et al. (2006) showed that the $CH_4$ lifetime under different 2030 scenarios responded in generally similar ways across 21 different models (Fig. 20). The results (from 10 models) all indicate that climate change will lead to a reduction of $CH_4$ lifetime. However, the absolute value for the $CH_4$ lifetime is more variable between models, which will have a significant bearing on the future evolution of $CH_4$.

### 4.3. Aerosol distribution and interaction

#### 4.3.1. Aerosol trends

Deep ice core drillings allow the identification of pre-industrial concentration levels of key aerosol components. The anthropogenic enhancement of these concentrations in the most recent snow deposits as compared to the preindustrial levels, which are significant for the main aerosol components, can be regarded as the minimum perturbation of aerosol levels in the atmosphere. The perturbation of the average global atmosphere is likely to be larger since glaciers are located far from major anthropogenic source regions and thus reflects the diluted state of the perturbed atmosphere.

Sulfate concentration levels increased from preindustrial levels by a factor of about 4 in 1980 at Greenland and the Canadian Arctic (Legrand et al., 1997; Goto-Azuma and Koerner, 2001). Ice cores in the Alps show larger increases due to the proximity of the European

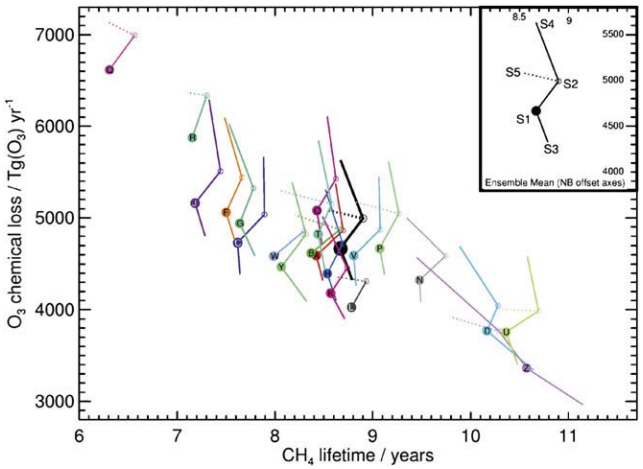


**Fig. 20.** Response of global $CH_4$ lifetime to various scenarios across 21 models (S1 = 2000; S2 = 2030 B2 + CLE; S3 = 2030 B2 + MFR; S4 = 2030 A2; S5 = 2030 B2 + CLE + climate change) (From Stevenson et al. (2006)).

sources. Nitrate levels in the Arctic from anthropogenic emissions have increased by a factor of 2–3 between 1950 and the 1980's (Goto-Azuma and Koerner, 2001). Ice core observations show that current BC levels exceed the 18th century levels by a factor 2 (McConnell et al., 2007).

Systematic surface measurements of in-situ aerosol properties such as aerosol extinction, absorption, aerosol composition and concentration and wet deposition have been analysis of recent trend. Quinn et al. (2007) report recent trends in aerosol sulfate at Alert, Alaska which show a significant decrease from 1982 to 2004. Peak black carbon levels at the same location decreased between 1990 and 2000, while absorption at Barrow shows almost no trend between 1990 and 2005.

Major technology developments are expected to lead to a shift in future emissions with a larger fraction emitted in tropical regions with higher levels of black carbon, primary organic particles and organic aerosol precursors and aerosol loads (Ramanathan and Carmichael, 2008).

### 4.3.2. Comparisons of aerosols and their precursors

Surface networks from which we can infer information about the global tropospheric distribution of aerosols make use of a diverse set of instruments with subsequent chemical analysis and mass weighting procedures (see Laj et al., 2009). The diversity of the instruments and the spatially unbalanced global distribution of sites with aerosol instrumentation have made satellite retrieved aerosol distributions a major source of information when it comes to describing the global distribution of aerosols. Calibration and precision of the satellite retrieved aerosol optical depth have improved over time with an important increase of available data over land and sea since the late 90's with the launch of satellite instruments such as POLDER, MODIS, MISR and CALIOP. Confidence in their products has been established through the synchronous deployment of ground-based sun photometers (AERONET, GAW, SKYNET, PHOTONS) and lidar systems (EARLINET, MPLNET). Note that the optical instruments can only retrieve the bulk property of column aerosol optical depth or extinction profiles which is ambiguous with respect to underlying aerosol composition and size. Intensive in-situ measurements of chemico-physical properties of the aerosol are being frequently used to interpret remote sensing products. The performance of state of the art global aerosol models and other satellites against the bulk aerosol optical depth derived from the satellite MODIS are shown in the Taylor diagram in Fig. 21. Considerable scatter of performance can be observed, while the median model outperforms individual models and some other satellite retrievals. Efforts continue in AEROCOM to understand the differences and hence uncertainty in simulated aerosol optical properties. For details about the comparisons, see Kinne et al. (2006) and Textor et al. (2006).

### 4.3.3. Diversity of simulated aerosol loads

Simulation of the global aerosol distributions suggest that the major contributors to global aerosol mass are dust and sea salt. Anthropogenic emissions contribute to the formation of secondary aerosol components such as sulfate, organic matter, soot and nitrate. Fig. 22 depicts the global simulated mass distributions for the major aerosol components, given as a median from nine models participating in the AeroCom project (Schulz et al., 2006). Note that the creation of a median model smoothes the distribution. Due to their short atmospheric life-time global particle distribution can be linked to the major source regions. From the distribution patterns of the different aerosol components, one can also infer considerable spatial variability in the aerosol composition.

Within the aerosol model inter-comparison initiative AeroCom, a large range of parameters have been incorporated, including those related to the mass balance, to optical properties and to the radiative forcing (see for further details http://nansen.ipsl.jussieu.fr/AEROCOM). The initial documentation showed significant and large diversity for almost all investigated parameters (Textor et al., 2006, Kinne et al., 2006 and Schulz et al., 2006. It is hard to explain the differences found in mass burdens and optical properties (Textor et al., 2007). As an example of these findings, Fig. 23 illustrates the global mass fraction of aerosol found above 5 km altitude in the AeroCom models in different experiments. The five major aerosol

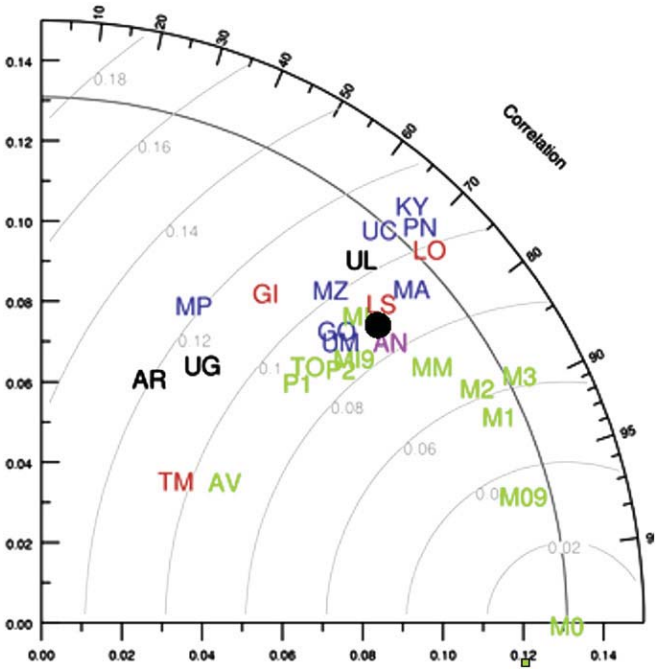


**Fig. 21.** Taylor plot exhibiting AOD standard deviation ($x$ & $y$ axis) and correlation (angular component), showing year 2000 performance of 16 AeroCom A models (blue and red symbols: higher and lower resolution CTM's or nudged GCMs, black symbols: not nudged GCMs) against 12 months (April 2000–March 2001) of MODIS satellite derived aerosol optical depth at 550 nm. Shown is also the performance of other satellite data sets (green symbols: Polder 1 and 2, AVHRR, TOMS MISR and Modis from other years). The black ball represents the behaviour of the AeroCom median model constructed from the 16 AeroCom A model results. Data correspond to model results documented in Textor et al. (2006) and Kinne et al. (2006).

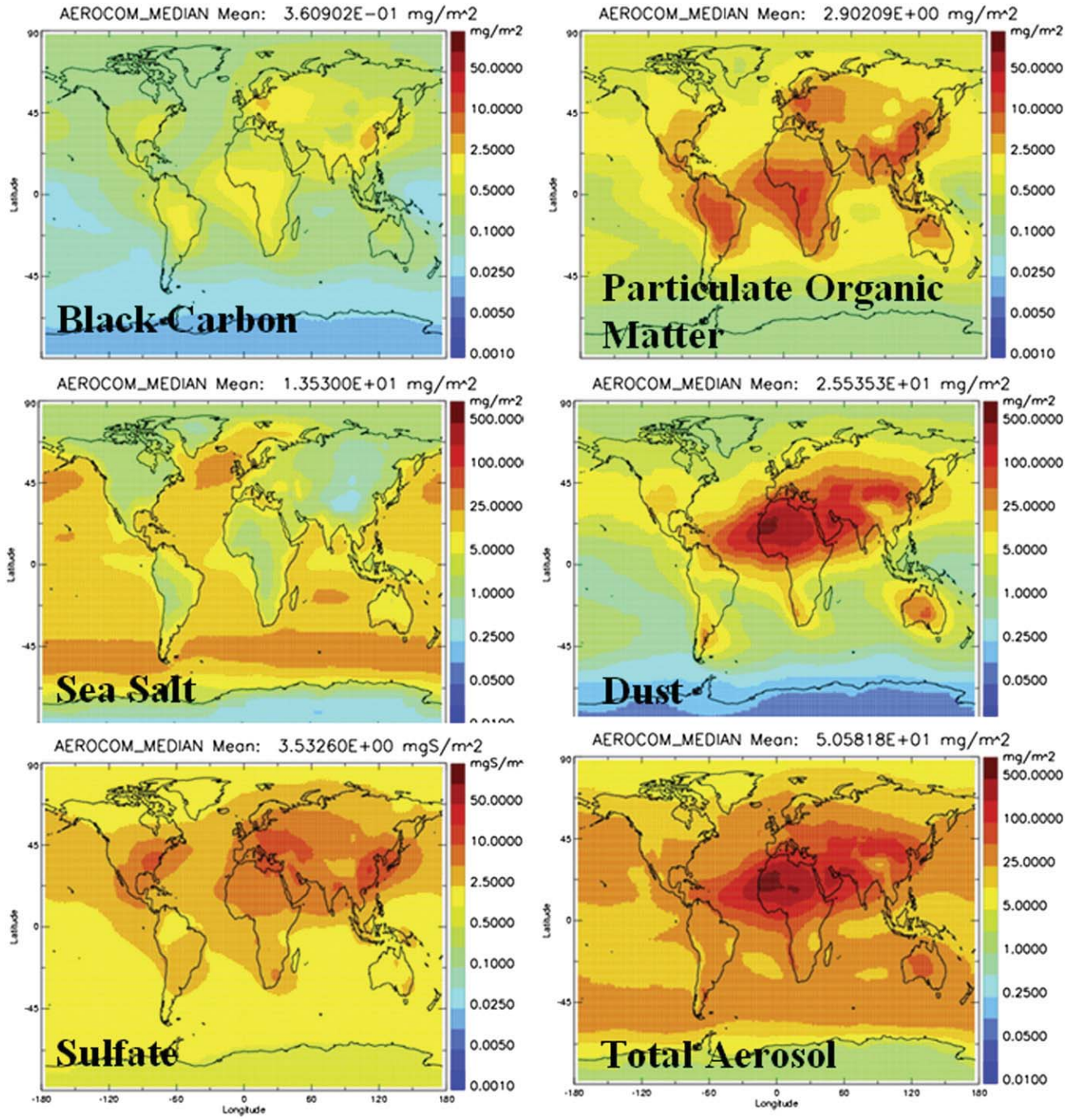


**Fig. 22.** Aerosol distribution of major components derived from the AeroCom B simulations (see models in Schulz et al, 2006) of year 2000. Shown is the median model constructed from the modeled distributions of 9 aerosol transport models.

components are depicted to show differences between the aerosol species. High fractions of sulfate mass above 5 km as compared to total column sulfate are found in all models and point to the slow production of aerosol sulfate in clouds and via OH oxidation. Surface emissions of relative coarse sea salt and dust aerosol particles translate into a relatively small sea salt and dust mass fraction in the upper troposphere. The mass fractions for the different model experiments of the same model are shown side by side to illustrate the impact of changing emissions on the vertical distribution.

The diversity among models and the resemblance among model experiments from a given model as documented by Fig. 23 with respect to the average vertical transport have led to several important conclusions: The current global models exhibit significant and important differences in the vertical mixing of aerosol mass. The way different species are affected by vertical mixing processes is varying from model to model. The experiment with harmonized emissions reveals that the internal structure of any aerosol model was by far more important for the vertical mixing and aerosol composition than the variations in spatial and temporal emissions imposed through AeroCom. The larger diversity in black carbon export from continental scale regions compared to that of carbon monoxide could be linked to the uncertainty in wet removal

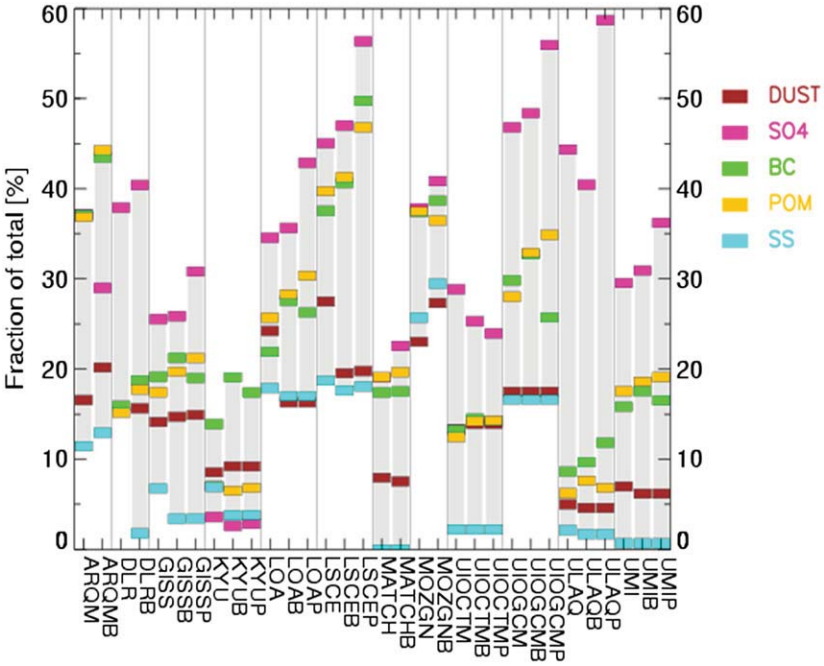


**Fig. 23.** Aerosol compound mass fraction found above 5 km altitude on global average. AeroCom A (original model state), B (present-day prescribed emissions) and P (preindustrial prescribed emissions) experiments are shown if available. Model names for experiments B and P are expanded by experiment abbreviation.

and thus long-range transport of aerosols (Shindell et al., 2008a,b). Other processes have been emphasized recently as possible source of diversity, such as humidity growth (Bian et al., 2009), meteorological drivers (Liu et al., 2007) and different aerosol compositions (Myhre et al., 2009). In general the recent works support the idea that differences in radiative forcing originate from different model constructions.

AeroCom comparisons documented considerable differences with respect to parameterization of several processes, including pole-ward transport, aerosol water mass, the split between large scale and convective scavenging, absorption of visible light, secondary sulfate formation, and radiative forcing related parameters. How these are couplings are achieved will have considerably impact on studies of aerosol-climate feedbacks (see eg Carslaw et al., 2009). It is clear that a systematic comparisons with observations, and more thorough analysis of the model structures is needed to reduce the differences in the future.

### 4.4. Observed brightening and dimming trends over the last 40 years

The major anthropogenic impact on climate occurs through a modification of the Earth's radiation balance by changing the amount of greenhouse gases and aerosol in the atmosphere. The amount of solar radiation reaching the Earth's surface is thereby particularly important as it provides the primary source of energy for life on the planet and states a major component of the surface energy balance, which governs the thermal and hydrological conditions at the Earth's surface.

Observational and modeling studies emerging in the past two decades suggest that surface solar radiation (SSR) is not necessary constant on decadal timescales as often assumed for simplicity, but shows substantial decadal variations. Largely unnoticed over a decade or more, this evidence recently gained a rapid growth of attention under the popular expressions "global dimming" and "brightening", which refer to a decadal decrease and increase in surface solar radiation, respectively.

Extensive measurements began in the late 1950s during the International Geophysical Year (IGY) in 1957/58. Many of these historic radiation measurements have been collected in the Global Energy Balance Archive (GEBA, Gilgen et al., 1998) at ETH Zurich and in the World Radiation Data Centre (WRDC) of the Main Geophysical Observatory St. Petersburg. In addition, more recently, high quality surface radiation measurements, such as those from the Baseline Surface Radiation Network (BSRN, Ohmura et al. 1998) and from the Atmospheric Radiation Measurement Program (ARM) have become available. These networks measure surface radiative fluxes at the highest possible accuracy with well-defined and calibrated state-of-the-art instrumentation at selected worldwide selected sites.

#### 4.4.1. Surface solar dimming from the 1960s to the 1980s

Changes in solar radiation from the beginning of worldwide measurements in the early 1960s until 1990 have been analyzed in numerous studies (e.g., Ohmura and Lang, 1989; Gilgen et al., 1998; Stanhill and Cohen, 2001 and references therein; Liepert, 2002; Wild, et al., 2004; Wild, 2009 and references therein). These studies report a general decrease of solar radiation at widespread locations over land surfaces between 1960 and 1990. This phenomenon is now popularly known as "global dimming". Fig. 24 shows the change in global dimming since 1950 for different locations.

Increasing air pollution and associated increase in aerosol concentrations are considered a major cause of the measured decline of surface solar radiation (e.g., Stanhill and Cohen, 2001). Changes in cloud amount and optical properties have also been proposed to contribute to the dimming (e.g., Liepert, 2002). Norris and Wild (2007) differentiate between aerosol and cloud impact on radiative changes over Europe. They show that changes in cloud amount cannot explain the changes in surface insolation, pointing to the aerosol direct and indirect effects as major cause of these variations. Alpert et al. (2005) found that the decline in surface solar radiation in the 1960 to 1990 period is particularly large in areas with dense population, which also suggests a significant anthropogenic influence through air pollution and aerosols. Several studies (e.g., Dutton et al. 2006) noted a dimming over the 1960 to 1990 period at

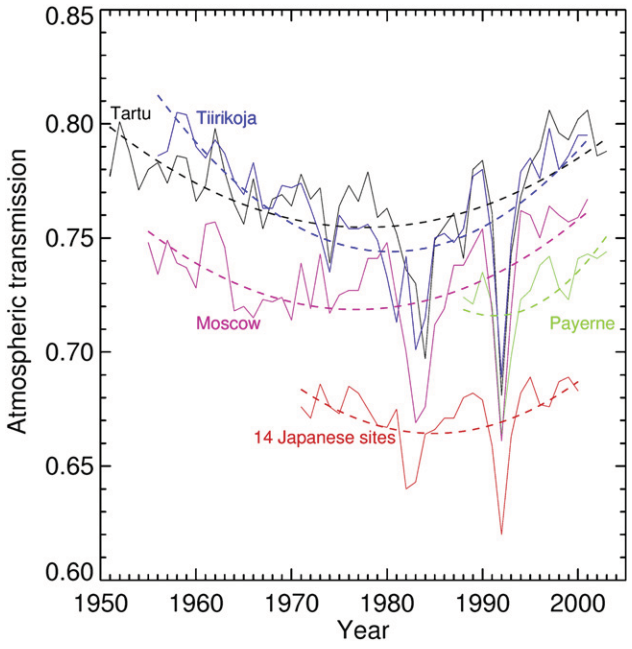


**Fig. 24.** Time series of annual mean atmospheric transmission under cloud free conditions determined from pyrheliometer measurements at various sites in Russia (Moscow), Estonia (Tartu–Toravere and Tiirikoja, Switzerland (Payerne) and Japan (average of 14 site, from Wild et al. 2005).

remote sites, suggesting that the phenomenon is not of purely local nature and air pollution may have far-reaching effects.

*4.4.2. Surface solar brightening from 1980s to present*

The studies on global dimming were all limited to data prior to 1990. ETH Zurich recently undertook a major effort to update the worldwide measured surface radiation data in GEBA for the period from 1990 to present. Wild et al. (2005) evaluated the newly available surface observational records in GEBA and BSRN to investigate the trends in surface solar radiation in the more recent years. This analysis showed that the decline in solar radiation at land surfaces seen in earlier data is no longer visible in the 1990s. Instead, the decline leveled off or even turned into a brightening since the mid 1980s at the majority of observation sites. This brightening is not just found under all sky conditions, but also under clear skies, pointing to aerosol as major cause of this trend reversal (Wild et al. 2005, Norris and Wild 2007). The trend reversal is reconcilable with recently estimated radiation trends derived from independent methods, such as satellite derived estimates and the independent Earthshine method (Pinker et al. 2005, Hatzianastassiou et al. 2005, Pallé et al., 2005). The transition from decreasing to increasing solar radiation is in line with a similar shift in atmospheric clear sky transmission determined from pyrheliometer measurements at a number of sites (Fig. 24).

In addition to the strong signals of major volcanic eruptions (such as Pinatubo and El Chichon), a general tendency of decreasing atmospheric transparency up to the early 1980s and a gradual recovery thereafter were found (Wild et al., 2005). The transition from dimming to brightening is also in line with changes in aerosol and aerosol precursor emissions derived from historic emission inventories, which also show a distinct trend reversal during the 1980s, particularly in the industrialized regions (Streets et al., 2006b). The documented trend reversal in aerosol emission towards a reduction and the associated increasing atmospheric transmission since the mid 1980s may be related to air pollution regulations and the breakdown of the economy in Eastern European countries (Wild et al., 2005; Streets et al,. 2006a). The observed reduction of black carbon and sulfur aerosol measured in the Canadian Arctic during the 1990s is likely related to the decreased emissions in Europe and the Former Soviet Union (Sharma et al. 2004). Since 1990, a reduction of aerosol optical depth over the world oceans was inferred from satellite data by Mishchenko et al. (2007). This fits well to the general picture of a widespread transition from dimming to brightening seen in the surface radiation observations at the same time.

*4.4.3. Impact of dimming and brightening on the climate system*

A growing number of studies provide evidence that the variations in surface solar radiation have a considerable impact on the climate system. Wild et al. (2007) investigated the impact of dimming and brightening on global warming. They present evidence that surface solar dimming was effective in masking and suppressing greenhouse warming, but only up to the mid-1980s, when dimming gradually transformed into brightening. Since then, the uncovered greenhouse effect reveals its full dimension, as manifested in a rapid temperature rise (+0.38 °C/decade over land since mid-1980s). Impacts of the global dimming and brightening transition can be further be seen in glaciers and snow cover retreats as well as an intensification of the hydrological cycle, which became evident as soon as the dimming disappeared in the 1990s (Wild, 2009).

Ramanathan and Carmichael (2008) estimate a reduced surface solar radiation of 1.7 W m$^{-2}$ due to BC. When including scattering aerosols and the indirect aerosol effect, a reduced surface radiation of 4.4 W m$^{-2}$ has been estimated. Global aerosol models produce weaker changes in the surface radiation (Schulz et al., 2006) than the observational based method used in Ramanathan and Carmichael (2008). Kvalevåg and Myhre (2007) show that other components such as gases and contrails (direct and indirect effect) contribute to the reduced surface solar radiation. It is further shown that the reduction in surface solar radiation calculated by models occurs mostly in industrialized regions, which could explain a large part of the observed dimming.

## 5. Climate impact from emission changes

This section describes the climate effects related to the changes in atmospheric constituents, including comparisons between the components of the system and how to define the metrics for mitigation purposes. Although various climate effects of aerosols and greenhouse gases are discussed, focus will be on the atmospheric components discussed in the previous chapters. Changes in land surface properties are not considered here.

The use of the radiative forcing concept is the most common way to compare the impact leading to climate change. This concept is used because surface temperature changes from GCMs are clearly model dependent (Hansen et al., 1997; Shine et al., 2003). The radiative forcing (RF) is defined as the net change in the irradiance (solar and terrestrial) at the tropopause after allowing the temperature in the stratosphere to adjust to radiative equilibrium (Forster et al., 2007). The surface and tropospheric temperatures are held fixed according to the definition and considered as a response. The impact of the temperature changes on water vapor and clouds, is for example considered as feedback.

For some of the aerosol effects the RF concept is particularly challenging. This is illustrated in Fig. 25 showing some of the main atmospheric aerosol effects. The direct aerosol effect and cloud albedo effect can be calculated in a way where only the aerosol abundance and cloud droplet sizes change, according to the radiative forcing concept. In the case of the semi-direct aerosol effect and the cloud lifetime effect (see Section 5.4), the calculation is much more

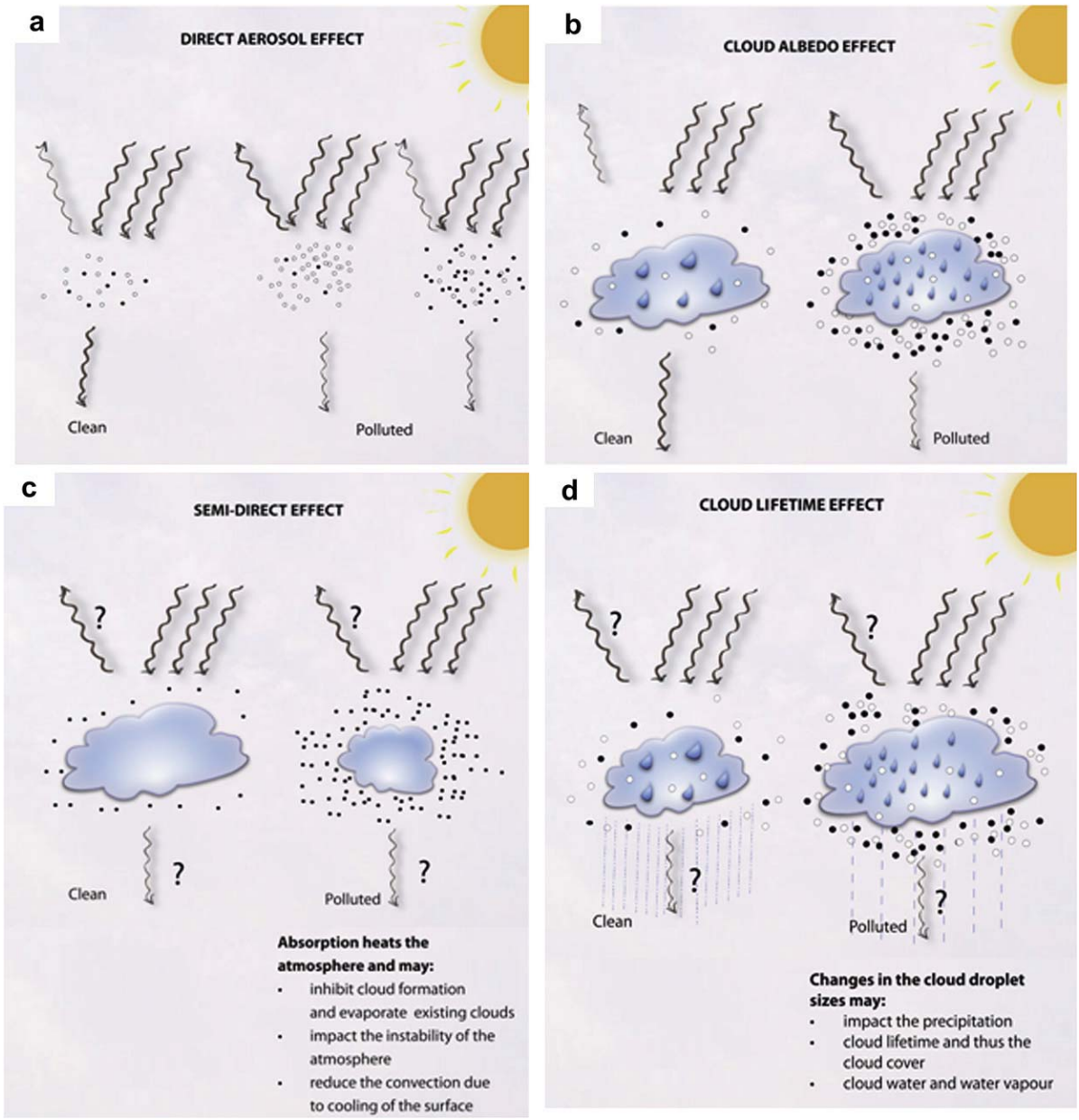


**Fig. 25.** Illustrations of the a) direct aerosol effect (with both anthropogenic scattering and absorbing aerosols), b) cloud albedo effect, c) semi-direct aerosol effect, d) and cloud lifetime effect d). Black circles represent absorbing aerosols and open circles represent scattering aerosols.

complex since not only atmospheric concentrations change, but cloud distribution and properties, water vapor abundance, and lapse rate as well as other factors may change. The uncertainties in the quantification of the semi-direct effect and the cloud lifetime effect were the reason why only the direct aerosol and the cloud albedo effect was quantified as radiative forcing mechanisms in IPCC AR4 (Forster et al., 2007). In this paper the semi-direct and the cloud lifetime are treated as radiative forcing mechanisms and a quantification of these based on available research is attempted.

The applicability of the radiative forcing concept is that the climate sensitivity relating surface temperature change, as proportional to the radiative forcing is similar for various climate forcing mechanisms. The climate efficacy has been defined as the climate sensitivity of a climate forcing mechanism divided by the climate sensitivity for $CO_2$ (Hansen et al., 2004; Hansen et al., 2005; Joshi et al., 2003). For most climate forcing mechanisms the climate efficacy is close to unity (mostly in the range 0.8–1.2) (Forster et al., 2007). The largest deviations from unity of the climate efficacy are found for idealized experiments on black carbon (Cook and Highwood, 2004; Hansen et al., 1997; Hansen et al., 2005) which is related to semi-direct effects. When considering the BC impact on surface albedo of snow and ice, a high climate efficacy is found (Flanner et al., 2007; Hansen et al., 2004).

### 5.1. Radiative forcing from gases

#### 5.1.1. Well-mixed greenhouse gases

The total RF due to the well-mixed greenhouse gases (WMGG) in 2005 relative to 1750 is 2.63 W $m^{-2}$ (Forster et al., 2007). Fig. 26 shows the percentage contribution of the RF due to $CO_2$ and other WMGG compared to the total RF from WMGG for two past period (preindustrial to current, 1998–2005) and the future. Estimates for

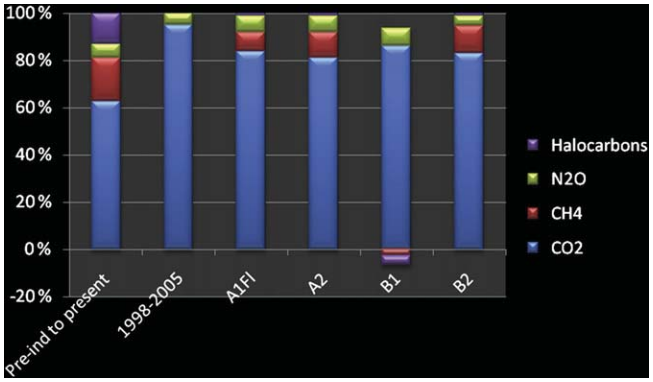


**Fig. 26.** Percentage contribution of the RF from $CO_2$, $CH_4$, N2O, and halocarbons to the total RF for 2 past time periods and 4 future SRES scenarios. The future scenarios are calculated for the time period 2000 to 2100. All values are taken from Forster et al. 2007 with regard to past changes and IPCC (2001) for the future.

4 IPCC SRES scenarios represent the future (2000–2100). The high contribution of $CO_2$ to the total WMGG RF in the future is evident even in the B1 scenario with a smallest $CO_2$ increase.

Total RF is expected to increase strongly during the 21st century. $CO_2$ is expected to be the dominating contributor to the total WMGG RF also in the future. The average global $CO_2$ concentration has increased to 384 ppm in 2007 and the RF is increasing at a rate higher than 0.03 W m$^{-2}$ yr$^{-1}$. It is worth to note that the RF due to $CO_2$ accounts for 63% of the total RF from WMGG over the industrial period. However, over the 1998 to 2005 time period, the increase of 0.2 W m$^{-2}$ in the RF of $CO_2$ is the same as the increase in the total WMGG RF (Forster et al., 2007).

The increased methane burden has contributed to about 20% of the anthropogenic climate forcing by greenhouse gases since the pre-industrial era ($0.48 \pm 0.05$ W m$^{-2}$; IPCC, 2007). An emission-based assessment of the climate forcing of methane (Shindell et al., 2005) showed that methane emissions are responsible for most of the increase in global tropospheric ozone, with minor contributions attributed to the increase of CO, VOC and $NO_x$ emissions. From this estimate the combined methane and tropospheric ozone forcing is about 0.8 W m$^{-2}$, almost half of the present-day $CO_2$ forcing of 1.66 W m$^{-2}$. Although the methane concentration increased between 2006 and 2007 by 0.63%, this had a small impact on the RF.

Currently CFC-12 has the highest RF among the CFCs and has the third highest RF of the WMGG (after $CO_2$ and $CH_4$). The RF due to $N_2O$ has been steadily increasing (Forster et al., 2007) and, as a result of more intensive agricultural practice, may enhance its growth. Since the CFC-12 concentration has leveled out the last years and is expected to decrease in the future the RF due $N_2O$ is expected to soon be the third largest among the WMGG.

The future IPCC scenarios show a spread of more than a factor of five for anthropogenic $CO_2$ emissions; in addition the impact of future warming on the carbon cycle is uncertain. This indicates large uncertainties in concentration changes (Friedlingstein et al., 2006; IPCC, 2007). A further uncertainty is caused by a recent suggestion that increased ozone may reduce the vegetation uptake of $CO_2$ (Sitch et al., 2007). Additionally, global dimming and changes in the direct and diffuse solar radiation at the surface may impact the vegetation and thus the $CO_2$ uptake (Mercado et al., 2009). Human activity has strongly altered the direct and diffuse solar radiation at the surface (Kvalevåg and Myhre, 2007; Mercado et al., 2009, see also Section 4.4).

### 5.1.2. Water vapor

Water vapor trends are significant in the troposphere (IPCC, 2007); they represent a feedback to the climate system). IPCC (2007) suggests an increase of 1.2%/decade for the 1988–2004 period, and an increase of the of the order of 5% over the 20th century. As an illustration, Boucher et al. (2004) estimate a forcing of 1.5 W m$^{-2}$ per 1% increase in the current water vapor content.

Direct human influence on water vapor is linked also to human practices such as through irrigation (Boucher et al., 2004) as well as to change in vegetation (Forster et al., 2007). However, these water vapor changes are small and difficult to quantify since they involve feedback mechanisms through perturbations of the hydrological cycle (Forster et al., 2007).

The trend in the stratospheric water vapor content is highly uncertain (Randel et al., 2006; Scherer et al., 2008) and its origin is not well established. A direct human influence on stratospheric water vapor originates from the water vapor emitted by aircraft and by the oxidation of increasing $CH_4$ in the stratosphere. The radiative forcing due to stratospheric water vapor increase from $CH_4$ oxidation has been estimated using two independent approaches by Hansen et al. (2005) and Myhre et al. (2007a). Calculated values of 0.07 and 0.08 W m$^{-2}$, are obtained respectively. The contribution of the stratospheric water from aircraft exhaust is very small (Sausen et al., 2005), but may be non-negligible in the future (Søvde et al., 2007).

### 5.1.3. Ozone

Within an ACCENT network study Gauss et al. (2006) applied ten global chemistry models to evaluate RF from ozone changes since pre-industrial time. The range of RF due to tropospheric ozone changes obtained by the different models is almost a factor of two. For stratospheric ozone changes, the sign of the RF varied among the models. The differences in RF due to tropospheric ozone changes were explained by significant differences in the calculated column tropospheric ozone changes (Gauss et al., 2006). Differences in the RF from stratospheric ozone change result mainly from differences in the vertical profile of ozone in the tropics (Forster and Shine, 1997; Hansen et al., 1997). The crossover altitude from an increase of ozone in the troposphere to a reduction in the stratosphere varies among the different models, from a level close to the tropical tropopause to about 25 km (Gauss et al., 2006). This crossover altitude depends on the increase in the ozone amount in the upper troposphere and the transport to the stratosphere. The causes to the differences in the ozone change between the models in the upper troposphere are mainly a result of applying different chemical schemes and parameterizations of boundary layer processes and convection (Gauss et al., 2006).

An indirect RF from ozone precursors emission, previously not accounted for, is the impact on vegetation from ozone enhancement, which has the potential to affect the carbon cycle. This indirect effect is linked to ozone damage on plants and crops resulting in smaller $CO_2$ uptake and higher atmospheric $CO_2$ abundance (Sitch et al., 2007). The indirect effect on RF from ozone through this process could be of similar magnitude as the direct RF from ozone changes (see Fig. 27 taken from Sitch et al., 2007).

### 5.1.4. $NO_2$

$NO_2$ strongly absorbs solar radiation, thereby contributing to RF. Due to its short life-time, the distribution of $NO_2$ is strongly heterogeneous with highest abundances in industrialized regions. Substantial changes in its concentrations have occurred over the past decade (Richter et al., 2005). A first estimate of RF due to $NO_2$ changes gives a value of 0.04 W m$^{-2}$ (Kvalevåg and Myhre, 2007) and is less than 2% of the total RF of the WMGG.

## 5.2. Direct aerosol effect

In the AR4 IPCC report (Forster et al., 2007) the total direct aerosol effect was quantified with a best estimate of −0.5 W m$^{-2}$,

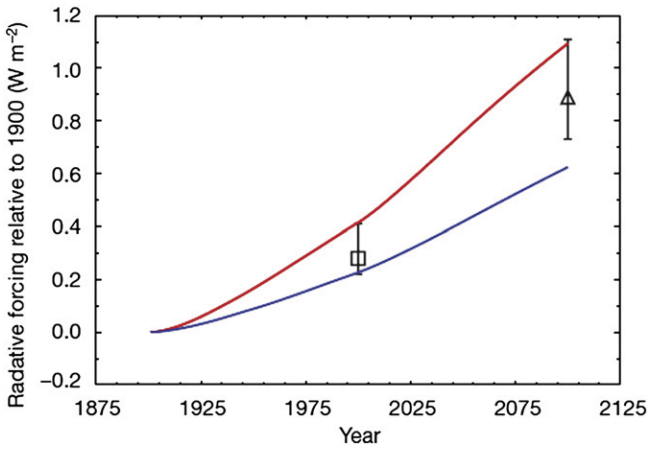


**Fig. 27.** Indirect radiative forcing due to ozone on plants affecting the $CO_2$ uptake for 'high' (red) and 'low' (blue) plant sensitivity to ozone (from Sitch et al. (2007)). Direct radiative forcing due to ozone is included as bars.

together with a rather large uncertainty range from −0.9 to −0.1 W m$^{-2}$. The large uncertainty range results from significant differences between estimates from global aerosol models (see also discussion in Section 4.3). Using a combination of models and satellite observations Myhre (2009) show that the RF due to the direct effect of aerosols is around −0.3 W m$^{-2}$, and that the uncertainty range can be halved compared to the estimate by IPCC (Forster et al., 2007). In the global aerosol inter-comparison study, AeroCom, nine models used identical emissions for calculations of RF (Schulz et al., 2006); they obtained a mean of −0.2 W m$^{-2}$ and an uncertainty range of 0.2 W m$^{-2}$. Schulz et al. (2006) summarized also some earlier model studies, which gave similar results. Studies based on observations estimate a much stronger RF for the total direct aerosol effect, with values between −0.8 and −0.5 W m$^{-2}$ (Bellouin et al., 2005; Chung et al., 2005). This section presents advances since the AR4 report in global aerosol models development, and in our understanding of the differences between model estimates and observational based studies.

*5.2.1. Recent progress in estimates of the RF*

Bellouin et al. (2008) have updated the simulation from Bellouin et al. (2005) using new satellite data and performed additional sensitivity simulations to investigate the difference between model calculations and methods based on observations. The latest version of the MODIS satellite retrieval, named Collection 5, is implemented instead of the MODIS Collection 4 used in Bellouin et al. (2005). This decreased the RF from −0.8 to −0.65 W m$^{-2}$. It was further shown that the treatment of clouds was a key cause to the difference between models (Bellouin et al., 2008). It was also shown that assumption of zero RF in cloudy region used in Bellouin et al. (2005) is questionable. In Schulz et al. (2006) the RF in cloudy region varied substantially among the global aerosol models.

Schulz et al. (2006) considered only sulfate, primary BC and OC from fossil and biomass burning as anthropogenic aerosols. Anthropogenic nitrate, secondary organic carbon (SOA), and dust were not included and these three aerosol components are all estimated to have a negative RF (Forster et al., 2007). The diversity of the RF estimates due to nitrate is large, from around −0.2 to −0.02 W m$^{-2}$ (Adams et al., 2001; Bauer et al., 2007; Jacobson, 2001; Liao and Seinfeld, 2005; Myhre et al., 2009; Myhre et al., 2006). The formation of nitrate particles is dependent on other aerosol components and precursors in a complex way and is likely the main reason for the large range in the RF due to nitrate. The formation of nitrate in the fine mode depends on the excess of ammonia and it is thus important to obtain a sufficiently low amount of sulfate to allow for the formation of ammonium nitrate. Observations show an important land – sea contrast, where fine mode nitrate dominates over land and coarse mode nitrate dominates over ocean (Putaud et al., 2004; Quinn and Bates, 2005). The size of the nitrate particles is important since coarse mode nitrate particles give a weak RF while fine mode nitrate generate a strong RF.

SOA particles were included in the Schulz et al. (2006) study, but only a natural component was considered, while the anthropogenic was not taken into contribution. Several global aerosol modeling studies of SOA have been performed (Chung and Seinfeld, 2002; Henze and Seinfeld, 2006; Hoyle et al., 2007; Tsigaridis and Kanakidou, 2003). The results show that SOA constitute a significant fraction of the total organic matter and even dominate in certain regions. Observations also show a dominance of SOA, when compared to primary organic matter in industrialized regions (Crosier et al., 2007; Gelencser et al., 2007).

As shown in Schulz et al. (2006) the spread in RF due to the direct aerosol effect among the models is substantial even though the emissions are similar. The diversity among the global aerosol models is found to be more related to the parameterizations of transport, removal chemistry, and aerosol microphysics than to the aerosol emissions used in the models (Textor et al., 2007). Substantial differences in RF were also found using a single model, with various meteorological input data (Liu et al., 2007).

*5.2.2. Atmospheric absorption by carbonaceous aerosols*

Ramanathan and Carmichael (2008) estimate that the direct aerosol effect of BC leads to a RF at the top of the atmosphere of 0.9 W m$^{-2}$ and a reduced radiation reaching the surface of 1.7 W m$^{-2}$. The estimate by Ramanathan and Carmichael (2008) is based on a method using a combination of observations, satellite retrievals, and models. It is important to note that the RF due to BC is a result of fossil fuel as well as biomass burning changes. The emission of BC from biomass burning is also associated with emissions of organic matter and the net effect of these emissions is a RF close to zero (Forster et al., 2007; Schulz et al., 2006). The RF due to BC is particularly strong in Asia (Ramanathan and Carmichael, 2008) and contributes to an enhanced solar heating rate in the atmosphere (Ramanathan et al., 2007).

The state of mixing of BC particles is important (Fuller et al., 1999; Haywood and Shine, 1995). The aerosol optical properties of BC have been quantified and better constrained by observations showing that aged BC is often coated with other aerosol components; while more fresh BC particles often are not mixed with other aerosol components (externally mixed) (Bond and Bergstrom, 2006; Bond et al., 2006). Suggestions that OC can absorb at short wavelengths in the solar spectrum (Jacobson, 1999; Dinar et al., 2008; Barnard et al., 2008; Sun et al., 2007), has not been quantified in terms of solar absorption or RF.

*5.3. Semi-direct effects of aerosols*

The degree of absorption versus scattering by aerosols depends on type and mixing state. Aerosol species that are efficient absorbers of solar radiation in the atmosphere are mainly BC, but also, to some extent, mineral dust and some organic compounds. An absorbing aerosol (e.g., soot) layer, as typically encountered in the boundary layer, may therefore lead to a substantial radiative heating in this layer and a corresponding reduction in the solar radiation reaching the surface (Kaufman et al., 2002; Ramanathan et al., 2001). The term *semi-direct aerosol effect* was first introduced by Hansen et al. (1997). They investigated the effects of radiative forcing in a global climate model (GCM) and found that the large-scale cloud cover was sensitive to the amount of absorbing aerosols

in the lowest model layers. A reduction in the low-level cloud cover corresponds to a positive radiative forcing at the top of the atmosphere (TOA), and thereby a warming of the Earth-atmosphere system.

However, the concept of absorbing aerosols influencing clouds had already been introduced by Grassl (1975). In this study, absorbing aerosols within cloud droplets and in cloudy air were found to reduce cloud albedo and heat the cloud layer. Observational support for absorbing aerosols influencing cloud cover in the Tropics was presented by Ackerman et al. (2000), as a minimum in trade cumulus cloud coverage was found in regions and seasons where clouds were typically embedded in dark haze. Ackerman et al. (2000) also presented large eddy-model (LES) simulations showing that absorbing aerosols may reduce trade cumulus cloud coverage by decreasing the boundary layer convection that drives stratocumulus formation.

This triggered a number of model studies investigating the semi-direct aerosol effect on a global scale. Some studies (Lohmann and Feichter, 2001; Jacobson, 2002; Cook and Highwood, 2004) found that absorbing aerosols decreased low-level cloud cover, in agreement with Hansen et al. (1997) and Ackerman et al. (2000), thereby reducing reflection of solar radiation and having a warming effect on the climate. Others, e.g., Menon et al. (2002) and Penner et al. (2003), found the opposite. In Menon et al. (2002) absorbing aerosols increased large-scale cloud cover. Penner et al. (2003) pointed out that the injection height of the absorbing aerosols is crucial for their effects on clouds, possibly explaining the apparently contradicting results arising from different GCM studies. The importance of the vertical structure of the absorbing aerosols for the semi-direct aerosol effect was also pointed out by Johnson et al. (2004). In LES model simulations of marine stratocumulus, they found absorbing aerosols located in the boundary layer to increase cloudiness, while the opposite was true for aerosol absorption above the clouds.

Stuber et al. (submitted for publication) performed idealized simulations with absorbing aerosols at different levels in the troposphere using two GCMs to investigate the robustness of the responses. Inclusion of absorbing aerosols in the lower part of the troposphere led to a surface warming, whereas absorbing aerosols in the middle and higher troposphere caused a surface cooling in both models. The GCM responses of absorbing aerosols clearly show changes in the local cloud distribution and water content (liquid and frozen) but also change in the instability of the troposphere. The climate sensitivity of absorbing aerosols was mostly higher than for a doubling of $CO_2$. These idealized experiments show that a realistic absorbing aerosol distribution may impact the clouds and tropospheric and surface temperature in a complex way.

Further observational support for the semi-direct aerosol effect was given by Koren et al. (2004), based on satellite observations from the MODIS instrument. Focusing on the Amazon basin they found cloud cover to be anti-correlated with smoke optical depth, and attributed this to absorption within the smoke layer, which stabilized the boundary layer and reduced the moisture fluxes from the surface. In Denman et al. (2007), the semi-direct aerosol effect was summarized to correspond to a negligible or slightly positive radiative forcing at the TOA.

In terms of radiative fluxes at the TOA, the semi-direct aerosol effect has been reported to be dominated by a more conventional aerosol effect on clouds, where aerosols acting as cloud condensation nuclei (CCN) increase cloud lifetime and coverage by delaying precipitation release (i.e. the cloud lifetime effect, see Section 6.4). However, a recent study by Koren et al. (2008) shed new light on the roles of these competing effects. Based on a theoretical framework and satellite observations from the MODIS instrument, they reported that, while the cloud lifetime effect dominates the semi-direct aerosol effect in regimes with relatively low aerosol optical depths (AODs), the opposite is true for larger AODs. AOD was in this study taken as a proxy for both CCN and the aerosol potential to absorb solar energy. The physical reason for this transition was that, while polluted clouds are relatively insensitive to further increases in CCN, there is no corresponding saturation effect for aerosol absorption, which increases steadily with aerosol loading. The study of Koren et al. (2008) uses satellite data over Amazon, but a similar pattern for the relationship between AOD and cloud cover is found in many regions in a global study using MODIS data (Myhre et al., 2007b). Koren et al. (2008) challenged the modeling community to test or incorporate this new concept in cloud-resolving or global models.

### 5.4. Aerosol indirect effects

More than three decades ago, Twomey (1974) stated the first theory on how anthropogenic aerosols may influence climate through their impact on clouds. According to this hypothesis, often called the first aerosol indirect effect, an increase in atmospheric pollution will lead to an increase in cloud albedo, everything else being equal. Since then, a number of hypotheses on how anthropogenic aerosols may influence climate through clouds were published. While some of the hypotheses have been studied extensively using models, satellite data or laboratory experiments, other hypotheses are new and controversial and have not yet been sufficiently tested.

Current suggestions for possible aerosol indirect effects are:

1) The first indirect effect or cloud albedo effect: in warm clouds, anthropogenic aerosols increase the cloud albedo by acting as cloud condensation nuclei (CCN), thereby increasing cloud droplet number concentrations and decreasing cloud droplet sizes in the case of constant liquid water content (Twomey, 1977 and Section 2.1.2).
2) The second indirect effect or cloud lifetime effect: The anthropogenic decrease in cloud droplet sizes causes a less efficient precipitation production, which could lead to increased cloud lifetimes or increased cloud horizontal and vertical extension (Albrecht, 1989).
3) The cloud glaciation effect: Ice formation in clouds at temperatures above approximately $-35\,^{\circ}C$ occurs by the aid of so-called ice nuclei (IN) (i.e. heterogeneous freezing). Such IN are typically insoluble particles with crystalline structure. Candidates are mineral dust, biological particles and soot (Pruppacher and Klett, 1997). Soot particles are largely of anthropogenic origin, so anthropogenic activity may have introduced additional IN into the atmosphere. Such an increase in IN would lead to an anthropogenic increase in freezing and cloud glaciation (e.g., Lohmann, 2002).
4) The de-activation effect: A relatively new idea is that anthropogenic sulfur coatings can potentially de-activate IN (Girard et al., 2004), or alternatively make them less efficient in mixed-phase clouds (Storelvmo et al., 2008b; Hoose et al., 2008).
5) The thermodynamic effect: As large droplets freeze more readily than small droplets (Pruppacher and Klett, 1997), the anthropogenic decrease in cloud droplet radius is expected to counteract freezing (e.g., Rosenfeld and Woodley, 2000).
6) Aerosol indirect effects on cirrus: The formation of pure ice clouds (i.e. cirrus) by homogeneous freezing of super cooled aerosols may occur at temperatures below approximately $-35\,^{\circ}C$. Although this freezing process can take place without the aid of IN, the presence of IN may delay or entirely prevent homogenous freezing, as heterogeneous freezing processes may deplete water vapor to the extent that the high super

saturation required for the onset of homogeneous freezing are not reached (e.g., DeMott et al., 1997).

Fig. 28 shows a schematic overview of how the above effects influence precipitation, cloud microphysical properties and radiation. Except from the deactivation effect, all of the above effects were discussed in IPCC AR4, (Denman et al., 2007) in light of recent publications. Rather than repeating what was already thoroughly discussed in IPCC AR4, we will here focus on aerosol indirect effects, which have recently received particular attention from the scientific community. The following sections review recent publications on aerosol indirect effects, and are further divided into sub-sections on warm and cold clouds, respectively. In Section 5.4.2, a discussion of the recent results and suggestions of future studies required for increased understanding of aerosol indirect effects, and ultimately the climate system, is given.

*5.4.1. Aerosol indirect effects associated with warm clouds*

As mentioned above, the aerosol indirect effect on warm clouds is typically divided further into the cloud albedo effect and the cloud lifetime effect. Both effects act to increase cloud albedo and cool the Earth-atmosphere system by increasing the amount of solar radiation reflected back to space. In IPCC AR4, the model estimates of radiative forcing (i.e. the perturbation to the global energy balance of the Earth/atmosphere system) associated with the cloud albedo effect range from $-0.22\ W\,m^{-2}$ to $-1.85\ W\,m^{-2}$, with a best estimate of $-0.7\ W\,m^{-2}$ (Forster et al., 2007). Low estimates are associated with model simulations using empirical relationships between aerosol mass and CDNC fitted to satellite data to estimate the cloud albedo effect (Ranging from $-0.22\ W\,m^{-2}$ to $-0.5\ W\,m^{-2}$). A recent study estimating the cloud albedo effect from satellite data alone (Quaas et al., 2008) gives an even lower estimate of $-0.2 \pm 0.1\ W\,m^{-2}$, suggesting that global models are exaggerating the effect compared to satellite measurements. Furthermore, based on ground-based remote sensing at the Southern Great Planes, Kim et al. (2008) reported that while the first aerosol indirect effect could be observed in adiabatic clouds, it was not readily observed in sub-adiabatic cases. A possible explanation is that entrainment and mixing-processes attenuate the effect. However, high uncertainties are associated not only with model estimates, but also with satellite retrievals and in-situ measurements.

McComiskey and Feingold (2008) recently demonstrated how measurements of aerosol-cloud interactions (termed ACI) differ substantially among various observational platforms, leading to radiative forcing that differ by several $W\,m^{-2}$ for the same anthropogenic aerosol perturbation in an idealized cloud case. Storelvmo et al. (2009) analyzed the cloud albedo effect in the IPCC AR4 models used for transient simulations of future climate. They found that about $1.3\ W\,m^{-2}$ of the $2\ W\,m^{-2}$ spread in estimated SW forcing for the year 2000 can be explained by the different empirical relationships between aerosol mass and CDNC used to calculate the aerosol indirect effect in the models.

The range of model estimates of the total anthropogenic aerosol effect on warm clouds (i.e. both the direct and indirect aerosol effects) range from $-0.2\ W\,m^{-2}$ to $-2.3\ W\,m^{-2}$ in IPCC AR4 (note that this range is based on a slightly different set of model studies than that of the cloud albedo effect) (Denman et al., 2007). The parameterization of auto conversion (i.e. warm-phase precipitation formation) is crucial when calculating the aerosol lifetime effect in the models. Many different parameterizations of auto conversion are available in the literature, yielding precipitation rates that differ by orders of magnitude for the same cloud liquid water content (LWC) and cloud droplet number concentration (CDNC) (e.g., Sotiropoulou et al., 2007). Consequently, an increase in CDNC caused by an anthropogenic aerosol perturbation can lead to substantially different precipitation responses, depending on the auto conversion scheme. Most, if not all, global climate model (GCM) estimates of the cloud lifetime effect predict increased cloud thicknesses and/or lifetimes as precipitation release is reduced in response to anthropogenic aerosol perturbations.

Furthermore, it has been suggested that in the presence of giant CCN (GCCN; typically large natural particles like sea salt and dust), the effect of increased CCN concentrations on precipitation release is significantly reduced (Feingold et al., 1999; Zhang et al., 2006; Cheng et al., 2007; Posselt and Lohmann, 2008). The GCCN initiate coalescence and precipitation, and thereby have the ability to trigger precipitation in otherwise non-precipitating clouds. To date, most GCM estimates of the aerosol lifetime effect have restricted themselves to warm stratiform clouds, despite several publications (e.g., Rosenfeld (1999) based on satellite data and Wang (2005) based on cloud-resolving modeling) suggesting a pronounced aerosol effect on convective clouds. Menon and Rotstayn (2006) provided the first global radiative forcing estimate of aerosol effects

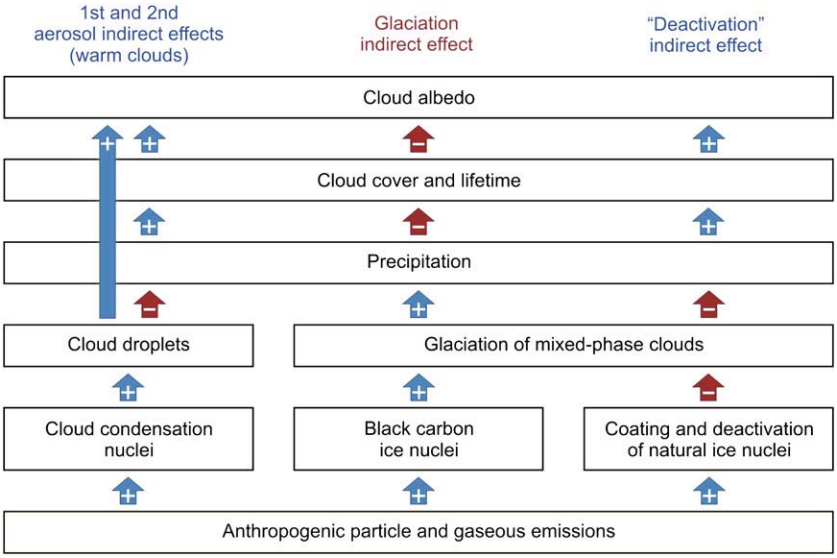


**Fig. 28.** Schematic of aerosol indirect effects on warm and mixed-phase clouds, originally published in Hoose et al. (2008).

on (warm) convective clouds, based on two GCMs (CSIRO and GISS). Whereas the CSIRO simulations suggested an enhanced total aerosol indirect effect when aerosol influences on convective clouds were included, the opposite was true for GISS simulations. Lohmann (2008) included aerosol effects on both warm and cold stratiform and convective clouds, and found a slight reduction in the total aerosol indirect effect due to aerosol influence on convective clouds.

*5.4.2. Aerosol indirect effects associated with cold clouds*

Similar to aerosol effects on convective clouds, aerosol effects on cold clouds have only very recently been included in global climate models. The first global estimate of the cloud glaciation effect was provided by Lohmann (2002), suggesting a reduced aerosol indirect effect under the extreme assumptions that IN are present in unlimited amounts compared to an atmosphere containing no IN at all. A more elaborate study of the cloud glaciation effect was presented by Lohmann and Diehl (2006), concluding that anthropogenic activity may lead to increased heterogeneous freezing and thereby influence cloud lifetime and precipitation processes, depending on the concentration and nature of the natural IN present. Mineral dust and certain primary biogenic aerosol particles (PBAPs) constitute natural IN in the atmosphere. While the impact of including realistic dust mineralogy was tested in a GCM by Hoose et al. (2008), no GCM has so far included PBAPs. Although realistic natural and anthropogenic IN concentrations are required for simulations of aerosol effects on mixed-phase clouds, the interaction of such particles with mixed-phase cloud microphysical processes like the Bergeron-Findeisen (BF) process is as important in this context. Such processes have typically been treated in a very simplistic manner in GCMs. Recent in-cloud observations from the high alpine research station Jungfraujoch (Verheggen et al. 2007) shed new light on the BF process and its interaction with aerosols. Further guidance on the BF process was given in terms of a theoretical framework presented in Korolev (2007); the implementation of this theoretical framework in a global model was found to have a strong impact on the simulated aerosol indirect effect (Storelvmo et al., 2008a).

Girard et al. (2004) were the first to test the hypothesis of IN deactivation by anthropogenic sulfate in a modeling framework, using a single column model to study arctic haze events. Assuming that sulfur coatings deactivated the IN entirely, they found pronounced impacts on precipitation rates and cloud radiative properties. A partial de-activation of IN as a result of sulfate coatings was also found in to recent modeling studies (in the ECHAM5 GCM (Hoose et al., 2008) and in the CAM-Oslo GCM (Storelvmo et al., 2008b). Rather than assuming that a sulfate coating deactivates the IN completely, both studies showed a shift of the IN from contact freezing nuclei to immersion freezing nuclei. In contact freezing mode, IN initiate freezing when colliding with cloud droplets. This freezing mechanism becomes efficient at relatively warm sub-zero temperatures, but requires insoluble IN particles. Coatings typically render IN slightly soluble, allowing them activate to form cloud droplets. Thereafter they may initiate freezing of the droplet from within (i.e. immersion freezing), but this freezing mechanism becomes efficient at lower temperatures. Although model studies have so far focused on de-activation due to sulfate coatings, other species may have the same coating effect. The fact that the efficiency of IN, such as mineral dust, may be reduced by physiochemical transformation of other aerosol species has recently been discussed in Baker and Peter (2008). In summary, the de-activation effect counteracts the cloud glaciation effect, and which effect dominates in any given case depends on the concentration of natural and anthropogenic IN, and the amount of anthropogenic material available for IN coating.

In a recent study, Penner et al. (2009) have shown that the effect on cirrus clouds of emission of anthropogenic aerosols, for instance from aircraft could have significant impact and reversing the sign of radiative forcing. Note that the results are preliminary, and further studies need to be done before conclusion can be made.

*5.4.3. Aerosol indirect effects associated with various cloud types*

A recent and comprehensive report on aerosol pollution impact on precipitation, produced by the International aerosol precipitation science assessment group (IAPSAG) (Levin and Cotton, 2007), concluded that despite the progress made in recent years, pollution effects on precipitation are not understood, neither on the scale of a local storm nor on the global scale. Obtaining observational evidence for pollution affecting precipitation release and cloud lifetimes is challenging, and recent modeling results render not only the magnitude but also the sign of this effect as highly uncertain. However, findings in recent publications suggest that the effect of increased aerosol concentrations on convective precipitation is to a large extent determined by environmental parameters like the unperturbed aerosol concentration or the relative humidity.

Fig. 29 gives an overview of the majority of global estimates of the aerosol indirect effect. Evidently, the spread in estimates has not decreased with time. On the contrary, estimates span a larger range than ever, much due to the new aerosol indirect effects recently taken into account.

### 5.5. Radiative forcing summary

In Chapter 5, new radiative forcing mechanisms are discussed and quantified, as well as the increases in WMGG concentrations affecting the RF estimates. Fig. 30 and Table 1 show estimates of the RF for seven different types of climate forcing mechanisms over the industrial era up to 2007. Only anthropogenic atmospheric compounds are included. For anthropogenic climate forcing on surface and natural climate forcing we refer to Forster et al. (2007). The WMGG dominates in terms of RF and consist of $CO_2$, $CH_4$, $N_2O$, and halocarbons. We group ozone, $NO_2$, and stratospheric water vapor into a common class of short-lived gases (SL-G). These gases have quite variable lifetimes that are too short for them to be well mixed in the atmosphere. Estimates for five groups of aerosol effects are included in Fig. 30. RF due to the direct aerosol effect and the cloud albedo effect have been estimated earlier, but separate estimates of the semi-direct aerosol effect and the cloud lifetime effect have not been provided earlier (Forster et al., 2007; Hansen et al., 2005). We also discuss here an estimate for indirect aerosol effects of mixed phase clouds.

## 6. Contributions to tropospheric changes from the transport sector and for different regions

Several recent studies on the impact of emissions from the transport sectors, in particular ship and aircraft have been performed (Eyring et al., 2009; Hoor et al., 2009; Collins et al., 2009; Dalsøren et al., 2009a). Both sectors differ from land-based sectors. A typical example of the differences is illustrated by emission from ship traffic. Ocean going ship types (e.g., bulk, oil transport, container ship) have highly different ship tracks, with different environmental impact, and highly different growth rates (Dalsøren et al., 2009a). Furthermore, the climate impact from the different transport sectors is different, which makes it necessary to treat sectors individually.

Ships and aircraft have so far not been affected by international policy measures to reduce emissions. Understanding and quantifying the impact of ship emissions is particularly challenging since

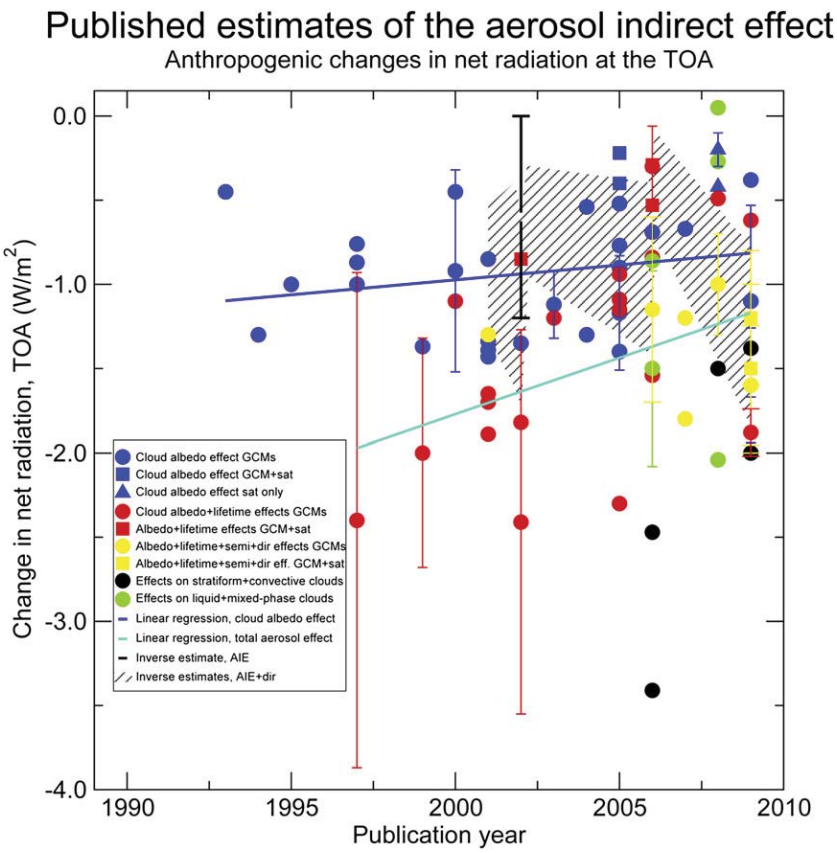


**Fig. 29.** Model and satellite estimates of the aerosol indirect effects over the last two decades. Blue represents estimates of the first AIE from GCMs (circles), GCMs combined with satellite measurements (triangles) and satellite only (square). Red represents estimates of both the first and second AIE from GCMs (circles) and GCMs combined with satellite estimates (triangles). The yellow circle represents an estimate of the first and second aerosol indirect effects, the direct and semi-direct effects. Green circles represent estimates of the first and second indirect aerosol effects on mixed-phase clouds, and black circles represent the first and second AIE on both stratiform and mixed-phase clouds.

the associated composition changes lead to large positive and negative global climate forcings.

Recent regional differences in $NO_x$ emissions play a significant role in the atmospheric oxidation process and on the impact on climate compounds like $O_3$ and $CH_4$ and oxidants like OH. For the period 1996–2004 substantial reductions of $NO_2$ were found over Europe and the United States, corresponding to regional emission decreases during this period, while emissions continued to increase in developing countries and accelerated in some transition economy regions, as demonstrated in Fig. 31 (Akimoto, 2003).

There has been a large increase in $NO_x$ emissions since pre-industrial time, which have led to significant increase in the atmospheric nitrogen burden. Tsigaridis et al. (2006) estimate a factor of global increase by a factor of 4. Galloway et al. (2004) calculated an increase in the nitrogen oxide deposition from 12.8 Tg(N)year$^{-1}$ in 1860 to 45.8 Tg(N)year$^{-1}$ in the early 1990s. Using emissions valid for 1992 and a critical load varying between different natural ecosystems, Bouwman et al. (2002) estimated that sulfur and nitrogen deposition exceeded critical loads over 7% of the region covered by natural vegetation (See also Fowler et al., 2009). Changes in modeled $NO_2$ concentrations during the 1990s qualitatively reproduce the different changes in regional emissions (Granier et al., 2003). Large decreases are found over Europe and Russia, smaller decreases are identified over western North America, and large increases in populated or industrialized areas in Asia and parts of Latin America, which is in line with reported emission trends in Fig. 31. For further discussions on chemical interactions of pollution emissions, in particular the regional impact of compounds like $NO_x$, CO, NMVOC and $SO_2$ we refer to the accompanying papers by Monks et al. (2009) and Fowler et al. (2009).

### 6.1. Composition change due to emission from the transport sectors

During recent years a strong focus has been on the atmospheric impact from the transport sectors. Several ongoing EU projects (ACCENT, QUANTIFY, ATTICA, ECATS) investigate the effects of aviation, shipping, road traffic and other land-based transport on the atmosphere (Eyring et al., 2007a; Hoor et al., 2009; Eyring et al., in preparation, Dalsøren et al., 2007; Dalsøren et al., 2009a; Lee et al., 2009). The focus in these projects is primarily on regional to global scales.

#### 6.1.1. Studies of current impact

The European Integrated Project QUANTIFY has investigated the impact of the various transport sectors on atmospheric composition and climate. A comprehensive model activity has evaluated the impact of transport emissions on ozone, methane and the resulting radiative forcing. Fig. 32 shows the combined effect of shipping, aviation and road traffic on column ozone. Perturbations are most pronounced during the summer months in the Northern Hemisphere, with local perturbations of 4% above the background levels, although individual model increases can be larger.

Gas and particle emissions from ocean going ships are a significant and growing contribution to the total emissions from the transportation sector. The EU financed ATTICA project has published a detailed review on the current state of research concerning the effects of shipping emissions on atmospheric chemistry and climate (Eyring et al., in preparation). Nearly 70% of ship emissions

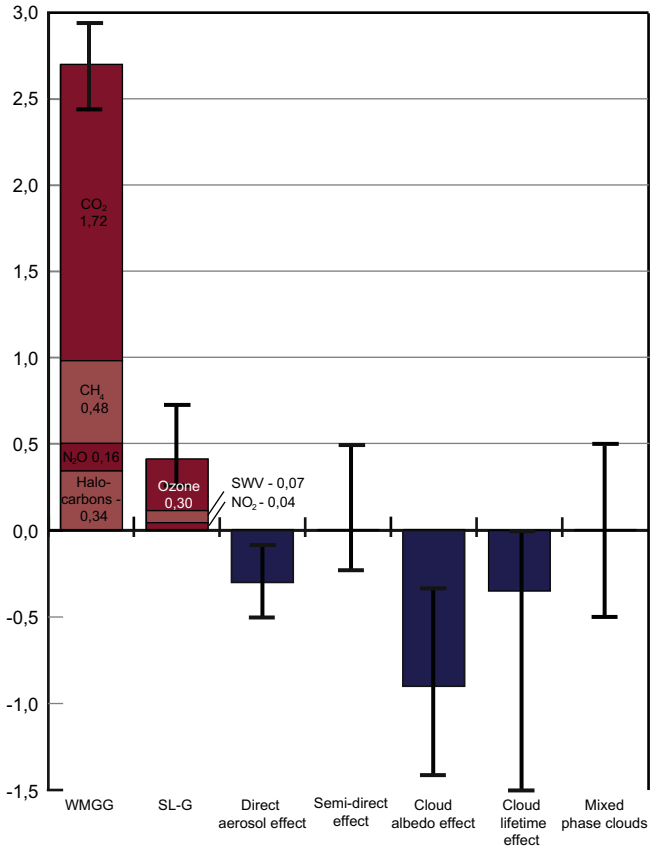


**Fig. 30.** Radiative forcing estimates of atmospheric compounds from the pre-industrial period 1750 to 2007. RF estimates of WMGG are similar to the one reported in Forster et al. (2007) except that it has been taken into account that growth in RF due to $CO_2$ is 0.03 W m$^{-2}$ yr$^{-1}$ between 2005 and 2007. Estimates for ozone and stratospheric water vapor are similar to the value given in Forster et al. (2007), whereas the estimate of $NO_2$ of 0.04 W m$^{-2}$ is from Kvalevåg and Myhre (2007). The estimate of the direct aerosol effect is from Myhre (2009). The RF for the cloud albedo effect is calculated based on Forster et al. (2007), with the modification that no model estimates have been excluded based on the number of aerosol species treated in the various models. Additionally, estimates published after Forster et al. (2007) have also been taken into account. While Forster et al. (2007) reported the median value of the estimates considered, we here report the mean. However, the mean and median values differ by only 2%. As few model studies report estimates of the cloud lifetime effect only, the estimate for cloud lifetime effect is calculated by subtracting the mean RF for the cloud albedo effect from the mean RF for both the albedo and lifetime effect. The latter is calculated based on studies reported in Denman et al. (2007), in addition to recently published estimates. This way of calculating the RF for the cloud lifetime effect relies on the assumption that the total (albedo and lifetime) effect equals the linear sum of the two separate effects to a good approximation (e.g., Kristjánsson, 2002). The few RF estimates for aerosol effects on mixed phase clouds available in the literature suggest a potentially large effect, but so far model studies are inconclusive in terms of the sign of this RF. Hence, we refrain from giving a RF estimate here, but rather give an uncertainty range from −0.5 W m$^{-2}$ to 0.5 W m$^{-2}$. The semi-direct effect is estimated based on a combination of published results of realistic BC atmospheric distributions and idealized experiments in Stuber et al. (submitted for publication). The absorption aerosol optical depth included in the idealized experiments in Stuber et al. (submitted for publication) is 0.05, which is an order of magnitude larger than the total (anthropogenic and natural) absorption aerosol optical depth from global aerosol models (Kinne et al., 2006). All the RF from the idealized semi-direct aerosol effect experiments are within the range −0.25 to +0.5 W m$^{-2}$ if the values are divided by 10 (Stuber et al., submitted for publication). The factor of 10 is adopted since the idealized experiments are performed with an absorption aerosol optical depth this magnitude larger than global aerosol models predicts for current condition.

occur within 400 km of coastlines, causing air quality problems through the formation of ground-level ozone, sulfur compounds and particulate matter in coastal areas. Ozone and aerosol precursors emitted to the atmospheres from ships are transported over several hundreds of kilometers, contributing to air quality

**Table 1**
Summary of radiative forcing (RF) for well-mixed and short-lived greenhouse gases, and the contribution from different aerosol effects. The uncertainty range is included.

| Radiative forcing mechanism | Best estimate | Range |
|---|---|---|
| WMGG | 2.69 | ±0.27 |
| $CO_2$ | 1.72 | ±0.17 |
| $CH_4$ | 0.48 | ±0.05 |
| $N_2O$ | 0.16 | ±0.02 |
| Halocarbons | 0.34 | ±0.03 |
| SL-GHG | 0.41 | 0.25, 0.73 |
| Ozone | 0.30 | 0.15, 0.60 |
| Stratospheric water vapor | 0.07 | ±0.05 |
| $NO_2$ | 0.04 | ±0.02 |
| Direct aerosol effect | −0.30 | ±0.20 |
| Semi-direct effect | NA | −0.25,+0.50 |
| Cloud albedo effect | −0.90 | −1.4,−0.3 |
| Cloud lifetime effect | −0.35 | −1.5,0 |
| Mixed phase clouds | NA | −0.5,+0.5 |

problems further inland. Fig. 33 shows satellite measurements of $NO_2$ columns retrieved by the SCIAMACHY instrument over marine areas (Richter et al., 2004), revealing large impact of shipping in the Indian Ocean, Eastern Mediterranean and coastlines in general, as well as further inland.

Fig. 34 shows global ozone enhancements from the OsloCTM2 model for year 2000 due to ship emissions (Dalsøren et al., 2007). The signal clearly follows the conventional ship tracks, but also affects continental areas. Calculations of ozone enhancements from ship emissions by Endresen et al. (2003) give maximum ozone perturbations of 12 ppb in the marine boundary layer during summer over the northern Atlantic and Pacific regions, while the multi-model study described in Eyring et al. (2007a) using EDGAR emissions obtained somewhat lower values, about 5–6 ppb, for the North Atlantic. In an update on ship emissions and their environmental impact, Dalsøren et al. (2009b) isolated the impacts of major ship types and ports. The large and increasing contribution from container ships was highlighted. In agreement with earlier studies, it was found that ship emissions contribute significantly to pollutants like ozone, sulfate, nitrate, BC and OC aerosols. In another study,

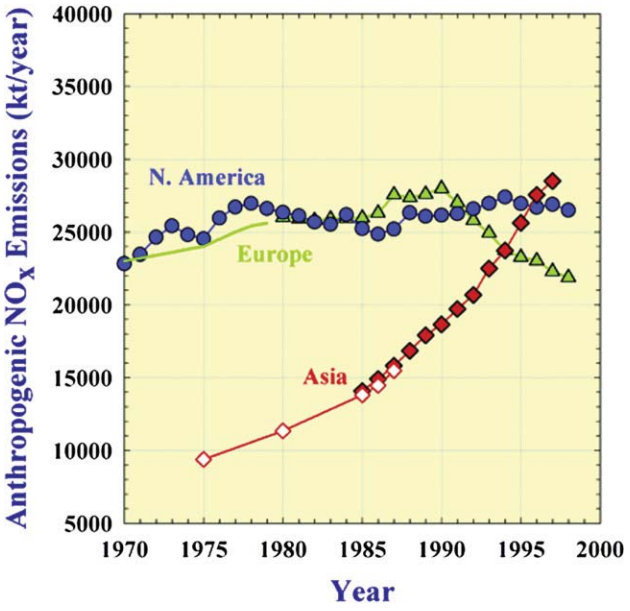


**Fig. 31.** Changes in anthropogenic $NO_x$ emissions in North America (United States and Canada), Europe (including Russia and the middle East), and Asia (East, Southeast, and South Asia), Akimoto, 2003.

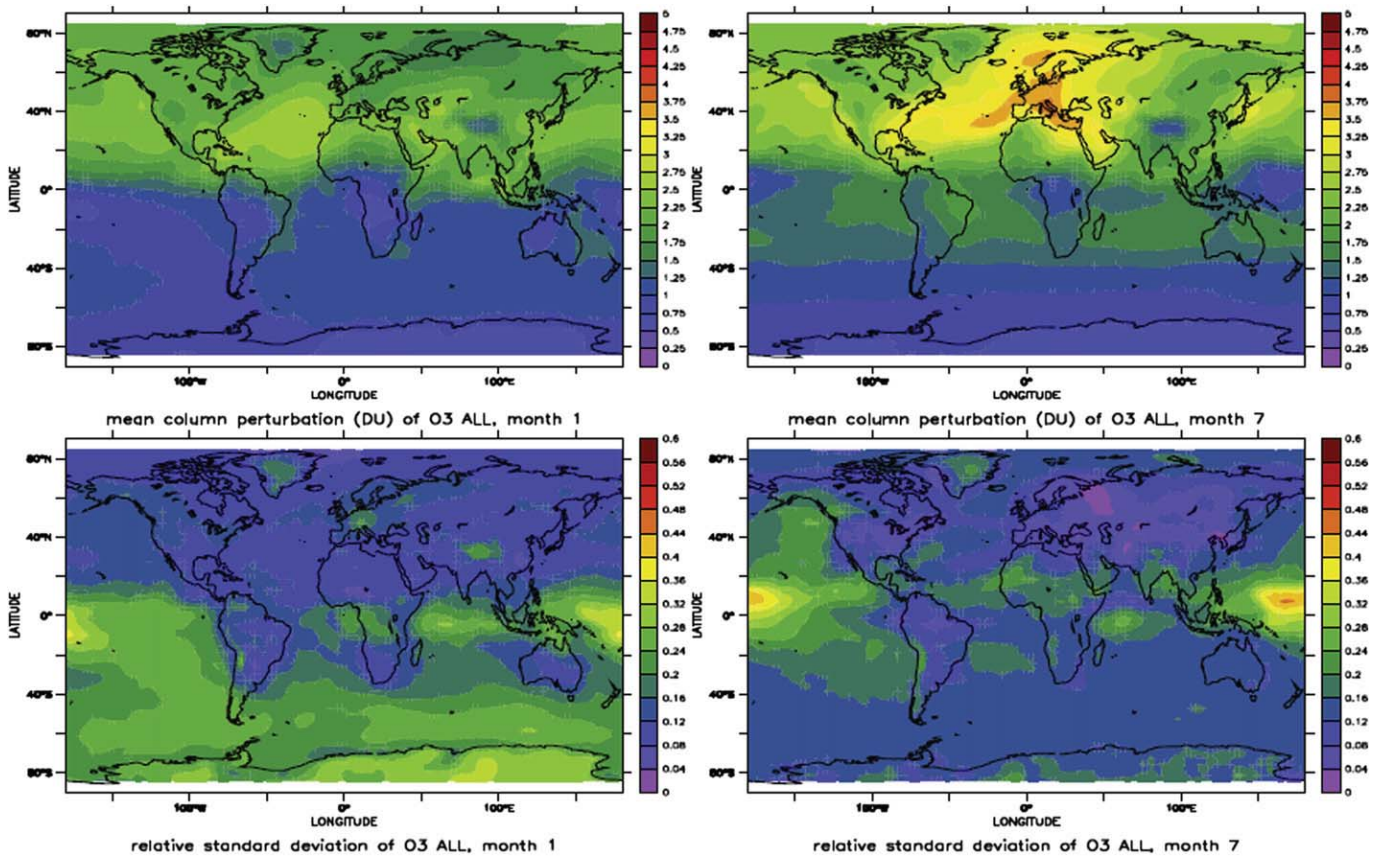


**Fig. 32.** Top panels: Mean column ozone perturbations due to all types of transport, as simulated by the TM4, LMDzINCA, OsloCTM2 and p-TOMCAT models (ensemble mean) for January (left) and July (right). Bottom panels: Corresponding relative standard deviations for January (left) and July (right) (from Hoor et al., 2009).

Dalsøren et al. (2009a) show that in regions where acidification still is of some concern (e.g., Northwest America and Scandinavia) ship emissions contribute heavily to wet deposition of nitrate.

For road emissions Matthes et al. (2007) found maximum surface ozone increases of 12% in northern mid-latitudes during July. New estimates of the impact of road traffic emissions on ozone, has been calculated by Hoor et al. (2009) using an ensemble of six global models. The result is shown in Fig. 35 along with impacts from the other sectors. Not surprisingly, significant enhancements due to shipping and road traffic are largely confined to marine and continental areas, respectively. However, the ship signals affect also coastal areas, and the impact of road traffic is not confined to the maximum emissions source regions in Europe and North America. Significant increases in ozone due to the aviation sector are confined to the Northern Hemisphere, where they are zonally mixed and, during summer, reach a maximum at high latitudes.

Scientific advances since the 1999 IPCC Special Report on Aviation and the Global Atmosphere (IPCC, 1999) have reduced key uncertainties, yet the basic conclusions remain the same. The ATTICA project has recently delivered a review of the current impact of aviation (Lee et al., 2009). Much progress has been made in the past ten years on characterizing aviation emissions, although major uncertainties remain, especially for particle emissions, and the combined effect on ozone and methane through $NO_x$ emissions.

The spatial variability in the effects of the transport sectors is large, not only because of the uneven distribution of emissions, but also because of differences in ambient chemical and radiative regimes, meteorological conditions, insolation, and surface properties.

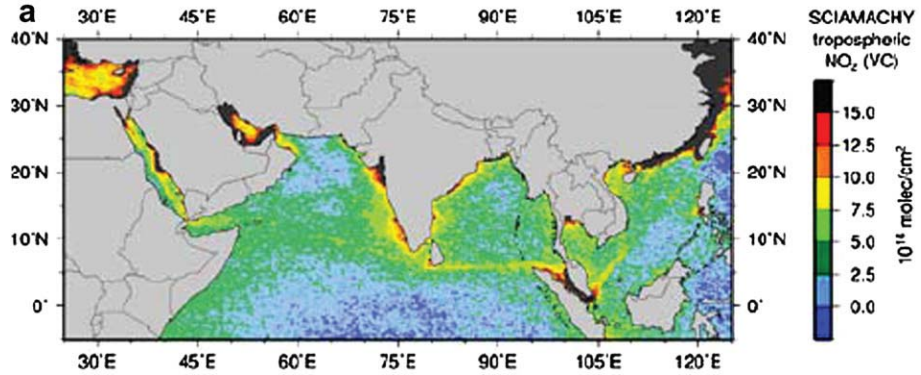


**Fig. 33.** $NO_x$ signature of shipping in the Indian Ocean as observed by satellite (from Richter et al., 2004).

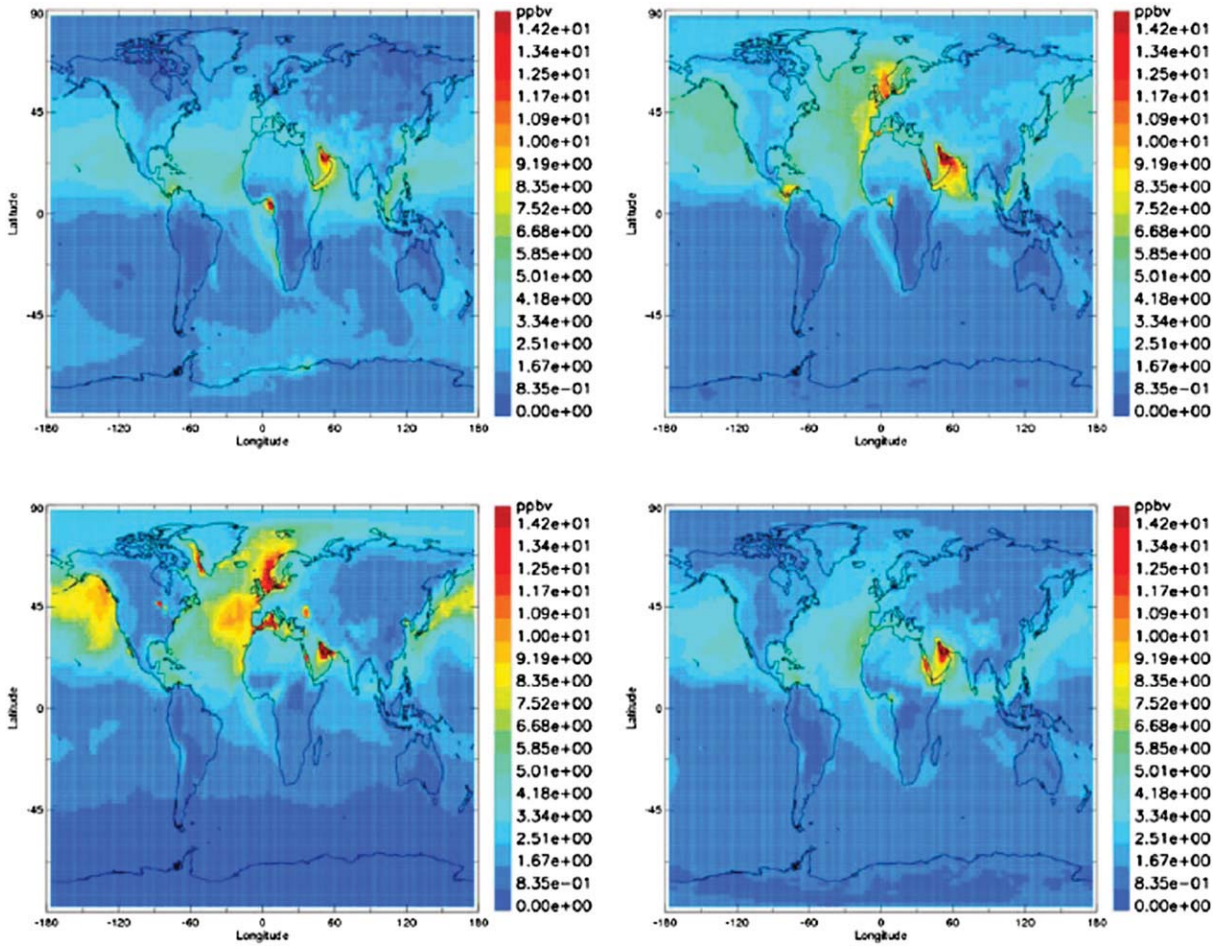


**Fig. 34.** Ozone change at the surface due to year 2000 ship emissions for January (top left), April (top right), July (bottom left), and October (bottom right) (from Dalsøren et al., 2007).

*6.1.2. Studies on future trends*

The model groups involved in the QUANTIFY project have performed detailed calculations of future impact from the transport sectors. The studies focus on the time evolution between 2000 and 2050, based on the different SRES scenarios. QUANTIFY project emission scenarios where provided for different transport sectors (road traffic, shipping and aviation) based on the IPCC SRES scenarios A1, A2, B1, and B2 (Nakicenovic et al., 2000). In addition, a low emission scenario was provided for aviation assuming the implementation of all available technology. The assumption is that emissions of ozone precursors from road traffic will drop to negligible amounts during this century, due to emission reduction technology. At the same time emissions from shipping and aviation are expected to increase during coming decades, since improving technology will not be able to compensate for the increased traffic. The climate impact from shipping is complex, since current emission trends lead to a global average negative radiative forcing (see Section 6.2.1). Future climate impact will, to a large extent, be determined by trend in emissions and on implementation of emission regulations. It should be recognized that environmental impact (on climate and air quality) from ships is local and regional in nature due to contributions from short-lived compounds such as sulfate aerosols. Dalsøren et al. (2007) have studied local effects of ship emissions in coastal regions and in the Arctic from future seaborne traffic.

Collins et al. (2009) have calculated the impact from ship emissions on atmospheric chemistry for the different land-based emissions in 2000 and 2030, ACCENT PhotoComp, presented in Section 4.2.1 (Fig. 36). The three plots show the change in the tropospheric ozone burden, production and methane lifetime due to ship emission. Shipping has the largest effect when using the 2030 MFR land-based scenario, a smaller impact when using the 2000 or 2030 CLE and an even smaller effect when using the high $NO_x$ SRES A2 scenario for the land-based emissions, illustrating the non-linearity of ozone chemistry with lower effects of emissions when added to a higher background. The non-linearity is stronger when looking at the change in the methane lifetime. Collins et al. (2009) have also performed calculations showing the effect of sulfur emissions, according to which the increase in sulfate aerosols and sulfur deposition due to the $SO_2$ from shipping will offset 75% of the benefits in air quality that would be expect from land-based emission controls under the SRES A2 scenario.

*6.2. Climate impact from the transport sectors*

*6.2.1. Impact from the different sectors*

In general, emissions from the transport sectors increase ozone and reduce methane. Ozone changes from the road sector result in stronger forcing because of the more effective vertical mixing over land that enhances the ozone change at higher altitudes where the forcing efficiency is higher.

In a recent study Fuglestvedt et al. (2008) show, that the net RF due to ship traffic from pre-industrial times to present is negative, opposite to what is found for other sectors. Aerosols are the main reason for the negative RF from shipping, but atmospheric reactive gases (e.g., methane) contribute to the negative RF. Fig. 37 depicts the combined

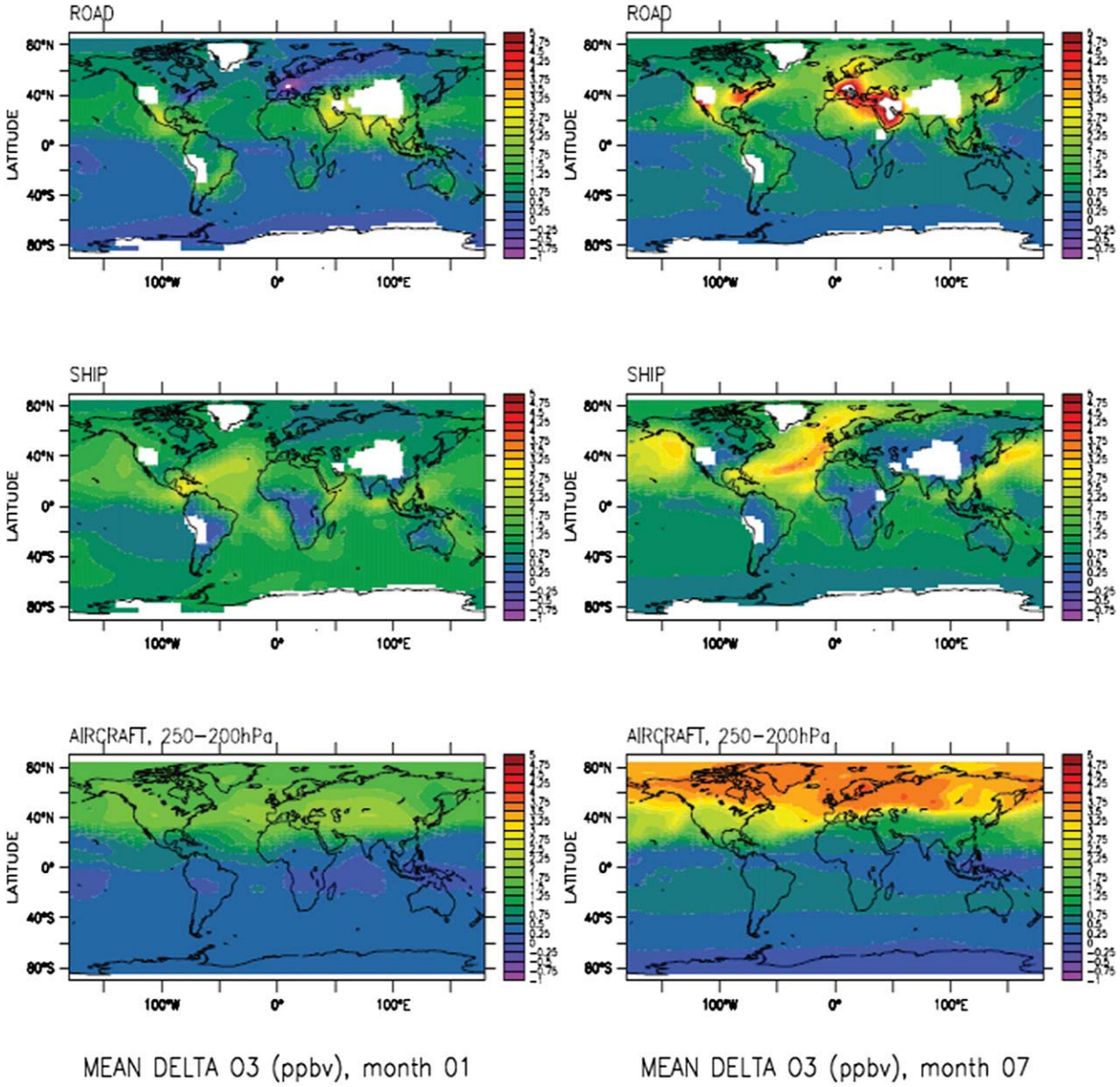


**Fig. 35.** Mean perturbations of ozone (ppbv) in the PBL (surface-800 hPa) for road emissions (upper row), ship emissions (middle row), and in the upper troposphere (200–250 hPa) for aircraft emissions (lower row) during January (left column) and July (right column) (Hoor et al., 2009).

RF from ozone changes and changes in methane. Ship emissions stand out with a combined negative effect. The reason for this is that $NO_x$ emissions from ship traffic occur over pristine areas where OH enhances efficiently, causing a strong reduction in the $CH_4$ lifetime and concentration (Dalsøren et al., 2009a; Fuglestvedt et al., 2008).

To investigate future impact, Fuglestvedt et al. (2008) have integrated radiative forcing for a current emission over different time horizons in order to compare the effect of different transport sectors and chemical components.

Fig. 38 shows the integrated radiative forcing due to the various components and sectors with a time horizon of 100 years, as used in the Kyoto Protocol. According to Fuglestvedt et al. (2008) $CO_2$ is by far the most important substance on this time scale, with the largest contribution coming from road transport. The second largest positive forcing comes from tropospheric ozone, again with a dominating contribution from road transport. Changes in methane and sulfate lead to a negative radiative forcing, with the larges contributions coming from the shipping sector. On the chosen time scale of 100 years the contributions from the short-lived and intermediate perturbations (ozone, aerosols, and methane) become significantly smaller compared with $CO_2$. Of the 100-year integrated net radiative forcing from total man made emissions the net radiative forcing from transport amounts to 16%.

### 6.2.2. *Comparison with other sectors*

Recent studies have improved our understanding of the contribution from various emission sectors and regions to RF from ozone and aerosol changes. Berntsen et al.(2006), Fuglestvedt et al. (2008), Unger et al. (2008) estimated the contribution to ozone radiative forcing. Unger et al. (2008) evaluated the RF due to ozone for the year 2030 from 6 emission sectors, as indicated in Fig. 39 with the largest contribution from the transportation and biomass burning sectors.

Koch et al. (2007) calculate the radiative forcing for the direct aerosol from six different sectors. The impacts of present-day aerosols emitted from particular regions and from particular

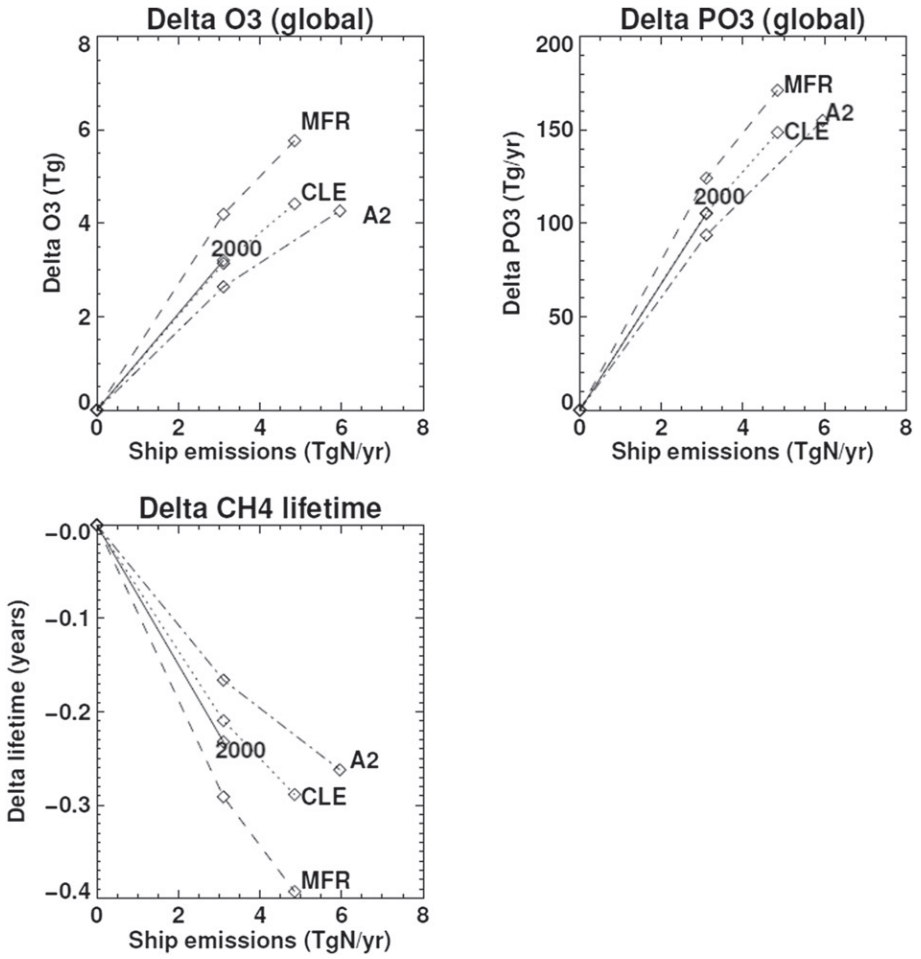


**Fig. 36.** Change in tropospheric ozone burden, production and methane lifetime for changes in ship emissions according to the four land-based emission scenarios (from Collins et al., 2009; their Fig. 11).

sectors using the Goddard Institute for Space Studies (GISS) GCM were studied. The conclusion from the work was that South-East Asia exports over 2/3 of its emitted black carbon and sulphate burden over the Northern Hemisphere. While Africa has the largest biomass burning emissions, South America generates a larger (about 20% of the global carbonaceous) aerosol burden; about 1/2 of this burden is exported and dominates the carbonaceous aerosol load in the Southern Hemisphere. The resulting calculated direct anthropogenic radiative forcings are −0.29, −0.06, and 0.24 W m$^{-2}$ calculated for sulfate, organic, and black carbon, respectively. Fig. 40 shows the percentage radiative forcing from various sectors for BC, OC, and sulfate. Two of the largest BC radiative forcings are from residential (0.09 W m$^{-2}$) and transport (0.06 W m$^{-2}$) sectors, making these potential targets to counter global warming suggested

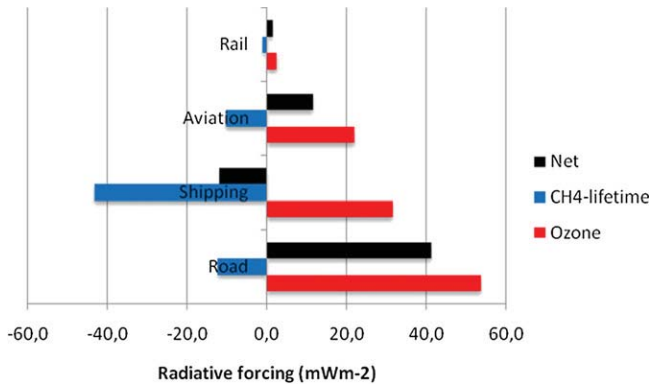


**Fig. 37.** Radiative forcing due to ozone, impact of changes in $CH_4$ lifetime, and the corresponding net radiative forcing for four transport sectors from pre-industrial to present, as calculated by Fuglestvedt et al. (2008).

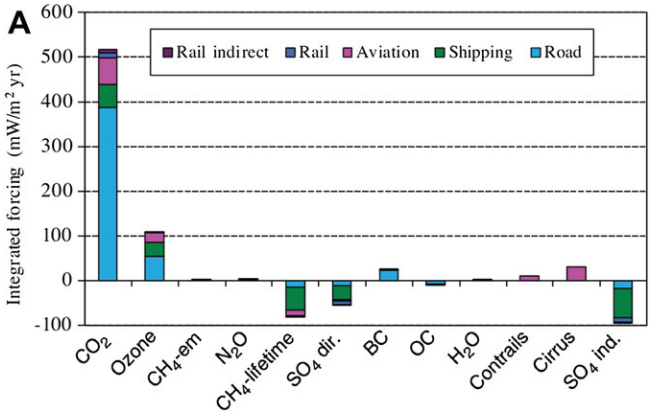


**Fig. 38.** Integrated radiative forcing of current emissions, by substance and transport subsector, over different time horizons. (A) Integrated global mean RF(mW m$^2$ yr) due to 2000 transport emissions, time horizon H = 100 years. (From Fuglestvedt et al., 2008)

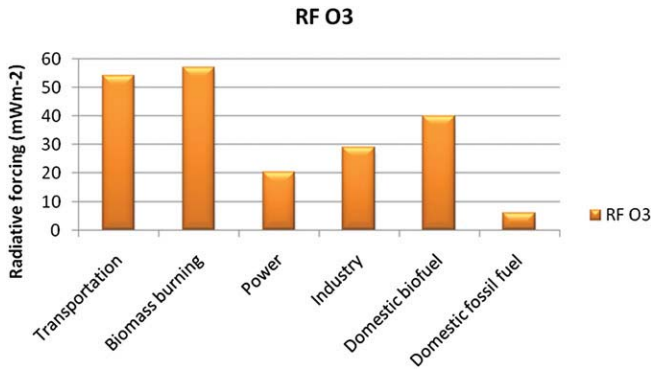


**Fig. 39.** Radiative forcing due to ozone changes in 2030 from different sectors, as calculated by Unger et al. (2008).

by Koch et al. (2007). Most anthropogenic sulfate comes from the power and industry sectors, and these sectors are responsible for the large negative aerosol forcings over the central Northern Hemisphere. Further studies have been performed by Shindell et al. (2008a,b), examining air quality (AQ) and radiative forcing due to emissions reductions by economic sector for different regions.

### 6.3. The impact of large emission increases in South-East Asia

South-East Asia where emission of pollutants have increased significantly, particularly during the last decade, and where it is likely that future emissions will continue to grow fast (Isaksen et al., 2009). These emissions are at such a high level that they have the potential to markedly increase transport of ozone to the US west coast (Zhang et al., 2009), and reduce global methane levels through enhanced OH levels (Dalsøren et al., 2009b). In the global model study by Dalsøren et al. (2009b) perturbations in 2000 and 2006, and future (2020) perturbations of OH and methane lifetimes are calculated. The adopted $NO_x$ emissions and results for the global average changes in OH and methane lifetime are given. For details of the adopted emissions in the model studies, see Dalsøren et al. (2009a). The high emission cases are based on the rapid growth in energy use after 2000, and assumption of future significant growth (see also Isaksen et al., 2009). Note that due to the methane response time of approximately 10 to 12 years to perturbation changes, there will be a lag in the methane response to lifetime changes.

In agreement with former studies it is found that global anthropogenic emission changes have resulted in small changes in OH and in methane lifetime from 1980 to 2000 (Table 2). As shown in Fig. 31 emission of $NO_x$, a main OH precursor, has decreased significantly during this time period in Europe. The model studies therefore indicate a significant cancellation of the increase in Southeast Asia from the overall global emission. Comparison for 2000 with satellite measurements show that the model is able to reproduce retrieved tropospheric $NO_2$ columns over Southeast Asia. In the high emission case the 2006 $NO_x$ emissions were fitted to the 2000–2006 increase in energy consumption in China. This case shows better agreement with the satellite retrieved 2000–2006 tropospheric $NO_2$ column trend over central and eastern China than the reference case. The satellite comparison thereby highlights an issue noted in other studies: The question addressed whether current emission inventories underestimate the recent increase in $NO_x$ emissions in Southeast Asia. The development of global OH and methane due to emission changes in Southeast Asia after 2000 is also dependent on the balance between changes in $NO_x$ and CO emissions. From 2000 to 2006 the sign of OH and methane lifetime changes are different in the reference case and the high $NO_x$ emission case. Though the high $NO_x$ emission case is an upper estimate of OH changes it is better than the reference scenario in reproducing measured $NO_2$ trends. From 2000 to 2020 the contributions from Southeast Asia are moderate in the base scenario but much larger than the small overall global emission impact from 1980 to 2000. In the 2020 high Southeast Asian $NO_x$ emission case the impact on global OH and methane is large. It is of comparable absolute magnitude to the international ship traffic (Endresen et al., 2003; Dalsøren et al., 2007; Dalsøren et al., 2009a). The OH increase in Southeast Asia is 4.7% in the 2020 high $NO_x$ case. Such a large change would have a significant effect on the oxidation of regional pollutants with short and intermediate lifetimes.

**Table 2**
Estimated changes in global average OH and methane lifetime due to changes in $NO_x$ emissions. 2000 changes are relative to 1980, and changes after 2000 are relative to 2000.

| | $NO_x$ | OH change (%) | $CH_4$ lifetime (%) |
|---|---|---|---|
| 1980 | 4.8 | | |
| 2000 | 8.2 | −0.1 | 0.22 |
| 2006 ref | 11.5 | −0.15 | 0.25 |
| 2006 high | 12.7 | 0.9 | −1.1 |
| 2020 ref | 15 | 0.25 | −0.5 |
| 2020 high | 22.3 | 2.75 | −2.7 |

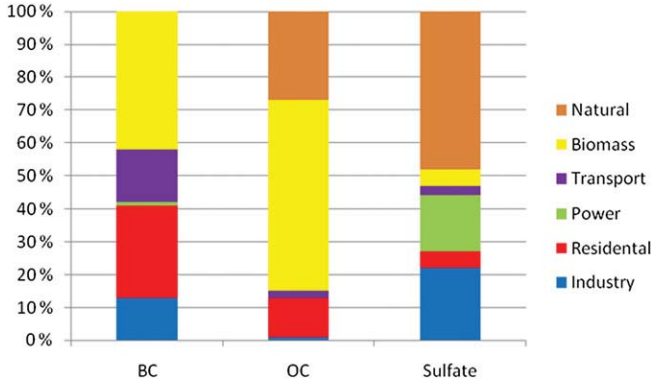


**Fig. 40.** Sectoral contributions to aerosol forcings shown as percentages relative to total TOA forcing for each species. Results are taken from Koch et al. (2007).

Zhang et al. (2009) compiled a detailed anthropogenic emission inventory for Asia for the spring 2006 period of INTEX-B but similar to Dalsøren et al. (2009b) used a higher estimate for Asian $NO_x$ emissions by constraining them to satellite observations. Zhang et al. (2009) found that Asian pollution enhanced surface ozone concentrations by 5–7 ppbv over western North America in spring 2006. The 2000–2006 rise in Asian anthropogenic emissions increased this influence by 1–2 ppbv.

### 6.4. Impact on the Arctic (Arctic Haze)

Human-induced climate–chemistry interactions could be of particular importance in the Arctic. The Arctic has warmed more rapidly during recent decades than most parts of the globe, and it is projected to warm even more during the 21st century. During the past 30 years, the extent of Arctic sea ice during the summer has decreased by about 25% (Stroeve et al., 2007), and the seasonal melt area of the Greenland Ice Sheet has increased rapidly, by ~7% per decade since 1979. While much of the Arctic warming originates from the same factors underlying global warming, studies suggest that both tropospheric aerosols and ozone play an important role in the Arctic.

*6.4.1. Observational data on trends*

Measurements of pollutants in the Arctic are relatively limited compared to more populated mid-latitude regions. Long-term (20–30 years) surface observations are available for ozone, sulfate, BC and dust, though only from a few stations. Data from Alert, Canada show no appreciable trends during the 1980s, followed by decreases in many aerosols concentrations (sulfate, nitrate, sea-salt) during the 1990s (Sirois and Barrie, 1999). Data from both Alert and Barrow, Alaska show likewise decreasing BC during the 1990s, but suggest that concentrations began to increase again around 2000 (Sharma et al., 2006). The trends in individual aerosol species are consistent with observations of the overall light scattering by aerosols, which peaks in spring as inflow of pollutants is large and near-surface temperature inversions inhibit deposition, leading to the seasonal aerosol build up known as Arctic Haze (Iversen and Joranger, 1995). Measurements of the Arctic Haze began in the late 1970s: they show a maximum scattering during the 1980s and 1990s, followed by decreases through around 2000 (Quinn et al., 2007).

Ozone data from Barrow show a slightly increasing trend from 1975–1995, but they are not statistically significant (Oltmans et al., 1998). In contrast, measurements of CO, the only ozone precursor (other than methane) with long-term Arctic records, show decreases at Northern high latitudes during the 1990s (Novelli et al., 1998). Only few long-term data on pollutants are available for the Eastern Hemisphere side of the Arctic.

On much longer timescales, the recent analysis of black carbon concentrations from a Greenland ice core has allowed reconstruction of BC deposition since the late 18th century (McConnell et al., 2007). These suggest that emissions in the main source regions, North America, Europe and more recently (and to a lesser extent) Asia, were extremely large in the early 1900s, declined thereafter through the middle of the century, and increased again during recent decades.

*6.4.2. Climate impact of chemically and radiatively active short-lived species in Arctic*

As emissions within the Arctic are relatively small, most Arctic pollution comes from distant sources. The relative importance of pollutants located within the Arctic as compared with those at lower latitudes is not clear, but remote radiative forcing appears to play a large role (Shindell et al., 2007). Direct radiative forcing due to changes in pollutants located within the Arctic can also be substantial, however, with seasonal values as large as $1\,W\,m^{-2}$ (Quinn et al., 2008). The contribution of various species to the total preindustrial to present-day Arctic surface temperature trends shows that BC, ozone and methane have together caused roughly as much warming as $CO_2$, while reflective aerosols have caused a cooling of comparable magnitude as seen in Fig. 41. Shortwave radiation is primarily perturbed via absorption by ozone and BC and reflection by sulfate, OC and nitrate. Long wave fluxes are affected by ozone (and other greenhouse gases) and by aerosols. While aerosol forcing is usually dominated by shortwave impacts, the long-wave effects play a larger role at high latitudes during polar darkness when observations show a distinct effect of Arctic Haze on thermal radiation (Ritter et al., 2005). Hence under Arctic conditions, aerosols can sometimes have similar impacts as those to greenhouse gases.

Indirect effects of aerosols can also be large in the Arctic. One prominent indirect effect is that of black carbon deposited onto snow or ice surfaces, darkening them and reducing their albedo (Warren and Wiscombe, 1980; Clarke and Noone, 1985; Jacobson, 2004). Another is the aerosol indirect effect on clouds, which can lead to very large radiative forcings ($>3\,W\,m^{-2}$) by increasing cloud cover under conditions of low insolation, which leads to a net warming effect due to absorption of outgoing long-wave radiation (Garrett and Zhao, 2006; Lubin and Vogelmann, 2006). There are limited understanding of any of these indirect processes. For example, aerosol indirect effects on clouds are not well characterized for ice phase clouds (Quinn et al., 2008).

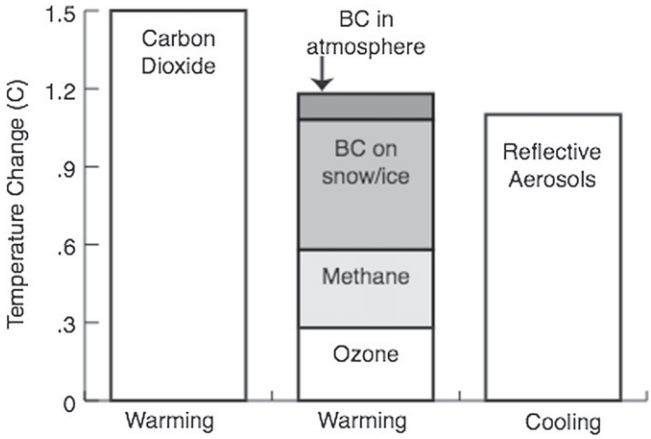


**Fig. 41.** Estimates of the contribution of particular species to preindustrial to present-day Arctic (60° to 90°N) surface temperature trends. Values are based on the assessment of modeling and observations of Quinn et al. (2008), and do not include aerosol indirect effects. Reflective aerosols include sulfate and organic carbon.

Forcing by Arctic aerosols has a strong seasonal variation for both shortwave and long-wave components, while forcing by ozone appears to maximize during boreal spring when Arctic ozone abundances are comparatively large and sunlight is relatively abundant (Quinn et al., 2008).

## 7. Impact on tropospheric composition from climate change and changes in stratospheric composition

Changes in climate have the potential to affect tropospheric composition and the distribution in several ways. Changes in circulation will alter the transport of pollutants, and in particular if stagnant conditions during high pressure situations become more/less frequent, conditions will be more/less favorable for the build up of high pollutions levels (e.g., Royal Society, 2008; Matsueda et al., 2009). Furthermore, higher temperatures will increase water vapor with enhanced OH production, and lightning activities could be enhanced in a warmer climate leading to enhanced $NO_x$ production. Changes in surface characteristics (dryness, wind speed) will affect the exchange of components between the biosphere and the atmosphere (see Fowler et al., 2009). Stratospheric/tropospheric exchange of, in particular, ozone is affected by climate change, and also by changes in ozone depletion in the stratosphere. For instance, the large stratospheric ozone depletion in the 1980s and 1990s had an impact on stratosphere–troposphere exchange and on ozone transport to the troposphere (e.g., van Noije et al., 2004).

### *7.1. Impact of climate change on future tropospheric composition*

*7.1.1. Ozone and its precursors*

Several modeling studies have investigated how future climate change may impact tropospheric composition, ozone in particular. An early study (Thompson et al., 1989) suggested that increases in water vapor, associated with warmer temperatures, would increase the flux through the reaction (R2: $O(^1D) + H_2O \rightarrow 2OH$), enhancing the loss of ozone and production of the hydroxyl radical. Subsequent work (e.g., Zeng and Pyle, 2003; Collins et al., 2003; Sudo et al., 2003) additionally found that climate change led to an increased flux of ozone from the stratosphere to the troposphere.

More recent results from climate models, with detailed stratospheric dynamics have confirmed that a more vigorous Brewer–Dobson circulation (the large-scale circulation that exerts a major control on stratosphere–troposphere exchange (STE)) is a robust feature of models (Butchart et al., 2006). Stevenson et al. (2006) presented results from ten models that simulated the impact of climate change between 2000 and 2030 on ozone. The main climate feedback processes affecting ozone in these models appeared to be the two discussed above. Some of the models were dominated by the negative water vapor feedback, whilst the positive STE feedback was more prominent in others.

Changes in lightning (and associated $NO_x$ production) in connection with climate change have been studied. Most model studies show an increase in lightning as climate warms (Schumann and Huntrieser, 2007), with increases of up to 60% per degree K of global mean surface warming (Lamarque et al., 2005), although other studies have shown no global trend, just a geographical shift from tropics to mid-latitudes (Stevenson et al., 2005), or decreases (Jacobson and Streets, 2009). Other studies show similar discrepancies, with no clear conclusions on climate change and lightning activity. Observations show no relationship between surface temperature and lightning in the tropics, but a strong positive correlation over Northern Hemisphere land areas (Reeve and Toumi, 1999). Some studies suggest that increases in lightning may be the dominant climate-related driver of future upper tropospheric $O_3$ increases (Wu et al., 2008a). Wild (2007) demonstrated that changes in lightning $NO_x$ emissions had a large influence over the tropospheric ozone burden.

Biogenic VOC emissions are a function of temperature, photosynthetically available radiation (PAR), leaf area index (LAI) and plant species (Guenther et al., 1995, 2006). Several global chemistry models account for some or all of these dependencies (e.g. Hauglustaine et al., 2005; Stevenson et al., 2006; Wu et al., 2008a). Most models show an increase in tropospheric $O_3$ as VOC emissions rise, particularly in regions with relatively high $NO_x$ levels; however, in low $NO_x$ regions, $O_3$ often decreases. VOC degradation chemistry influences ozone's sensitivity to VOC emissions, in particular whether isoprene nitrate formation represents a temporary or terminal sink for $NO_x$ (Giacopelli et al., 2005; Wu et al., 2008b). Horowitz et al. (2007) present observational evidence that isoprene nitrates do permanently remove $NO_x$, and in models that reflect this finding, the surface $O_3$ response to rising biogenic VOC emissions quite rapidly saturates (Wu et al., 2008b), and can even result in $O_3$ reductions. For example, Wu et al. (2008b) find that future surface $O_3$ levels in the SE US are reduced as isoprene emissions rise. One study by Arneth et al. (2007) links biogenic VOC emissions also to $CO_2$ levels (Arneth et al., 2007) and land-use change. The process is not well known, and has generally not yet been considered in global models.

Changes in the biosphere associated with climate change may have other important effects. Soil $NO_x$ emissions, produced from bacterial activity, are likely to increase as the land warms (Granier et al., 2003; Hauglustaine et al., 2005; Liao et al., 2006; Wu et al., 2008a). Changes in the hydrological cycle, and in particular soil moisture, may significantly affect stomatal opening and hence dry deposition fluxes of ozone and other gases (e.g., Solberg et al., 2008). Enhanced deposition will occur under wetter conditions and visa versa. Increases in $CO_2$ levels may reduce stomatal opening and hence ozone deposition (Sanderson et al., 2007). Furthermore, higher temperatures will increase evaporative anthropogenic VOC emissions (e.g., Rubin et al., 2006).

Trends in cloud optical depth, aerosol loading and the solar cycle in the tropics (Chandra et al., 1999; Fusco and Logan, 2003) might modulate tropospheric ozone to some extent. Climate related changes in temperature, humidity, meteorology, and land use/vegetation can also affect ozone. Fusco and Logan (2003) estimate a 3% ozone increase over Western Europe and 1% decline over much of North America due to 1970–1995 temperature increase and decrease respectively. The overall change in tropospheric ozone due to climate change since the pre-industrial period was positive in 5 of 6 studies in a model assessment (Gauss et al., 2006). However, model studies based on future scenarios taking into account climate changes (Hauglustaine et al., 2005; Stevenson et al., 2006; Dentener et al., 2005; Dentener et al., 2006c) report a significantly reduced global tropospheric burden due to the effects of climate change, partly as a result of enhanced OH formation. It should however be noted that the signs of the changes vary in different regions of the troposphere both for past and future changes.

More prolonged and frequent occurrence of heat waves of the type experienced over Western Europe in August 2003 is expected to occur in a future warmer climate. Solberg et al. (2008) applied meteorological data in a global scale Chemical Transport Model (the Oslo CTM2), covering the heat wave period, and showed that under such extreme weather situations large ozone levels build up in the planetary boundary layer with current emissions for extended time periods (in excess of 100 ppb for several days). If the 2003 heat wave is taken as a proxy for more frequent severe weather situations during future warmer climates, the effect of measures to control regional pollution could be strongly reduced.

#### 7.1.2. Methane

The natural source of methane from wetlands is climate-sensitive (Gedney et al., 2004; Shindell et al., 2004). Changes in hydroxyl radical (OH) concentrations directly affect the rate of methane oxidation. Higher levels of water vapor lead to higher levels of OH (reaction (R2)). The reaction of methane with OH is strongly temperature dependent, and proceeds faster at higher temperatures. Several model studies have noted the negative feedback of climate on methane through these mechanisms (e.g., Johnson et al., 2001; Stevenson et al., 2005). All ten of the models in Stevenson et al. (2006) showed a reduction in the methane lifetime in a warmer climate, with an average reduction of 4% for a global mean surface warming of around 0.7 K.

Thawing of permafrost represents a potential significant source of methane to the atmosphere, and may constitute a positive feedback mechanism in the climate–chemistry system (Osterkamp, 2005; Lawrence and Slater, 2005; Walter et al., 2006a,b). With strongly enhancing temperatures in the Arctic, permafrost degradation has been observed to occur rapidly (Jorgensen et al., 2006), and methane has been observed to be bubbling from melting lakes at an increasing rate (Walter et al., 2006a,b). Large amounts of organic carbon are stored in the permafrost, which partly is converted to methane and emitted to the atmosphere, following the thawing of the permafrost (Walter et al., 2006a,b; Zimov et al., 2006). There is a non-linear response in atmospheric methane concentrations to enhanced emissions, currently giving an additional 40% increase in atmospheric concentrations (positive feedback) (Prather and Ehhalt, 2001). The non-linear feedback is likely to be much larger with strong enhancements in methane concentrations, since a larger fraction of the OH loss is through the methane reaction. Methane emissions over periods of decades to several centuries in connection with permafrost thawing (Walter et al., 2006a,b), combined with a methane lifetime of the order of 10 years, makes the impact of methane permafrost emissions depends critically on the time horizon of permafrost thawing. Similar and rapid impact on methane can occur if large amounts of methane trapped as methane hydrates under Arctic sea ice (Buffett and Archer, 2004) are released following ocean temperature increases and extensive sea ice melting. Although the contributions from the described processes are uncertain, observations of emission from

melting permafrost lakes, nevertheless show increase, although at a small rate compared with other methane sources (Walter et al., 2006a,b). Sea ice melting in the Arctic is recently found to be faster than predicted (Stroeve et al., 2007).

#### 7.1.3. Aerosol

A few studies have considered the effects of climate change on aerosol concentrations. Higher levels of oxidants tend to increase secondary aerosol formation rates (Stevenson et al., 2005; Unger et al., 2006; Tsigaridis and Kanakidou, 2007). Changes in the hydrological cycle have strong regional influences on wet removal processes, generally increasing wet deposition (Liao et al., 2006; Racherla and Adams, 2006). The thermodynamic equilibrium of some aerosol species may be shifted by changes in climate (Liao et al., 2006). Some sources of aerosols, such as biomass burning, may increase as climate warms (Jacob and Winner, 2009). Following the A2 scenario, global aerosol burdens are reduced by 20% (2100–2000) in the study of Liao et al. (2006), and by 2–18% (2050–1990) in that of Racherla and Adams (2006), mainly due to enhanced deposition.

Feedback mechanisms between the physical climate state (wind, land cover, ice cover, vegetation distribution and temperature), and natural emissions lead to changes in aerosol abundances (dust loads, sea salt and biogenic organic aerosols) (Mahowald and Luo, 2003; Jones et al., 2007; Tsigaridis and Kanakidou, 2007). The quantification of such changes will require considerable research efforts on relevant parameterizations in global models, in order to define credible scenarios including such feedbacks.

Large uncertainties still exist in terms of natural emissions, e.g., DMS from the oceans and hydrocarbons from land vegetation, and their response to climate change. There are also large uncertainties in the contribution of biomass burning, which occurs both naturally and due to human activity and is characterized by large interannual variations, thus complicating trend analyses.

#### 7.1.4. Effects of climate change on Arctic composition

Climate change can influence Arctic pollutants in many ways. Changes in the transport of pollutants to the Arctic region could occur because enhanced polar warming would reduce the gradient between the Arctic and lower latitude pollutant source regions, facilitating transport which is currently limited by the polar front (constant potential temperature surfaces which intersect the Earth's surface and form a dome over the polar region) (Stohl, 2006). Additionally, climate models generally project an enhancement of the strength of Northern Hemisphere mid-latitude westerly winds associated with the large climate variability patterns of the North Atlantic Oscillation and Northern Annular Mode (Miller et al., 2006), which would lead to enhanced transport of pollutants to the Arctic (Eckhardt et al., 2003; Duncan and Bey, 2004; Sharma et al., 2006).

Emissions of ozone precursors in and near the Arctic may also increase as boreal regions warm and forest fire frequency increases. Release of methane from enhanced boreal wetland productivity is an additional possible consequences of Arctic warming, whose effects would however be global given methane's long lifetime. The retreat of Arctic sea ice cover during springtime is also likely to alter the ozone-depleting halogen chemistry that takes place in the marine boundary layer (Simpson et al., 2007).

The relative importance of climate-induced changes on Arctic pollutants versus anthropogenic emission changes will clearly depend upon future emissions. A shift of pollutant emissions from industrialized nations to developing nations at lower latitudes is already taking place. This may have a greater impact on pollutant transport to the Arctic than the climate-induced changes discussed above as pollution transport from lower latitude Asian sources is substantially less efficient per unit emission than transport from Europe (Stohl, 2006; Shindell et al., 2008a,b). Furthermore, substantial increases in local emissions are possible under a scenario where shipping in the Arctic ocean increases substantially as sea ice cover retreats (Granier et al., 2006; Dalsøren et al., 2007). Hence much work remains to better understand climate–chemistry interactions in the Arctic and to project their role in future Arctic climate change.

### 7.2. Impact of stratospheric changes on tropospheric composition

The stratosphere can affect tropospheric ozone by direct downward transport of stratospheric high-ozone air, and by changes in the stratospheric ozone column affecting the penetration of UV radiation, and hence tropospheric photolysis rates. Changes in the stratosphere can also affect tropospheric circulation patterns particularly in the polar regions such as Antarctic circumpolar westerly winds (e.g., Perlwitz et al., 2008), and the Arctic oscillation (Hess and Lamarque, 2007), and hence indirectly affect tropospheric ozone distributions.

#### 7.2.1. Contributions of stratosphere–troposphere exchange to the tropospheric ozone budget

Irreversible exchange of air between the stratosphere and troposphere occurs largely in synoptic scale events. Global estimates have been made using correlations between $N_2O$ and $O_3$ (e.g., Murphy and Fahey, 1994), by 3D chemistry models (e.g., Roelofs and Lelieveld, 1995; Jöckel et al., 2006), and by combining satellite ozone observations with meteorological analyses (e.g., Olsen et al., 2003). These typically give fluxes in the range 450–600 $Tg(O_3)\,yr^{-1}$. However there are some discrepancies in the definition of the flux. Some studies quote a flux through a fixed pressure level, others through a PV surface. Many tropospheric chemistry models use the 150 ppbv ozone surface as a definition of the tropopause.

Stevenson et al. (2006) assessed the ozone budgets of 26 tropospheric chemistry models. They inferred the STE flux in the models across the 150 ppbv ozone surface by assuming a balance between the stratospheric input, net chemical production and dry deposition of ozone. The results gave a mean STE ozone flux of 552 $Tg\,yr^{-1}$ with a range of 151–930 $Tg\,yr^{-1}$. This compares to a mean tropospheric chemical production of 5110 $Tg\,yr^{-1}$. Hence STE contributes about 10% to the total tropospheric ozone budget. This does not necessarily mean that STE contributes 10% to the tropospheric burden since the ozone is injected into the upper troposphere where the ozone lifetime is longer. By tagging stratospheric ozone in their model simulation, Sudo and Akimoto (2007) calculated that STE contributed 23% to the tropospheric ozone burden. Variations in STE account for 25% of the variance in the tropospheric ozone burden between models (Wild, 2007).

#### 7.2.2. Trends in STE

The exchange of mass between the stratosphere and troposphere depends on the Brewer–Dobson circulation in the stratosphere (upwelling in the tropics, downwelling in the extra-tropics), which is driven by extra-tropical wave forcing. A study by Butchart and Scaife (2001) found that the rate of global mass exchange between the stratosphere and troposphere will increase by 3% per decade in future. They put this down to an increased wave forcing from more vigorous extra-tropical planetary waves in the warmer climate. The overall trend of the Brewer–Dobson circulation is a consistent feature of coupled chemistry climate models. Butchart et al. (2006) estimated an average 2% per decade increase in the tropical upwelling in 11 models over the 21st century.

The ozone concentrations in the lower stratosphere depend on chemistry and transport, and could be strongly influenced by

climate change. Zeng and Pyle (2003) found a substantial increase in lower stratospheric ozone, with a future climate in their model with a top at 36 km. Another study, using a model with an 85 km top, found that while lower temperatures increased ozone in the upper stratosphere, this reduced the lower stratospheric ozone as less UV could penetrate to the lower levels.

*7.2.3. Trends in tropospheric ozone*

Collins et al. (2003), Sudo et al. (2003) and Zeng and Pyle (2003) found that STE of ozone by 2100 would increase by 40%, 130% and 80% respectively. These models were tropospheric chemistry models with tops between 36 and 40 km. The three studies investigated changes in both circulation and lower stratospheric ozone. In all these cases the change in lower stratospheric ozone had a large effect on STE. Increased water vapor in a warmer climate is expected to increase destruction of tropospheric ozone, but in the above three studies increased STE partially or completely offset the increased destruction. In the Stevenson et al. (2006) model intercomparison, models had varying methods of accounting for STE of ozone. These gave STE increases with 2030s climate of 0–19%.

Recent trends in tropospheric ozone may be at least partly due to changes in the lower stratosphere. Ordóñez et al. (2007) have shown that a 16%/decade trend in lowermost stratospheric ozone over Europe (1992–2004) correlates well with a 5–10%/decade trend in lower tropospheric background ozone (Fig. 42).

Stratospheric ozone depletion and its subsequent recovery will affect lower stratospheric concentrations and hence influx of ozone into the troposphere. Ozone depletion may have offset two thirds of the tropospheric ozone burden increase from pre-industrial times to the present day, according to Shindell et al. (2006). They also suggest that of their expected 124% increase in STE in future, only 33% is due to climate change, the rest is due to ozone recovery.

*7.2.4. Impact of UV changes*

Since chemical processes in the troposphere are initiated by solar UV-B penetration into the troposphere, changes in stratospheric ozone could affect the impact on the tropospheric oxidation. Available measurements show that surface UV radiation levels have generally increased with a geographic pattern similar to the observed reductions in stratospheric ozone. In addition surface UV levels will be strongly influenced by cloud cover, local ground albedo and the atmospheric aerosol content. UV increases lead to

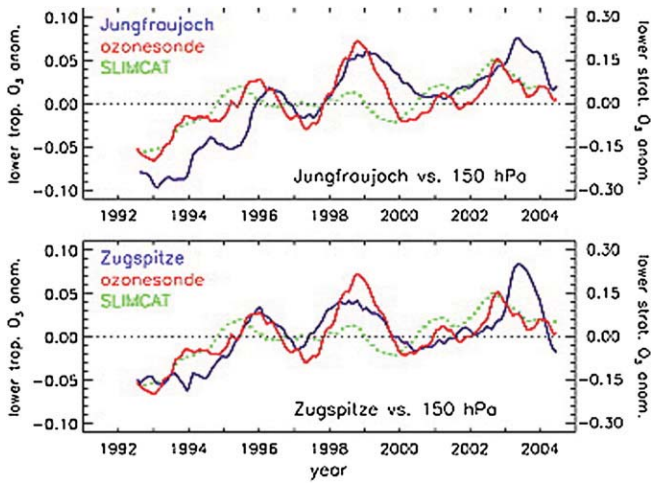


**Fig. 42.** 12-month running means of the normalized monthly anomalies with respect to the 1992–2004 mean annual cycle of lower free tropospheric ozone (blue) at (top) Jungfraujoch and (bottom) Zugspitze, and 150 hPa (~13.6 km altitude) ozone averaged for Payerne and Hohenpeissenberg (red). From Ordóñez et al., 2007.

an enhanced OH production, which reduces the lifetime of methane and influences ozone production and loss rates. The impact on ozone is more complex (Isaksen et al., 2005). While decreased ozone columns, enhanced surface ozone in polluted regions, surface ozone decreased in pristine background regions with low $NO_x$. Collins et al. (2009) showed that during summer with very high $NO_x$ levels titration lowered ozone production. Shindell et al. (2006) calculated that ozone depletion since 1979 had increased OH levels by 3.5%. This would correspond to a 5% decrease in methane concentrations (using the factor 1.4 feedback adjustment, from Prather and Ehhalt (2001), and assuming initial reduction in methane lifetime is the same as the global OH increase). Conversely ozone recovery would be expected to increase methane and hence tropospheric ozone.

## 8. Cross cutting issues (policy relations, integration)

The 1992 UN Framework Convention on Climate Change (UNFCCC) states that policies and measures to address a human-induced climate change shall stabilize atmospheric concentrations of greenhouse gases (GHGs) "at a level that would prevent dangerous anthropogenic interference with the climate system" (Art. 2), and that the measures should be "comprehensive" and "cost-effective" (Art. 3.3). Article 2 forms the basis for determining the total reductions in emissions. However, due to incomplete understanding of the climate system it is difficult to determine the appropriate level of mitigation. One major issue is the possibility that natural fluctuations such as the solar forcing have contributed significantly to the observed global temperature increase. One way to assure Comprehensiveness and Cost-effectiveness as stated in Article 3.3 is to allow flexibility with respect to which species should be mitigated. This requires an emission metric whereby the global impact of emissions of different gases or aerosols with different atmospheric lifetimes and different radiative properties can be compared and weighted.

In the 1997 Kyoto Protocol, the target is formulated in terms of "$CO_2$ equivalents" using the Global Warming Potential (GWP) metric concept. The principle of comprehensiveness and cost effectiveness are made operative as the aggregate anthropogenic carbon dioxide equivalent emissions of six specified GHGs or groups of GHGs: carbon dioxide ($CO_2$), methane ($CH_4$), nitrous oxide ($N_2O$), hydrofluorocarbons (HFCs), perfluorocarbons (PFCs) and sulfur hexafluoride ($SF_6$) (Art. 3.1, Annex A). Note that apart from being used in binding agreements emission metrics can also be used to form a basis for common understanding of the climate impact that can be used for example when new technology standards are developed.

While a number of interactions between atmospheric chemistry and climate are now recognized, quantifying these interactions and their relative importance is more difficult and many uncertainties remain. Part of the difficulty in fully quantifying the relative importance of different climate–chemistry interactions is that the composition of the atmosphere and the climate processes are strongly coupled, thus a change in the emissions or concentration of one gas or particle can feedback on the atmospheric composition and climate in multiple ways. Furthermore, the large variability both in time and space in the secondary compounds like ozone and sulfate and organic particles make the quantification of the climate–chemistry interactions and adopting suitable metric for policy measures highly complex.

### *8.1. Climatic response to solar forcing: overview of theories*

Variations in solar activity may give rise to changes in Earth's atmosphere both in terms of energy as well as its composition.

Furthermore, some hypotheses suggest that cloud formation and the creation of cloud condensation nuclei may be linked indirectly to the level of solar activity through the action of galactic cosmic rays.

The notion that changes in the sun may affect weather on Earth is old and can be traced back to early discussions in the late 17th century (Benestad, 2002). It was established in 1896 (Kristian Birkeland) that Aurora was connected to the solar activity, and in more modern times an unequivocal response has been found in the upper atmosphere (Labitzke, 1987; Labitzke and van Loon, 1988; Haigh, 1994, 2003; Salby and Callagan, 2000, 2004; Shindell et al., 1999, 2001). But no definite and convincing evidence has yet been found suggesting a strong link for the troposphere and Earth's surface climate, although changes in the temperature structure in the stratosphere may affect the planetary wave dynamics and hence the advection of heat.

There have been many speculations over the past centuries about a solar connection to variations in quantities such as temperature, precipitation, and sea level pressure, and attempts to find a solar link. Friis-Christensen & Lassen (1991) presented an analysis suggesting a strong association between the warming over the 20th century in the northern hemisphere and the solar cycle length, but Laut (2003) and Damon & Laut (2004) reported errors in their analysis and argued that their conclusions were invalid. Subsequent analysis by Benestad (2005) also failed to reproduce their results. Furthermore, it is not clear how the temperature on Earth would be sensitive to the solar cycle length and exact which physical processes that would be involved.

Analysis by Crook and Gray (2005a,b) and Lean and Rind (2008) found a solar cycle signature in climatic variables, although these were weak compared to the internal variability. Furthermore, simulations with general circulation models (GCMs) also suggest a solar response, albeit modest (Cubash et al., 1997; Meehl et al., 2003). The level of solar activity is estimated to be high for this millennium (Solanki et al., 2004), however, direct modern instrument measurements indicate that the level of solar activity has not increased significantly over the last 30–50 years (Richardson et al., 2002; Lockwood and Frölich, 2007; Benestad, 2005).

Traditional studies have relied on empirical evidence and sunspot observations. More recently, additional indices as well as more physical variables, such as the total solar irradiance (TSI) and magnetic indices (Lockwoo, 2002) have been included in similar analyses. The level of solar output is however, still uncertain (Lean, 2006), and although several reconstructions of past variations have been published (Lean et al., 1995; Lean, 2004; Wang et al., 2005), there are still holes in our knowledge of past variations in solar forcings. Forster et al. (2007) estimated a radiative forcing due to an increase in TSI (1750–2005) of +0.12 (0.06–0.18) $W m^{-2}$ (90% confidence interval).

There are three main explanations for how changes in the sun may affect Earth's climate: (a) direct effect from TSI, (b) stratospheric response (Haigh, 1994, 2003), and (c) modification of clouds through shielding of galactic cosmic rays (GCR; Dickinson, 1975; Carslaw et al., 2002; Marsh and Svensmark, 2000).

Climatic response involving the stratosphere is believed to involve chemical reactions in the stratosphere (e.g. ozone), and the fact that solar UV varies strongly over a solar cycle compared to the total solar irradiance strongly suggests a mechanisms involving both atmospheric chemistry and a response in the atmospheric dynamics (e.g. wave propagation). However, the importance of this mechanism depends on whether the variations in the stratosphere have an influence on the lower troposphere.

While the direct TSI effect and stratospheric mechanism have been investigated in several modeling studies, the effect of GCR has been difficult to test in the GCMs. One problem with GCR and clouds is that the physical mechanisms are poorly known, and neither is it firmly established whether the GCR mechanism takes place in Earth's atmosphere. There have been several studies questioning the hypothesis due to a lack of empirical basis (Kristjánsson et al., 2008; Sloan and Wolfendale, 2008; Erlykin et al., 2009), but also some suggesting an effect of GCRs on clouds (Harrison and Stephenson, 2006; Knudsen and Riisager, 2009). However, the fact that clouds may be affected by either GCR or the atmospheric electric field does not necessarily imply the mechanism proposed by Marsh and Svensmark (2000), where GCR is alleged to produce higher low-cloud coverage, higher planetary albedo, and hence lower temperatures. Pierce and Adams (2009) attempted to model the effect of GCR on the low clouds, but found that the changes from the cloud condensation nuclei (CCN) due to changes in the GCR were two orders of magnitude too small to account for the observed variations in the cloud properties. For instance, while Knudsen and Riisager (2009) reported high correlation between $^{18}O$ records and the Earth's magnetic dipole moment and concluded that the tropical precipitation has been influenced by variations in the geomagnetic field, they also argued that their findings gives some support to the link between GCR particles, cloud formation, and climate. However, if GCRs result in an increase in the planetary albedo and hence a cooler climate, it is unclear how this could lead to higher rainfall in the tropics. On the other hand, the rainfall in the region of their study is strongly linked to the Monsoon system, and a latitudinal shift in the position of the system can easily translate into large increases or decreases locally. There have also been other claims of strong solar-terrestrial links even over the most recent decades (e.g. Scafetta and West, 2005), but these are controversial and have been disputed (Lean, 2006; Benestad and Schmidt, 2009). Furthermore, a lack of trend in the GCR since 1952 suggests that GCR is not responsible for the most recent global warming (Benestad, 2005), and recent trends in the stratosphere further disagree with the notion of recently enhanced levels of solar activity (IPCC, 2007).

### 8.2. Metrics

#### 8.2.1. Definition of a metric

In general the "$CO_2$ equivalents" emissions of any component is not linked exclusively to the GWP metric, but can be derived for any metric M by

$$Em(CO_2 - eq) = Em_i \cdot M_i \quad (1)$$

Where $M_i$ is the metric value for component $i$ and $Em_i$ is the emissions of component $i$. The metric value ($M_i$) will not ensure $CO_2$-equivalence in all aspects of climate change, but only with respect to the definition of the metric (O'Neill, 2000). For example the climate impact of emissions of 1 kg of methane (with $GWP_{100} = 25$) is only equal to that of 25 kg emission of $CO_2$ in that the integrated radiative forcing over 100 years after the emissions are equal. The more the physical properties (e.g., atmospheric lifetime) of component $i$ deviates from that of $CO_2$ (e.g., as for $NO_x$ and aerosols) the larger differences can be expected for other climate impacts (e.g., on other timescales) than the impacts that defines the metric.

The Kyoto Protocol excludes emissions of short-lived species including all types of aerosols, or their precursors, despite the fact that they are believed to contribute significantly to climate change. This could weaken efforts to mitigate climate change by weakening the comprehensive approach embodied in the UNFCCC; indeed, the U.S. administration has cited the absence of black carbon and tropospheric ozone from the Protocol as one reason why they have not become signatories. The absence could also lead to a distortion (for example, away from economically more efficient measures) of priorities in emission reductions.

It is important to stress that the choice of a given metric do not define the policy – they are tools that enable implementation of the policy. However, different policy frameworks require different metric concepts (e.g., Manne and Richels, 2001; Fuglestvedt et al., 2003; Shine et al., 2007; IPCC, 2009). For example the Global Temperature Potential (GTP, Shine et al., 2005) is more consistent with a climate policy with a long-term temperature target (e.g., EU 2 °C target) than the GWP metric used in the Kyoto Protocol.

*8.2.2. Special challenges for metrics of chemically active short-lived species*

Inclusion of chemically active short-lived components like aerosols and ozone precursors together with long-lived greenhouse gases in a climate policy using a common metric concept gives rise to several challenges. There are significant uncertainties in our quantitative understanding of the climate impacts for these species. This includes quantitative and even qualitative understanding of the many chemical and physical indirect effects. As an example of indirect effects, the current definition of $GWP_{100}$ for methane that is in operational use in the Kyoto Protocol, includes indirect effects on ozone and stratospheric water vapor (IPCC, 2001; Forster et al., 2007), but there may be further indirect effects of ozone on the carbon-cycle as discussed in Section 5.1.3 (Sitch et al., 2007). In addition, and maybe more importantly, there are also more fundamental methodological issues caused by the very wide range of lifetimes for the chemically active species compared to the long-lived greenhouse gases including $CO_2$. An emission pulse of a short-lived component will naturally give a climate response on a much shorter time scale. The climate response is dominated by the response time of the mixed layer of the ocean, i.e. 5–10 years (e.g., Hartmann, 1996).

Emissions of short-lived components will not lead to globally or hemispheric scale well mixed increases. A global metric value for each component as indicated in equation (1) (and applied in the form of GWPs in the Kyoto Protocol) may not be applicable to short-lived components, and metric values that are regionally dependent and possibly also time (e.g., seasonally) dependent should be used. However, policy makers may decide that metric values that depend on region and time are too difficult to handle in a negotiation process and instead accept the inaccuracies that are embedded in a global metric value if inclusion of short-lived species is deemed to be important.

Radiative forcing is the basis for the GWP metric based on the assumption that other climate impacts such as global mean temperature increase is scaling linearly with radiative forcing, i.e. that the efficacy (cf. Section 5) is equal for all forcing mechanisms. For most of the short-lived components there are indications that the efficacy is relatively close to 1.0 (Hansen et al., 2005; Forster et al., 2007), there are indications that the efficacy can be significantly enhanced for forcing mechanisms that is spatially correlated with regions of strong feedbacks or if species specific processes are involved. In particular will black carbon aerosols that are deposited on snow trigger a strong snow-albedo feedback with efficacy estimates in the range from 1.8 to 3.5 (Hansen et al., 2004; Flanner et al., 2007). If indirect cloud effects of aerosols, except the cloud–albedo effect (e.g., the cloud lifetime and semi-direct effects) are not considered as forcing mechanisms but rather as feedbacks (as in Forster et al., 2007) the net effect of these emissions may have a quite different efficacy than the LLGHGs.

Chemically active components and aerosols frequently cause negative radiative forcing and thus a cooling. For some components like $SO_2$ and organic carbon aerosols there will be a net cooling, while for other like $NO_x$ the warming (ozone) and cooling (decreased methane through increased OH and formation of nitrate aerosols) effects can be of similar magnitude. In the case of $NO_x$ the warming and cooling may cancel on a global and time-integrated level, but since the methane perturbation is much more long-lived, the cooling will affect both hemispheres while the warming will mainly be confined to the hemisphere where $NO_x$ is emitted. To what extent these cooling effects should be included in the metric values and thus in a policy aimed at reducing global warming is basically a political questions. For instance, whether or not to include $SO_2$ with a negative metric value is in many ways similar to the discussion about the use of geo-engineering to mitigate global warming (Crutzen, 2006; Rasch et al., 2008; Latham et al., 2008).

Emissions of chemically active short-lived species often lead to other non-climate environmental effects such as degradation of air quality, acid deposition and eutrophication. To the extent that these effects do not influence the climate parameter used to calculate the metric value, these effects should not be included in the metric value, but will, of course, in the end affect the policy development.

As discussed above there are significant uncertainties in our quantitative understanding of the climate impact of the chemically active short-lived species. A metric that is to be used in binding agreements needs to be relatively transparent and robust, robust in the sense that the scientific understanding must be sufficiently mature so that the metric value is not expected to change significantly with every new study. The many indirect effects are probably the main source of uncertainty (e.g. indirect aerosol effects, Section 5.4).

*8.2.3. Examples of published metrics*

Metrics have been developed by economists based on different kinds of optimization frameworks such as cost-benefit analysis (e.g., Kandlikar, 1995) and cost-effectiveness (e.g., Manne and Richels, 2001). Common for these metrics is that mitigation cost estimates and discount rates are needed and in the case of cost-benefit analysis also damage costs (could be positive or negative) of climate change are needed. These cost estimates are highly uncertain, and the determination of an appropriate discount rate is highly controversial.

Purely physical metrics have also been developed, the Global Warming Potential (GWP) being the most widely known and used through its inclusion in the Kyoto Protocol. The AGWP(H) (Absolute GWP) of a component *i* is defined as the integrated radiative forcing over a given time horizon (H) following a pulse emission of 1 kg of *i*.

$$\mathrm{AGWP}_i(\mathrm{H}) = \int_0^{\mathrm{H}} \mathrm{RF}_i(t)\cdot \mathrm{d}t \tag{2}$$

where $RF_i$ is the radiative forcing following a pulse emission of 1 kg of *i* at $t = 0$. The $GWP_i$ is defined as the ratio of $AGWP_i$ and the AGWP for $CO_2$ which is used as a reference gas.

If component *i* is decaying with a constant lifetime then

$$\mathrm{AGWP}_i(\mathrm{H}) = a_i \int_0^{\mathrm{H}} C_i(t)\mathrm{d}t = a_i \int_0^{\mathrm{H}} C_0\cdot \mathrm{e}^{-t/\tau}\cdot \mathrm{d}t \tag{3}$$

where $a_i$ is the radiative efficiency (RF per unit concentration change) and $C_i(t)$ is the concentration perturbation following a pulse emission of 1 kg of *i*, $C_0$ is the initial concentration perturbation at $t = 0$ and $\tau$ is the lifetime of component *i*.

A second purely physical metric, the Global Temperature Potential (GTP) has more recently been proposed (Shine et al., 2005). The AGTP(H) (absolute GTP) is defined as the temperature perturbation (global annual mean) at time H following a pulse emission at time $t = 0$ of 1 kg of component *i*. As for the GWP the GTP is defined as the ratio of $AGTP_i$ and the AGTP for $CO_2$. To derive

values for the GTP metric knowledge of the temporal response of the climate system to a perturbation is needed. Several methods have been proposed and used (Shine et al., 2005; Shine et al., 2007; Boucher and Reddy, 2008; Berntsen and Fuglestvedt, 2008), using both simple analytical climate models and impulse response functions fitted to AOGCMs. Consensus about what is the appropriate method has not yet been established.

Fig. 43 shows examples of published and derived metric values for $NO_x$ and BC particles (see Fuglestvedt et al., in press). For $NO_x$ it is the indirect effects through ozone formation (positive RF), and decrease in methane lifetime (negative RF) that is included. Due to the integrating nature of the GWP concept the strong, but short-term, positive RF caused by ozone production have a strong impact on the GWP even with a 100 year time horizon. For the GTP metric even after 20 years most of the warming of the ozone has disappeared and the more long-term cooling of methane reductions dominates giving negative GTP values.

Tol et al. (2008) show that the purely physical metrics GWP and GTP are special cases that can be derived through a number of simplifications from a cost-benefit analysis (GWP) and a cost-effective analysis (GTP).

Although there are significant uncertainties and it can be discussed if the GWP and GTP concepts are appropriate measures of the climate impacts due to emissions short-lived chemically active components, the metric values can be readily calculated based on results from chemistry-transport models (CTM) of GCMs with chemistry. Fuglestvedt et al. ( in press) give an overview of metric values for both the GWP and GTP for ozone precursors, $SO_2$, and carbonaceous aerosols with some information about regional differences.

### 8.3. Future directions for climate–chemistry research

#### 8.3.1. The role of model-observation and model-model comparisons

Studies of future climate–chemistry interactions rely heavily on how models can reproduce distribution and changes in the chemical active greenhouse gases. It has been demonstrated that there are significant uncertainties with the models, which should be demonstrated by a couple of examples: The global tropospheric concentration of OH, which is a key component in tropospheric oxidation, show large spread in the comparison given in Fig. 14 (Shindell et al., 2006). Likewise, aerosol burdens in state of the art models, given in Fig. 23 (the AeroCom experiment), reveal large uncertainties in model estimates.

One of the key first steps in quantifying climate–chemistry interactions and perform assessments of coupled climate–chemistry models is to improve the modeling tools through extensive comparisons with observations. Some past efforts have already been made towards assessing CCMs, including Austin et al. (2003), Eyring et al. (2005a,b, 2006).

There are a number of ongoing activities around the world to study various aspects of climate–chemistry interactions, in the troposphere and stratosphere. The international Aerosol model inter-Comparison (AeroCom), the ACCENT model inter-comparison, the assessment of the atmospheric impact of the transport sector in the EU funded project ATTICA and the Task Force on Hemispheric Transport of Atmospheric Pollutants (TF HTAP) focus on climate relevant modeling studies. Under AeroCom, global tropospheric aerosol models were compared and tested against satellite, lidar, and sun photometer measurements. The ACCENT-MIP effort previously focused on coordinating and comparing IPCC scenarios (Nakicenovic et al., 2000), contrasting the climate in 2030 vs. 2000 across a suite of tropospheric chemistry–climate models, with a goal towards capturing how climate change might affect air quality (gas species only). This effort is extended to encompass the activities of the TF HTAP. The activities focus on understanding and quantifying northern hemispheric transport of gaseous and particulate air pollutants and their precursors from source to receptor regions.

A major new international effort towards analyzing climate–chemistry models is being coordinated, called the Atmospheric Chemistry and Climate (AC&C) Initiative. The focus of AC&C is on identifying science issues, providing analysis tools, coordinating and integrating activities, and furthermore to provide input on climate–chemistry interactions to the IPCC process.

#### 8.3.2. Other issues in improved modeling of chemistry–climate interactions

As noted already, advancing the quantification of climate–chemistry interactions will also require improvement in the fundamental building blocks of our understanding of tropospheric and stratospheric chemical and physical processes. These include improvements in characterizing the rates of gas phase, heterogeneous, and photolytic processes; process studies in the atmosphere to test our understanding of the chemical processes; and incorporation of these processes in a realistic way in global climate–chemistry models.

Long-term monitoring and observation is a prerequisite to better understand and quantify the key atmospheric processes affecting climate–chemistry interactions. These observations are also a key to determining the scientific basis for understanding how and why changes are occurring. Although significant

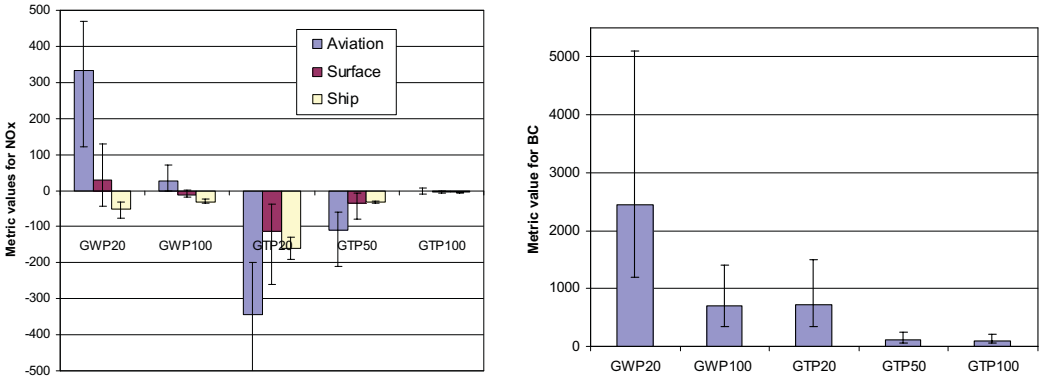


**Fig. 43.** Overview of published and derived metric values for $NO_x$ and BC emissions (based on Fuglestvedt et al., in press). The metrics shown are GWPs with 20 and 100 year time horizons, and GTPs with 20, 50 and 100 years time horizons. The error bars indicate the full range of values across regions of emissions and published studies. For $NO_x$ it is distinguished between emissions from aviation, shipping and surface land sources.

amounts of data for large-scale model validation and process studies have been made available during the last decade, in particular satellite observations, the actual needs for observing the Earth's system are expanding and require more complex experiments covering a wide range of instruments and observed species on a global spatial and temporal scale. The value of an integrated global observing system is worldwide recognized as the only way to produce systematic, coherent data, capable of addressing climate related issues on a global scale. The different platforms used for data collection play complementary roles in the establishment of long-term monitoring capability of global coverage for process and global changes studies, and remain essential to constrain models and predict the future of our planet with reduced uncertainties.

## 9. Summary and conclusions

Potentially significant contributions to the climate impact are provided by compounds like $CO_2$, $CH_4$, $O_3$, particles and cirrus clouds. For the chemically active gases processes in the atmosphere are important, with large spatial and temporal variations. The climate–chemistry interactions are therefore characterized by significant regional differences with regions as Southeast Asia being a future key region due to significant increases in energy use, and pollution emission (Akimoto, 2003; Kupiainen and Klimont, 2007; Amann et al., 2008; Klimont et al., 2009; Isaksen et al., 2009). Likewise, ship and air traffic represent important sectors because of significant increases in emissions in recent years (Eyring et al., 2005a,b, 2007a; Dalsøren et al., 2009a; Lee et al., 2009). The relative contributions to the emissions from various sectors are expected to change significantly over the next few decades due to differences in mitigation options and costs.

Our ability to predict the extensive interaction between climate and chemistry has improved significantly over the last decade due to an extensive increase in observational data and computer resources, which has led to improved large-scale modeling capability for tropospheric distribution and trends. Both CTMs and CCMs are available (Eyring et al., 2005a,b; Bousquet et al., 2006; Gauss et al., 2006; Stevenson et al., 2006) with more extensive chemical processes included and higher resolutions, and with observations available for model evaluation and long-term model analysis, in particular satellite observations (Gerasopoulos et al., 2005; Richter et al., 2005; Laj et al., 2009). Extensive multi-model comparisons and studies of emission impact have been performed in projects like ACCENT, AEROCOM, and QUANTIFY during the last few years. This demonstrates our ability to model man made impact on atmospheric composition of chemically active climate compounds (Shindell et al., 2006; Stevenson et al., 2006; Textor et al., 2006, Textor et al., 2007; Hoor et al., 2009; Fiore et al., 2009). These model comparisons show, however, that there are significant model to model differences.

New satellite observations have provided data on the global distribution of tropospheric column burden of ozone and methane, as well as a number of ozone precursors ($NO_2$, CO, and HCHO) (Laj et al., 2009). Over the last two decades tropospheric ozone trends from surface observations give a mixed signal depending on regional trends in emissions of ozone precursors and possibly an influence of a reversed trend in the influx of stratospheric ozone (Ordóñez et al., 2007). Shindell et al. (2006) report that a significant fraction of the increase in tropospheric ozone since preindustrial time may have been reduced due to stratospheric ozone depletion. Referring to changes since the 1970s Ordóñez et al. (2007) came to the same conclusion. Models driven by changes in emissions are capable of capturing some but not all of the features of the observed trends in tropospheric ozone. A key point here is the difference in emissions from different emission sectors, and a number of studies have focused specifically on attributing changes in atmospheric concentrations to specific emission sectors. For instance, it is possible that the large increase in emissions during the last decade (Eyring et al., in preparation; Dalsøren et al., 2009a), from ocean going ship, may have led to increases in observed ozone at costal stations in Europe and the western US.

OH is the key compound in the tropospheric oxidation process (Monks et al., 2009). Long-term trend in global OH is significant for methane trend. Observations show that methane concentrations leveled off during the last decade, although there was a significant increase between 2007 and 2008. It is debated if the leveling off in methane is primarily caused by a leveling off in the emissions or if the primary cause is an increase in global OH levels, possibly caused by an increase in the NO/CO ratio in global emissions (Dalsøren and Isaksen, 2006). Although there is a general understanding of the OH distribution, there are significant uncertainties connected to OH trends and to processes affecting distribution and trends (Cariolle et al., 2008). $NO_x$ emissions from ship traffic represent a particularly important source for atmospheric OH (Eyring et al., in preparation; Hoor et al., 2009; Dalsøren et al., 2009a). Surface emissions of $NO_x$ in pristine areas from ship efficiently increase OH, thereby reducing methane lifetime and atmospheric methane. It has been shown that the efficient methane reduction together with aerosol emissions give a negative radiative forcing for current ship traffic. Future long-term impact will depend on mitigation measures adopted to reduce emissions (reduction of sulfur and $NO_x$ emissions).

For aerosols a number of satellite retrievals of bulk aerosol properties backed up by surface measurements and in-situ campaigns have improved the understanding of the global distribution of aerosols significantly. Extensive model validation and inter-comparisons within the AEROCOM project have revealed significant inter-model differences and discrepancies compared to observations. Differences are mainly originating from differences in model constructions (Textor et al., 2006; Schulz et al., 2006; Textor et al., 2007). Anthropogenic aerosols' ability to alter the radiative budget has been singled out as the most uncertain contributor to the total anthropogenic forcing of the Earth-atmosphere system (Forster et al., 2007). Several recent studies improve our understanding of the RF from different climate compounds. In a new study, combining models and satellite data, Myhre (2009) estimates the RF due to the direct effect of aerosols to be around $-0.3\ W\,m^{-2}$, with halved uncertainty range compared to the estimates by IPCC (Forster et al., 2007).

Although the cloud albedo effect has been studied extensively for several decades, it is still characterized by a low level of understanding. A number of studies on aerosol indirect effects have been published since IPCC AR4, showing that the scientific community is currently making an effort to increase the knowledge and reduce uncertainties associated with aerosol indirect effects. Continued use of satellite data combined with models, and continuous improvements of cloud parameterizations, may reduce the uncertainties in model estimates (Anderson et al., 2003) of the aerosol indirect effect. The comparison of the spread in estimates of indirect aerosol effects in Fig. 29 shows that the uncertainties have not decreased with time. In fact, estimates span a larger range than ever, much due to the new aerosol indirect effects recently taken into account.

A number of climate processes that influence the levels of methane, tropospheric ozone and the oxidation capacity have been identified through recent studies and to some extent quantified through sensitivity experiments in models. These processes include: Change in OH from temperature and humidity perturbations, change in tropospheric ozone through STE exchange and changes in stratospheric ozone; enhancements in methane emissions from melting permafrost, changes in $NO_x$ emissions from lightning, and

change in biogenic VOC and $NO_x$ emissions from changes in surface characteristics (humidity, temperature) (Zeng and Pyle, 2003; Collins et al., 2003; Isaksen et al., 2005; Horowitz et al., 2007; Sitch et al., 2007; Walter et al., 2006a,b; Wu et al., 2008b).

Models have been used for sensitivity studies and for studies of changes in tropospheric and surface ozone for 2030, 2050 and 2100 due to both emission changes and climate change (Prather et al., 2003; Stevenson et al., 2006; Royal Society, 2008). Differences in assumptions about improvements in control of precursor emissions have significant impacts on future tropospheric ozone concentrations over the 30-year period from 2000 to 2030. An increase between 10 and 14 ppb in annual zonal-mean ozone at 30 °N is calculated for the unregulated SRES A2 case, and a decrease of up to 6 ppb for the B2 + MFR (Maximum feasible reduction) case. Changes in climate are found to slightly reduce the amount of tropospheric ozone, through enhanced OH formation. Model studies of OH concentrations in 2030 and 2050 indicate that global OH concentrations will increase slightly due to emission changes, but that this increase will be more than compensated by effects of climate change. Higher temperatures give more water vapor and enhanced OH production.

Changes in chemically active greenhouse gases and aerosols have contributed significantly to the overall radiative forcing since pre-industrial times. Two considerations are important in for estimates of future climate impact from man-made emissions: The short chemical lifetime of most of the important chemically active climate compounds as compared to $CO_2$, and the possibility for mitigation options to reduce emissions. It is likely that in the future the relative contribution from the chemically active climate compounds become smaller compared to the contribution from $CO_2$. A consequence of the large differences in the lifetimes of the climate compounds is that future effects are strongly dependent on the scenarios adopted for emissions, and it is not obvious what type of metric should be adopted (Shine et al., 2005; Shine et al., 2007; Berntsen and Fuglestvedt, 2008; Boucher and Reddy, 2008; Fuglestvedt et al., in press). Continued growth in emissions, for instance, favors impact from the short-lived compounds.

Long-term monitoring and observation is a prerequisite to better understand and quantify the key atmospheric processes affecting climate–chemistry interactions. These observations are also a key to building the scientific basis for understanding how and why changes are occurring. Although significant amounts of data for large-scale model validation and process studies have been made available during the last decade, in particular satellite observations (see Laj et al., 2009), the actual needs for observing the Earth's system are expanding and require more complex experiments covering a wide range of instruments and observed species on a global spatial and temporal scale. A key question is the issue of the natural variability of composition on different scales associated with the climate variability, which indicate that longer, and possibly ensemble simulations, may be required to extract the signal of anthropogenic climate change on composition from that related to natural climate variability.

## Acknowledgements

Significant parts of the work reported in this article are based on studies performed in the EU projects ACCENT, ATTICA, QUANTIFY, EUCAARI and HYMN. We are thankful to Dr. Corinna Hoose for making Fig. 28 available and to Dr. Keith Shine for valuable discussions and for his contribution to the article. We are thankful to the ACCENT project office for their support in the preparation of the article.

## References

Abbot, D.S., Palmer, P.I., Martin, R.V., Chance, K.V., Jacob, D.J., Guenther, A., 2003. Seasonal and inter-annual variability of North American isoprene emissions as determined by formaldehyde column measurements from space. Geophysical Research Letters 30 (17), 1886. doi:10.1029/2003GL017336.

Ackerman, A.S., et al., 2000. Effects of aerosols on cloud albedo: evaluation of Twomey's parameterization of cloud susceptibility using measurements of ship tracks. Journal of Atmospheric Science 57, 2684–2695.

Adams, P.J., Seinfeld, J.H., Koch, D., Mickley, L., Jacob, D., 2001. General circulation model assessment of direct radiative forcing by the sulfate–nitrate–ammonium–water inorganic aerosol system. Journal of Geophysical Research 106 (D1), 1097–1111.

Akimoto, H., 2003. Global air quality and pollution. Science 302 (5651), 1716–1719. doi:10.1126/science.1092666.

Albrecht, B.A., 1989. Aerosols, cloud microphysics, and fractional cloudiness. Science 245, 1227–1230.

Allen, R.J., Sherwood, S.C., 2008. Warming maximum in the tropical upper troposphere deduced from thermal wind observations. Nature Geoscience 65, 399–403.

Alpert, P., Kishcha, P., Kaufman, Y.J., Schwarzbard, R., 2005. Global dimming or local dimming?: effect of urbanization on sunlight availability. Geophysical Research Letters 32, L17802. doi:10.1029/2005GL023320.

Amann, M., Cofala, J., Heyes, C., Klimont, Z., Mechler, R., Posch, M., Schöpp, W., 2004. The RAINS Model. Documentation of the Model Approach Prepared for the RAINS Review. International Institute for Applied Systems Analysis (IIASA), Laxenburg, Austria.

Amann, M., Bertok, I., Cofala, J., Heyes, C., Klimont, Z., Rafaj, P., Schöpp, W., Wagner, F., 2008. National emission Ceilings for 2020 based on the 2008 Climate & Energy Package. NEC Report 6. Final report to the European Commission. Available at: www.iiasa.ac.at/rains/reports/NEC6-final110708.pdf.

Anderson, T.L., Charlson, S.E., Schwartz, S.E., Knutti, R., Boucher, O., Rodhe, H., Heintzenberg, J., 2003. Climate forcing by a aerosols – a hazy picture. Science 300, 1103–1104.

Arneth, A., Miller, P.A., Scholze, M., Hickler, T., Schurgers, G., Smith, B., Prentice, I.C., 2007. $CO_2$ inhibition of global terrestrial isoprene emissions: potential implications for atmospheric chemistry. Geophysical Research Letters 34, L18813. doi:10.1029/2007GL030615.

Austin, J., Shindell, D., Beagley, S.R., Brühl, C., Dameris, M., Manzini, E., Nagashima, T., Newman, P., Pawson, S., Pitari, G., Rozanov, E., Schnadt, C., Shepherd, T.G., 2003. Uncertainties and assessments of chemistry–climate models of the stratosphere. Atmospheric Chemistry and Physics 3, 1–27.

Aw, J., Kleeman, M.J., 2003. Evaluating the first-order effect of intra-annual temperature variability on urban air pollution. Journal of Geophysical Research 108, 4365. doi:10.1029/2002JD002688.

Baker, M.B., Peter, T., 2008. Small-scale cloud processes and climate. Nature 451, 299–300.

Barnard, J.C., Volkamer, R., Kassianov, E.I., 2008. Estimation of the mass absorption cross section of the organic carbon component of aerosols in the Mexico City Metropolitan Area. Atmospheric Chemistry and Physics 8, 6665–6679.

Bauer, S.E., Koch, D., Unger, N., Metzger, S.M., Shindell, D.T., Streets, D.G., 2007. Nitrate aerosols today and in 2030: a global simulation including aerosols and tropospheric ozone. Atmospheric Chemistry and Physics 7 (19), 5043–5059.

Beirle, S., Platt, U., von Glasow, R., Wenig, M., Wagner, T., 2004. Estimate of nitrogen oxide emissions from shipping by satellite remote sensing. Geophysical Research Letters 31 (18).

Beirle, S., Spichtinger, N., Stohl, A., Cummins, K.L., Turner, T., Boccippio, D., Cooper, O.R., Wenig, M., Grzegorski, M., Platt, U., Wagner, T., 2006. Estimating the NOx produced by lightning from GOME and NLDN data: a case study in the Gulf of Mexico. Atmospheric Chemistry and Physics 6, 1075–1089.

Bellouin, N., Boucher, O., Haywood, J., Reddy, M.S., 2005. Global estimate of aerosol direct radiative forcing from satellite measurements. Nature 438 (7071), 1138–1141.

Bellouin, N., Jones, A., Haywood, J., Christopher, S.A., 2008. Updated estimate of aerosol direct radiative forcing from satellite observations and comparison against the Hadley Centre Climate Model. Journal Geophysical Research 113 (D10), D10205.

Benestad, R.E., 2002. Solar Activity and Earth's Climate. Praxis-Springer, Berlin and Heidelberg.

Benestad, R.E., 2005. A review of the solar cycle length estimates. Geophysical Research Letters 32. doi:10.1029/2005GL023621.

Benestad, R.E., Schmidt, G.A., 2009. Solar trends and global warming. Journal of Geophysical Research 114, D14101. doi:10.1029/2008JD011639.

Benson, D.R., Young, L.-H., Lee, S.-H., Campos, T.L., Rogers, D.C., Jensen, J., 2008. The effects of airmass history on new particle formation in the free troposphere: case studies. Atmospheric Chemistry and Physics 8, 3015–3024.

Bergamaschi, P., Frankenberg, C., Meirink, J.F., Krol, M., Dentener, F., Wagner, T., Platt, U., Kaplan, J.O., Körner, S., Heimann, M., Dlugokencky, E.J., Goede, A., 2007. Satellite chartography of atmospheric methane from SCIAMACHY on board ENVISAT: 2. Evaluation based on inverse model simulations. Journal of Geophysical Research 112, D02304. doi:10.1029/2006JD007268.

Bergin, M.S., West, J.J., Keating, T.J., Russell, A.G., 2005. Regional Atmospheric pollution and transboundary air quality management. Annual Review of Environment and Resources 30, 1–37. doi:10.1146/annurev.energy.30.050504.144138.

Berntsen, T.K., Isaksen, I.S.A., Myhre, G., Fuglestvedt, J.S., Stordal, F., Larsen, T.A., Freckleton, R.S., Shine, K.P., 1997. Effects of anthropogenic emissions on tropospheric ozone and its radiative forcing. Journal of Geophysical Research 102 (D23), 28101–28126. 10.1029/97JD02226.

Berntsen, T.K., Fuglestvedt, J., Myhre, G., Stordal, F., Berglen, T.F., 2006. Abatement of greenhouse gases: does location matter? Climatic Change 74 (4), 377–411.
Berntsen, T., Fuglestvedt, J.S., 2008. Global temperature responses to current emissions from the transport sectors. Proceedings of the National Academy of Sciences 105 (49), 19154–19159.
Berresheim, H., Plass-Dülmer, C., Elste, T., Mihalopoulos, N., Rohrer, F., 2003. OH in the coastal boundary layer of Crete during MINOS: measurements and relationship with ozone photolysis. Atmospheric Chemistry and Physics 3, 639–649.
Bertram, T.H., Heckel, A., Richter, A., Burrows, J.P., Cohen, R.C., 2005. Satellite measurements of daily variations in soil $NO_x$ emissions. Geophysical Research Letters 32 (24).
Bian, H., Chin, M., Rodriguez, J., Yu, H., Penner, J.E., Strahan, S., 2009. Sensitivity of aerosol optical thickness and aerosol direct radiative effect to relative humidity. Atmospheric Chemistry and Physics 9, 2375–2386.
Bloss, W.J., Lee, J.D., Heard, D.E., Salmon, R.A., Bauguitte, S.J.-B., Roscoe, H.K., Jones, A.E., 2007. Observations of OH and $HO_2$ radicals in coastal Antarctica. Atmospheric Chemistry and Physics 7, 4171–4185.
Boersma, K.F., Eskes, H.J., Meijer, E.W., Kelder, H.M., 2005. Estimates of lightning $NO_x$ production from GOME satellite observations. Atmospheric Chemistry and Physics 5, 2311–2331.
Bond, T.C., Streets, D.G., Yarber, K.F., Nelson, S.M., Woo, J.H., Klimont, Z., 2004. A technology-based global inventory of black and organic carbon emissions from combustion. Journal of Geophysical Research 109, D14203. doi:10.1029/2003JD003697.
Bond, T.C., Bergstrom, R.W., 2006. Light absorption by carbonaceous particles: an investigative review. Aerosol Science And Technology 40 (1), 27–67.
Bond, T.C., Habib, G., Bergstrom, R.W., 2006. Limitations in the enhancement of visible light absorption due to mixing state. Journal of Geophysical Research 111 (D20), D20211.
Bond, T.C., Bhardwaj, E., Dong, R., Jogani, R., Jung, S., Roden, C., Streets, D.G., Trautmann, N.M., 2007. Historical emissions of black and organic carbon aerosol from energy-related combustion, 1850–2000. Global Biogeochemical Cycles 21, GB2018. doi:10.1029/2006GB002840.
Boucher, O., Myhre, G., Myhre, A., 2004. Direct human influence of irrigation on atmospheric water vapour and climate. Climate Dynamics 22 (6–7), 597–603.
Boucher, O., Reddy, M.S., 2008. Climate trade-off between black carbon and carbon dioxide emissions. Energy Policy 36, 193–200.
Bousquet, P., Hauglustaine, D.A., Peylin, P., Carouge, C., Ciais, P., 2005. Two decades of OH variability as inferred by an inversion of atmospheric transport and chemistry of methyl chloroform. Atmospheric Chemistry and Physics 5, 2635–2656.
Bousquet, P., Ciais, P., Miller, J.B., Dlugokencky, E.J., Hauglustaine, D.A., Prigent, C., Van der Werf, G.R., Peylin, P., Brunke, E.G., Carouge, C., Langenfelds, R.L., Lathiere, J., Papa, F., Ramonet, M., Schmidt, M., Steele, L.P., Tyler, S.C., White, J., 2006. Contribution of anthropogenic and natural sources to atmospheric methane variability. Nature 443, 439–443.
Bouwman, A.F., von Duuren, D.P., Derwent, R.G., Posch, M., 2002. A global analysis of acidification and eutrophication of terrestrial ecosystems. Water, Air, and Soil Pollution 141, 349–382.
Bovensmann, H., Burrows, J.P., Buchwitz, M., Frerick, J., Noël, S., Rozanov, V.V., Chance, K.V., Goede, A.P.H., 1999. SCIAMACHY: mission objectives and measurement modes. Journal of the Atmospheric Sciences 56 (2), 127–150.
Brunner, D., Staehelin, J., Rogers, H.L., Kohler, M.O., Pyle, J.A., Hauglustaine, D.A., Jourdain, L., Berntsen, T.K., Gauss, M., Isaksen, I.S.A., Meijer, E., van Velthoven, P., Pitari, G., Mancini, E., Grewe, V., Sausen, R., 2005. An evaluation of the performance of chemistry transport models – part 2: detailed comparison with two selected campaigns. Atmospheric Chemistry and Physics 5, 107–129.
Buchwitz, M., de Beek, R., Burrows, J.P., Bovensmann, H., Warneke, T., Notholt, J., Meirink, J.F., Goede, A.P.H., Bergamaschi, P., Korner, S., Heimann, M., Schulz, A., 2005. Atmospheric methane and carbon dioxide from SCIAMACHY satellite data: initial comparison with chemistry and transport models. Atmospheric Chemistry and Physics 5, 941–962.
Buffett, B., Archer, D., 2004. Global inventory of methane clathrate: sensitivity to changes in the deep ocean. Earth and Planetary Science Letters 227, 185–199.
Burrows, J.P., Weber, M., Buchwitz, M., Rozanov, V., Landstätter-Weißenmayer, A., Richter, A., Debeek, R., Hoogen, R., Bramstedt, K., Eichmann, K.-U., Eisinger, M., Perner, D., 1999. The global ozone monitoring experiment (GOME): mission concept and first scientific results. Journal of the Atmospheric Sciences 56 (2), 151–175.
Butchart, N., Scaife, A.A., 2001. Removal of chlorofluorocarbons by increased mass exchange between the stratosphere and troposphere in a changing climate. Nature 410 (6830), 799–802.
Butchart, N., et al., 2006. Simulations of anthropogenic change in the strength of the Brewer–Dobson circulation. Climate Dynamics 27, 727–741.
Butkovskaya, N., Kukui, A., Le Bras, G., 2007. $HNO_3$ forming channel of the $HO_2 + NO$ reaction as a function of pressure and temperature in the ranges of 72−600 Torr and 223–323 KJ. Physics and Chemistry A 111 (37), 9047–9053. doi:10.1021/jp074117m.
Butler, T.M., Rayner, P.J., Simmonds, I., Lawrence, M.G., 2005. Simultaneous mass balance inverse modeling of methane and carbon monoxide. Journal of Geophysical Research 110, D21310. doi:10.1029/2005JD006071.
Callies, J., Corpaccioli, E., Eisinger, M., Hahne, A., Lefebvre, A., 2000. GOME-2-MetOp's second generation sensor for operational ozone monitoring. ESA Bulletin 102.
Cariolle, D., Morcrette, J.-J., 2006. A linearized approach to the radiative budget of the stratosphere: influence of the ozone distribution. Geophysical Research Letters 33, L05806. doi:10.1029/2005GL025597.
Cariolle, D., Evans, M.J., Chipperfield, M.P., Butkovskaya, N., Kukui, A., Le Bras, G., 2008. Impact of the new $HNO_3$-forming channel of the $HO_2 + NO$ reaction on tropospheric $HNO_3$, $NO_x$, $HO_x$ and ozone. Atmospheric Chemistry and Physics 8, 4061–4068.
Carslaw, K.S., Harrison, R.G., Kirkby, J., 2002. Cosmic rays, clouds, and climate. Science 298, 1732–1737.
Carslaw, K.S., Boucher, O., Spracklen, D.V., Mann, G.W., Rae, J.G.L., Woodward, S., Kulmala, M., 2009. Atmospheric aerosols in the earth system: a review of interactions and feedbacks. Atmospheric Chemistry and Physics Discussions 9, 11087–11183.
Chance, K., Palmer, P.I., Spurr, R.J.D., Martin, R.V., Kurosu, T.P., Jacob, D.J., 2000. Satellite observations of for, Corpaccioli, E., Eisinger, M., Hahne, A., Lefebvre, A., 2000. GOME-2-MetOp's second generation sensor for operational ozone monitoring maldehyde over North America from GOME. Geophysical Research Letters, 27 (21), 3461–3464.
Chandra, S., Ziemke, J.R., Stewart, R.W., 1999. An 11-year solar cycle in tropospheric ozone from TOMS measurements. Geophysical Research Letters 26 (2), 185–188.
Chen, Y.H., Prinn, R.G., 2006. Estimation of atmospheric methane emissions between 1996 and 2001 using a three-dimensional global chemical transport model. Journal of Geophysical Research 111. doi:10.1029/2005JD006058.
Cheng, C.-T., Wang, W.-C., Chen J.-, P., 2007. A modeling study of aerosol impacts on cloud microphysics and radiative properties. Quarterly Journal of the Royal Meteorological Society 133, 283–297.
Chung, C.E., Ramanathan, V., Kim, D., Podgorny, I.A., 2005. Global anthropogenic aerosol direct forcing derived from satellite and ground-based observations. Journal of Geophysical Research 110 (D24), D24207.
Chung, S.H., Seinfeld, J.H., 2002. Global distribution and climate forcing of carbonaceous aerosols. Journal of Geophysical Research 107 (D19), 4407.
Clarke, A.D., Noone, K.J., 1985. Soot in the Arctic snowpack: a cause for perturbations in radiative transfer. Atmospheric Environment 19, 2045–2053.
Clerbaux, C., Boynard, A., Clarisse, L., George, M., Hadji-Lazaro, J., Herbin, H., Hurtmans, D., Pommier, M., Razavi, A., Turquety, S., Wespes, C., Coheur, P.-F., 2009. Monitoring of atmospheric composition using the thermal infrared IASI/MetOp sounder. Atmospheric Chemistry and Physics 9, 6041–6054.
Cofala, J., Amann, M., Klimont, Z., Kupiainen, K., Höglund-Isaksson, L., 2007. Scenarios of global anthropogenic emissions of air pollutants and methane until 2030. Atmospheric Environment 41, 8486–8499. doi:10.1016/j.atmosenv.2007.07.010.
Collins, W.J., Stevenson, D.S., Johnson, C.E., Derwent, R.G., 2000. The European regional ozone distribution and its links with the global scale for the years 1992 and 2015. Atmospheric Environment 34, 255–267.
Collins, W.J., Derwent, R.G., Garnier, B., Johnson, C.E., Sanderson, M.G., Stevenson, D.S., 2003. The effect of stratosphere–troposphere exchange on the future tropospheric ozone trend. Journal of Geophysical Research 108. doi:10.1029/2002JD002617.
Collins, W.J., Sanderson, M.G., Johnson, C.E., 2009. Impact of increasing ship emissions on air quality and deposition over Europe by 2030. Meteorologische Zeitschrift 18, 25–39.
Cook, J., Highwood, E.J., 2004. Climate response to tropospheric absorbing aerosols in an intermediate general-circulation model. Quarterly Journal of the Royal Meteorological Society 130 (596), 175–191.
Crook, S.A., Gray, L.J., 2005a. Characterization of the 11-year solar signal using a multiple regression analysis of the ERA-40 dataset. Journal of Climate 18, 996–1015.
Crosier, J., Allan, J.D., Coe, H., Bower, K.N., Formenti, P., Williams, P.I., 2007. Chemical composition of summertime aerosol in the Po Valley (Italy), northern Adriatic and Black Sea. Quarterly Journal of the Royal Meteorological Society 133, 61–75.
Crook, S.A., Gray, L.J., 2005. Characterization of the 11-year solar signal using a multiple regression analysis of the ERA-40 dataset. 18, 996–1014.
Crutzen, P.J., 2006. Albedo enhancement by stratospheric sulfur injections: A contribution to resolve a policy dilemma? Climate Change 77, 211–220. doi:10.1007/s10584-006-9101-y.
Cubash, U., Voss, R., Hegerl, G.C., Waszkewitz, J., Crowley, T.J., 1997. Simulation of the influence of solar radiation variations on the global climate with an ocean–atmosphere general circulation model. Climate Dynamics 13, 757–767.
Curry, C.L., 2007. Modeling the soil consumption of atmospheric methane at the global scale. Global Biogeochemistry Cycles 21, GB4012. doi:10.1029/2006GB002818.
Dalsøren, S.B., Isaksen, I.S.A., 2006. CTM study of changes in tropospheric hydroxyl distribution 1990–2001 and its impact on methane. Geophysical Research Letters 33, L23811. doi:10.1029/2006GL027295.
Dalsøren, S.B., Endresen, Ø., Isaksen, I.S.A., Gravir, G., Sørgård, E., 2007. Environmental impacts of the expected increase in sea transportation, with a particular focus on oil and gas scenarios for Norway and northwest Russia. Journal of Geophysical Research 112, D02310. doi:10.1029/2005JD006927.
Dalsøren, S.B., Eide, M.S., Endresen, Ø., Mjelde, A., Gravir, G., Isaksen, I.S.A., 2009a. Update on emissions and environmental impacts from the international fleet of ships: the contribution from major ship types and ports. Atmospheric Chemistry and Physics 9, 2171–2194.
Dalsøren, S.B., Isaksen, I.S.A., Li, L., Richter, A., 2009b. Effect of emission changes in Southeast Asia on global hydroxyl and methane lifetime. Tellus B 61 (4), 588–601. doi:10.1111/j.1600-0889.2009.00429.x.

Damon, P.E., Laut, P., 2004. Pattern of strange errors plagues solar activity and terrestrial climate data. Eos 85 (39), 370.

Damoah, R., Spichtinger, N., Servranckx, R., Fromm, M., Eloranta, E.W., Razenkov, I.A., James, P., Shulski, M., Forster, C., Stohl, A., 2006. A case study of pyro-convection using transport model and remote sensing data. Atmospheric Chemistry and Physics 6, 173–185.

Dawson, J.P., Adams, P.J., Pandis, S.N., 2007. Sensitivity of PM2.5 to climate in the Eastern US: a modeling case study. Atmospheric Chemistry and Physics 7, 4295–4309.

De Smedt, I., Müller, J.-F., Stavrakou, T., van der, A.R., Eskes, H., Van Roozendael, M., 2008. Twelve years of global observation of formaldehyde in the troposphere using GOME and SCIAMACHY sensors. Atmospheric Chemistry and Physical 8, 4947–4963.

Delmonte, B., Basile-Doelsch, I., Petit, J.-R., Maggi, V., Revel-Rolland, M., Michard, A., Jagoutz, E., Grousset, F., 2004. Comparing the Epica and Vostok dust records during the last 220,000 years: stratigraphical correlation and provenance in glacial periods. Earth-Science Reviews 66, 63–87.

DeMott, P.J., Rogers, D.C., Kreidenweis, S.M., 1997. The susceptibility of ice formation in upper tropospheric clouds to insoluble aerosol components. Journal of Geophysical Research 102, 19575–19584.

Denman, K.L., Brasseur, G., Chidthaisong, A., Ciais, P., Cox, P.M., Dickinson, E.E., Hauglustaine, D., Heinze, C., Holland, E., Jacob, D., Lohmann, U., Ramachandran, S., da Silva Dias, P.L., Wofsy, S.C., Zhang, X., 2007. Couplings between changes in the climate system and biogeochemistry. In: Solomon, S., Qin, D., Manning, M., Chen, Z., Marquis, M., et al. (Eds.), Climate Change 2007: the Physical Science Basis. Contribution of Working Group I to the Fourth Assessment Report of the Intergovernmental Panel on Climate Change. Cambridge University Press, United Kingdom and New York, NY, USA.

Dentener, F., Stevenson, D., Cofala, J., Mechler, R., Amann, M., Bergamaschi, P., Raes, F., Derwent, R., 2005. The impact of air pollutant and methane emission controls on tropospheric ozone and radiative forcing: CTM calculations for the period 1990–2030. Atmospheric Chemistry and Physics 5, 1731–1755.

Dentener, F., Drevet, J., Lamarque, J.F., Bey, I., Eickhout, B., Fiore, A.M., Hauglustaine, D., Horowitz, L.W., Krol, M., Kulshrestha, U.C., Lawrence, M., Galy-Lacaux, C., Rast, S., Shindell, D., Stevenson, D., Van Noije, T., Atherton, C., Bell, N., Bergman, D., Butler, T., Cofala, J., Collins, B., Doherty, R., Ellingsen, K., Galloway, J., Gauss, M., Montanaro, V., Müller, J.F., Pitari, G., Rodriguez, J., Sanderson, M., Solmon, F., Strahan, S., Schultz, M., Sudo, K., Szopa, S., Wild, O., 2006. Nitrogen and sulfur deposition on regional and global scales: a multimodel evaluation. Global Biogeochemistry Cycles 20, GB4003. doi:10.1029/2005GB002672.

Dentener, F., Stevenson, D., Ellingsen, K., van Noije, T., Schultz, M., Amann, M., Atherton, C., Bell, N., Bergmann, D., Bey, I., Bouwman, L., Butler, T., Cofala, J., Collins, B., Drevet, J., Doherty, R., Eickhout, B., Eskes, H., Fiore, A., Gauss, M., Hauglustaine, D., Horowitz, L., Isaksen, I.S.A., Josse, B., Lawrence, M., Krol, M., Lamarque, J.F., Montanaro, V., Müller, J.F., Peuch, V.H., Pitari, G., Pyle, J., Rast, S., Rodriguez, J., Sanderson, M., Savage, N.H., Shindell, D., Strahan, S., Szopa, S., Sudo, K., Van Dingenen, R., Wild, O., Zeng, G., 2006a. Global atmospheric environment for the next generation. Environmental Science and Technology 40, 3586–3594.

Dentener, F., Kinne, S., Bond, T., Boucher, O., Cofala, J., Generoso, S., Ginoux, P., Gong, S., Hoelzemann, J.J., Ito, A., Marelli, L., Penner, J.E., Putaud, J.-P., Textor, C., Schulz, M., van der Werf, G.R., Wilson, J., 2006b. Emissions of primary aerosol and precursor gases in the years 2000 and 1750 prescribed data-sets for AeroCom. Atmospheric Chemistry and Physics 6, 4321–4344.

Derwent, R.G., Simmonds, P.G., O'Doherty, S., Stevenson, D.S., Collins, W.J., Sanderson, M.G., Johnson, C.E., Dentener, F., Cofala, J., Mechler, R., Amann, M., 2006. External influences on Europe's air quality: baseline methane, carbon monoxide and ozone from 1990 to 2030 at Mace Head, Ireland. Atmospheric Environment 40, 844–855.

Dickinson, R.E., 1975. Solar variability and the lower atmosphere. Bulletin of the American Meteorological Society 56, 1240–1248.

Dinar, E., Abo Riziq, A., Spindler, C., Erlick, C., Kiss, G., Rudich, Y., 2008. The complex refractive index of atmospheric and model humic-like substances (HULIS) retrieved by a cavity ring down aerosol spectrometer (CRD-AS). Faraday Discussions 137, 279–295.

Drummond, J.R., Mand, G.S., 1996. The measurements of pollution in the troposphere (MOPITT) instrument: overall performance and calibration requirements. Journal of Atmospheric and Oceanic Technology 13 (2), 314–320.

Duncan, B.N., Bey, I., 2004. A modeling study of the export pathways of pollution from Europe: seasonal and interannual variations (1987–1997). Journal of Geophysical Research 109, D08301. doi:10.1029/2003JD004079.

Dutton, E.G., Nelson, D.W., Stone, R.S., Longenecker, D., Carbaugh, G., Harris, J.M., Wendell, J., 2006. Decadal variations in surface solar irradiance as observed in a globally remote network. Journal of Geophysical Research 111. doi:10.1029/2005JD006901.

Eckhardt, S., Stohl, A., Beirle, S., Spichtinger, N., James, P., Forster, C., Junker, C., Wagner, T., Platt, U., Jennings, S.G., 2003. The North Atlantic oscillation controls air pollution transport to the Arctic. Atmospheric Chemistry and Physics 3, 1769–1778.

EMEP, 2004. EMEP assessment part I European perspective. Lövblad G., Tarrasón L., Tørseth K., Dutchak S. (Eds.), Oslo, ISBN 82-7144-032-2.

EMEP, 2006. Transboundary acidification, eutrophication and ground level ozone in Europe since 1990 to 2004, EMEP Status Report 1/06 to support the Review of Gothenburg Protocol.

Emmerson, K.M., Carslaw, N., Carslaw, D.C., Lee, J.D., McFiggans, G., Bloss, W.J., Gravestock, T., Heard, D.E., Hopkins, J., Ingham, T., Pilling, M.J., Smith, S.C., Jacob, M., Monks, P.S., 2007. Free radical modelling studies during the UK TORCH Campaign in Summer 2003. Atmospheric Chemistry and Physics 7, 167–181.

Endresen, Ø., Sørgård, E., Sundet, J.K., Dalsøren, S.B., Isaksen, I.S.A., Berglen, T.F., Gravir, G., 2003. Emission from international sea transportation and environmental impact. Journal of Geophysical Research 108 (D17), 4560. doi:10.1029/2002JD002898.

EPA, 2003. Environmental Protection Agency: National Air Quality and Emissions Trends Report, 2003 Special Studies Edition Available at: http://www.epa.gov/air/airtrends/aqtrnd03.

Erlykin, A.D., Sloan, T., Wolfendale, A.W., 2009. Solar activity and the mean global temperature. Environmental Research Letters 4. doi:10.1088/1748-9326/4/1/014006, 014006 (5 pp.).

Eyring, V., Harris, N.R.P., Rex, M., Shepherd, T.G., Fahey, D.W., Amanatidis, G.T., Austin, J., Chipperfield, M.P., Dameris, M., Forster, P.M., De, F., Gettelman, A., Graf, H.F., Nagashima, T., Newman, P.A., Pawson, S., Prather, M.J., Pyle, J.A., Salawitch, R.J., Santer, B.D., Waugh, D.W., 2005a. A strategy for process-oriented validation of coupled chemistry–climate models. Bulletin of the American Meteorological Society 86, 1117–1133.

Eyring, V., Köhler, H.W., van Aardenne, J., Lauer, A., 2005b. Emissions from international shipping: 1. The last 50 years. Journal of Geophysical Research 110, D17305. doi:10.1029/2004JD005619.

Eyring, V., Butchart, N., Waugh, D.W., Akiyoshi, H., Austin, J., Bekki, S., Bodeker, G.E., Boville, B.A., Brühl, C., Chipperfield, M.P., Cordero, E., Dameris, M., Deushi, M., Fioletov, V.E., Frith S., M., Garcia, R.R., Gettelman, A., Giorgetta, M.A., Grewe, V., Jourdain, L., Kinnison, D.E., Mancini, E., Manzini, E., Marchand, M., Marsh, D.R., Nagashima, T., Newman, P.A., Nielsen, J.E., Pawson, S., Pitari, G., Plummer, D.A., Rozanov, E., Schraner, M., Shepherd, T.G., Shibata, K., Stolarski, R.S., Struthers, H., Tian, W., Yoshiki, M., 2006. Assessment of temperature, trace species and ozone in chemistry–climate model simulations of the recent past. Journal of Geophysical Research 111, D22308. doi:10.1029/2006JD007327.

Eyring, V., Stevenson, D.S., Lauer, A., Dentener, F.J., Butler, T., Collins, W.J., Ellingsen, K., Gauss, M., Hauglustaine, D.A., Isaksen, I.S.A., Lawrence, M.G., Richter, A., Rodriguez, J.M., Sanderson, M., Strahan, S.E., Sudo, K., Szopa, S., van Noije, T.P.C., Wild, O., 2007a. Multi-model simulations of the impact of international shipping on atmospheric chemistry and climate in 2000 and 2030. Atmospheric Chemistry and Physics 7, 757–780.

Eyring, V., Waugh, D.W., Bodeker, G.E., Cordero, E., Akiyoshi, H., Austin, J., Beagley, S.R., Boville, B., Braesicke, P., Brühl, C., Butchart, N., Chipperfield, M.P., Dameris, M., Deckert, R., Deushi, M., Frith, S.M., Garcia, R.R., Gettelman, A., Giorgetta, M., Kinnison, D.E., Mancini, E., Manzini, E., Marsh, D.R., Matthes, S., Nagashima, T., Newman, P.A., Nielsen, J.E., Pawson, S., Pitari, G., Plummer, D.A., Rozanov, E., Schraner, M., Scinocca, J.F., Semeniuk, K., Shepherd, T.G., Shibata, K., Steil, B., Stolarski, R., Tian, W., Yoshiki, M., 2007b. Multimodel projections of stratospheric ozone in the 21st century. Journal of Geophysical Research 112, D16303. doi:10.1029/2006JD008332.

Eyring, V., Isaksen, I.S.A., Berntsen, T., Collins, W.J., Corbett, J.J., Endresen, O., Grainger, R.G., Moldanova, J., Schlager, H., Stevenson, D.S. Assessment of transport impacts on climate and ozone: shipping. Atmospheric Environment, in preparation.

Feingold, G., Cotton, W.R., Kreidenweis, S., Davis, J.T., 1999. The impact of giant cloud condensation nuclei on drizzle formation in stratocumulus: implications for cloud radiative properties. Journal of Atmospheric Sciences 56, 4100–4117.

Fiore, A.M., et al., 2009. Multimodel estimates of intercontinental source–receptor relationships for ozone pollution. Journal of Geophysical Research 114, D04301. doi:10.1029/2008JD010816.

Flanner, M.G., Zender, C.S., Randerson, J.T., Rasch, P.J., 2007. Present-day climate forcing and response from black carbon in snow. Journal of Geophysical Research 112, D11202. doi:10.1029/2006JD008003.

Folkins, I., Chatfield, R., 2000. Impact of acetone on ozone production and OH in the upper troposphere at high $NO_x$. Journal of Geophysical Research 105 (D9), 11585–11600.

Forster, P.M., de, F., Shine, K.P., 1997. Radiative forcing and temperature trends from stratospheric ozone changes. Journal of Geophysical Research 102, 10841–10857.

Forster, P., Ramaswamy, V., Artaxo, P., Berntsen, T., Betts, R., Fahey, D.W., Haywood, J., Lean, J., Lowe, D.C., Myhre, G., Nganga, J., Prinn, R., Raga, G., Schulz, M., van Dorland, R., Bodeker, G., Boucher, O., Collins, W.D., Conway, T.J., Dlugokencky, E., Elkins, J.W., Etheridge, D., Foukal, P., Fraser, P., Geller, M., Joos, F., Keeling, C.D., Kinne, S., Lassey, K., Lohmann, U., Manning, A.C., Montzka, S., Oram, D., O'Shaughnessy, K., Piper, S., Plattner, G.-K., Ponater Michael, Ramankutty, N., Reid, G., Rind, D., Rosenlof, K., Sausen, R., Schwarzkopf, D., Solanki, S.K., Stenchikov, G., Stuber, N., Takemura, T., Textor, C., Wang, R., Weiss, R., Whorf, T., 2007. Changes in atmospheric constituents and in radiative forcing. In: Solomon, S., Qin, D., Manning, M., Chen, Z., Marquis, M., et al. (Eds.), Climate Change 2007: the Physical Science Basis. Contribution of Working Group I to the Fourth Assessment Report of the Intergovernmental Panel on Climate Change. Cambridge University Press, United Kingdom and New York, NY, USA.

Fowler, D., Pilegaard, K., Sutton, M.A., Ambus, P., Raivonen, M., Duyzer, J., Simpson, D., Fagerli, H., Schjoerring, J.K., Neftel, A., Burkhardt, J., Daemmgen, U., Neirynck, J., Personne, E., Wichink-Kruit, R., Butterbach-Bahl, K., Flechard, C., Tuovinen, J.P., Coyle, M., Fuzzi, S., Gerosa, G., Granier, C., Loubet, B., Altimir, N., Gruenhage, L., Ammann, C., Cieslik, S., Paoletti, E., Mikkelsen, T.N., Ro-Poulsen, H., Cellier, P.,

Cape, J.N., Isaksen, I.S.A., Horváth, L., Loreto, F., Niinemets, Ü., Palmer, P.I., Rinne, J., Laj, P., Maione, M., Misztal, P., Monks, P., Nemitz, E., Nilsson, D., Pryor, S., Gallagher, M.W., Vesala, T., Skiba, U., Brüeggemann, N., Zechmeister-Boltenstern, S., Williams, J., O'Dowd, C., Facchini, M.C., de Leeuw, G., Flossman, A., Chaumerliac, N., Erisman, J.W., 2009. Atmospheric composition change: ecosystems – atmosphere interactions 43, 5138–5192.

Frankenberg, C., Meirink, J.F., van Weele, M., Platt, U., Wagner, T., 2005. Assessing methane emissions from global space-borne observations. Science 308 (5724), 1010–1014.

Frankenberg, C., Meirink, J.F., Bergamaschi, P., Goede, A.P.H., Heimann, M., Körner, S., Platt, U., van Weele, M., Wagner, T., 2006. Satellite chartography of atmospheric methane from SCIAMACHY on board ENVISAT: analysis of the years 2003 and 2004. Journal of Geophysical Research 111, D07303. doi:10.1029/2005JD006235.

Frankenberg, C., Bergamaschi, P., Butz, A., Houweling, S., Meirink, J.F., Notholt, J., Petersen, A.K., Schrijver, H., Warneke, T., Aben, I., 2008. Tropical methane emissions: a revised view from SCIAMACHY onboard ENVISAT. Geophysical Research Letters 35, L15811. doi:10.1029/2008GL034300.

Friedlingstein, P., Cox, P., Betts, R., Bopp, L., Von Bloh, W., Brovkin, V., Cadule, P., Doney, S., Eby, M., Fung, I., Bala, G., John, J., Jones, C., Joos, F., Kato, T., Kawamiya, M., Knorr, W., Lindsay, K., Matthews, H.D., Raddatz, T., Rayner, P., Reick, C., Roeckner, E., Schnitzler, K.-G., Schnur, R., Strassmann, K., Weaver, A.J., Yoshikawa, C., Zeng, N., 2006. Climate–carbon cycle feedback analysis: results from the $C^4$MIP model intercomparison. Journal of Climate 19 (14), 3337–3353.

Friis-Christensen, E., Lassen, K., 1991. Length of the solar cycle: an indicator of solar activity closely associated with climate. Science 254, 698–700.

Fu, T.M., Jacob, D.J., Palmer, P.I., Chance, K., Wang, Y.X.X., Barletta, B., Blake, D.R., Stanton, J.C., Pilling, M.J., 2007. Space-based formaldehyde measurements as constraints on volatile organic compound emissions in east and south Asia and implications for ozone. Journal of Geophysical Research-Atmosphere 112 (D6). doi:10.1029/2006JD007853.

Fuglestvedt, J.S., Berntsen, T., Godal, O., Sausen, R., Shine, K.P., Skodvin, T., 2003. Metrics of climate change: assessing radiative forcing and emission indices. Climatic Change 58 (3), 267–331.

Fuglestvedt, J., Berntsen, T., Myhre, G., Rypdal, K., Skeie, R.B., 2008. Climate forcing from the transport sectors. Proceedings of the National Academy of Sciences USA 105 (2), 454–458.

Fuglestvedt, J.S., Shine, K.P., Cook, J., Berntsen, T., Lee, D.S., Stenke, A., Skeie, R.B., Velders, G.J.M., Waitz, I.A. Assessment of transport impacts on climate and ozone: metrics. Atmospheric Environment, in press. Available online 5 May 2009.

Fuller, K.A., Malm, W.C., Kreidenweis, S.M., 1999. Effects of mixing on extinction by carbonaceous particles. Journal of Geophysical Research 104 (D13), 15941–15954.

Fusco, A.C., Logan, J.A., 2003. Analysis of 1970–1995 trends in tropospheric ozone at Northern Hemisphere midlatitudes with the GEOS–CHEM model. Journal of Geophysical Research 108, 4449. doi:10.1029/2002JD002742.

Galloway, J.N., Dentener, F.J., Capone, D.G., Boyer, E.W., Howarth, R.W., Seitzinger, S.P., Asner, G.P., Cleveland, C., Green, P., Holland, E., Karl, D.M., Michaels, A.F., Porter, J.H., Townsend, A., Vörösmarty, C., 2004. Nitrogen cycles: past, present and future. Biogeochemistry 70 (2), 153–226.

Garrett, T.J., Zhao, C., 2006. Increased Arctic cloud longwave emissivity associated with pollution from mid-latitudes. Nature 440, 787–789.

Gauss, M., Myhre, G., Isaksen, I.S.A., Grewe, V., Pitari, G., Wild, O., Collins, W.J., Dentener, F.J., Ellingsen, K., Gohar, L.K., Hauglustaine, D.A., Iachetti, D., Lamarque, J.-F., Mancini, E., Mickley, L.J., Prather, M.J., Pyle, J.A., Sanderson, M.G., Shine, K.P., Stevenson, D.S., Sudo, K., Szopa, S., Zeng, G., 2006. Radiative forcing since preindustrial times due to ozone change in the troposphere and the lower stratosphere. Atmospheric Chemistry and Physics 6, 575–599.

Gedney, N., Cox, P.M., Huntingford, C., 2004. Climate feedback from wetland methane emissions. Geophysical Research Letters 31, L20503. doi:10.1029/2004GL020919.

Gelencser, A., May, B., Simpson, D., Sanchez-Ochoa, A., Kasper-Giebl, A., Puxbaum, H., Caseiro, A., Pio, C., Legrand, M., 2007. Source apportionment of PM2.5 organic aerosol over Europe: primary/secondary, natural/anthropogenic, and fossil/biogenic origin. Journal of Geophysical Research 112 (D23), D23S04.

Gerasopoulos, E., Kouvarakis, G., Vrekoussis, M., Kanakidou, M., Mihalopoulos, N., 2005. Ozone variability in the marine boundary layer of the eastern Mediterranean based on 7-year observations. Journal of Geophysical Research 110, D15309. doi:10.1029/2005JD005991.

Giacopelli, P., Ford, K., Espada, C., Shepson, P.B., 2005. Comparison of the measured and simulated isoprene nitrate distributions above a forest canopy. Journal of Geophysical Research 110, D01304. doi:10.1029/2004JD005123.

Gilgen, H., Wild, M., Ohmura, A., 1998. Means and trends of shortwave irradiance at the surface estimated from GEBA. Journal of Climate 11, 2042–2061.

Girard, E., Blanchet, J.-P., Dubois, Y., 2004. Effects of arctic sulphuric acid aerosols on wintertime low-level atmospheric ice crystals, humidity and temperature at Alert, Nunavut. Atmosperich Research 73, 131–148.

Goto-Azuma, K., Koerner, R.M., 2001. Ice core studies of anthropogenic sulfate and nitrate trends in the Arctic. Journal of Geophysical Research 106 (D5), 4959–4969.

Granier, C., Niemeier, U., Müller, J.F., Olivier, J., Richter, A., Nuess, H., Burrows, J., 2003. Variation of the atmospheric composition over the 1990–2000 period. POET Report 6, EU project EVK2-1999-00011.

Granier, C., Niemeier, U., Jungclaus, J.H., Emmons, L., Hess, P., Lamarque, J.-F., Walters, S., Brasseur, G.P., 2006. Ozone pollution from future ship traffic in the Arctic northern passages. Geophysical Research Letters 33, L13807. doi:10.1029/2006GL026180.

Grassl, H., 1975. Albedo reduction and radiative heating of clouds by absorbing aerosol particles. Contributinos to Atmospheric Physics 48, 199–210.

Guenther, A., Hewitt, C.N., Erickson, D., Fall, R., Geron, C., Graedel, T., Harley, P., Klinger, L., Lerdau, M., Mckay, W.A., Pierce, T., Scholes, B., Steinbrecher, R., Tallamraju, R., Taylor, J., Zimmerman, P.A., 1995. Global-model of natural volatile organic-compound emissions. Journal of Geophysical Research – Atmosphere 100 (D5), 8873–8892.

Guenther, A., Karl, T., Harley, P., Wiedinmyer, C., Palmer, P.I., Geron, C., 2006. Estimates of global terrestrial isoprene emissions using MEGAN (Model of Emissions of Gases and Aerosols from Nature). Atmospheric Chemistry and Physics 6, 3181–3210.

Haigh, J.D., 1994. The role of stratospheric ozone in modulating the solar radiative forcing of climate. Nature 370, 544–546.

Haigh, J.D., 2003. The effects of solar variability on the Earth's climate. Philosophical Transactions of the Royal Society London A 361, 95–111.

Hansen, J., Sato, M., Ruedy, R., 1997. Radiative forcing and climate response. Journal of Geophysical Research 102, 6831–6864.

Hansen, J., Nazarenko, L., 2004. Soot climate forcing via snow and ice albedos. Proceedings of the National Academy of Sciences U S A 101, 423–428.

Hansen, J., Sato, M., Ruedy, R., Nazarenko, L., Lacis, A., Schmidt, G.A., Russell, G., Aleinov, I., Bauer, M., Bauer, S., Bell, N., Cairns, B., Canuto, V., Chandler, M., Cheng, Y., Del Genio, A., Faluvegi, G., Fleming, E., Friend, A., Hall, T., Jackman, C., Kelley, M., Kiang, N., Koch, D., Lean, J., Lerner, J., Lo, K., Menon, S., Miller, R., Minnis, P., Novakov, T., Oinas, V., Perlwitz, J., Perlwitz, J., Rind, D., Romanou, A., Shindell, D., Stone, P., Sun, S., Tausnev, N., Thresher, D., Wielicki, B., Wong, T., Yao, M., Zhang, S., 2005. Efficacy of climate forcings. Journal of Geophysical Research – Atmospheres 110, D18104.

Harries, J.E., Brindley, H.E., Sagoo, P.J., Bantges, R.J., 2001. Increases in greenhouse forcing inferred from the outgoing longwave radiation spectra of the Earth in 1970 and 1997. Nature 410, 355–357.

Harrison, G.R., Stephenson, D.B., 2006. Empirical evidence for a nonlinear effect of galactic cosmic rays on clouds 462 (2068), 1221–1233. doi:10.1098/rspa.2005.1628.

Hartmann, D.L., 1996. Global Physical Climatology. Academic.

Hatzianastassiou, N., Matsoukas, C., Fotiadi, A., Pavlakis, K.G., Drakakis, E., Hatzidimitriou, D., Vardavas, I., 2005. Global distribution of Earth's surface-shortwave radiation budget. Atmospheric Chemistry and Physics 5, 2847–2867.

Hauglustaine, D.A., Brasseur, G.P., 2001. Evolution of tropospheric ozone under anthropogenic activities and associated radiative forcing of climate. Journal of Geophysical Research 106 (32), 337–32 360.

Hauglustaine, D.A., Lathière, J., Szopa, S., Folberth, G.A., 2005. Future tropospheric ozone simulated with a climate–chemistry–biosphere model. Geophysical Research Letters 32, L24807. doi:10.1029/2005GL024031.

Haywood, J.M., Shine, K.P., 1995. The effect of anthropogenic sulfate and soot aerosol on the clear-sky planetary radiation budget. Geophysical Research Letters 22 (5), 603–606.

Hein, R., Crutzen, P.J., Heimann, M., 1997. An inverse modeling approach to investigate the global atmospheric methane cycle. Global Biogeochem. Cycles 11 (1), 43–76.

Henze, D.K., Seinfeld, J.H., 2006. Global secondary organic aerosol from isoprene oxidation. Geophysical Research Letters 33 (9), L09812.

Hess, P.G., Lamarque, J.-F., 2007. Ozone source attribution and its modulation by the Arctic oscillation during the spring months. Journal of Geophysical Research 112, D11303. doi:10.1029/2006JD007557.

Hogrefe, C., Lynn, B., Civerolo, K., Ku, J.-Y., Rosenthal, J., Rosenzweig, C., Goldberg, R., Gaffin, S., Knowlton, K., Kinney, P.L., 2004. Simulating changes in regional air pollution over the eastern United States due to changes in global and regional climate and emissions. Journal of Geophysical Research 109, D22301. doi:10.1029/2004JD004690.

Hoor, P., Borken-Kleefeld, J., Caro, D., Dessens, O., Endresen, O., Gauss, M., Grewe, V., Hauglustaine, D., Isaksen, I.S.A., Jöckel, P., Lelieveld, J., Meijer, E., Olivie, D., Prather, M., Schnadt Poberaj, C., Staehelin, J., Tang, Q., van Aardenne, J., van Velthoven, P., Sausen, R., 2009. The impact of traffic emissions on atmospheric ozone and OH: results from QUANTIFY. Atmospheric Chemistry and Physics 9, 3113–3136. 18219–18266.

Hoose, C., Lohmann, U., Erdin, R., Tegen, I., 2008. Global influence of dust mineralogical composition on heterogeneous ice nucleation. Environmental Research Letters 3 025003.

Horowitz, L.W., Fiore, A.M., Milly, G.P., Cohen, R.C., Perring, A., Wooldridge, P.J., Hess, P.G., Emmons, L.K., Lamarque, J.-F., 2007. Observational constraints on the chemistry of isoprene nitrates over the Eastern United States. Journal of Geophysical Research 112, D12S08. doi:10.1029/2006JD007747.

Houweling, S., Rockmann, T., Aben, I., Keppler, F., Krol, M., Meirink, J.F., Dlugokencky, E.J., Frankenberg, C., 2006. Atmospheric constraints on global emissions of methane from plants. Geophysical Research Letters 33 ISI:000239991400002.

Hoyle, C.R., Berntsen, T., Myhre, G., Isaksen, I.S.A., 2007. Secondary organic aerosol in the global aerosol – chemical transport model Oslo CTM2. Atmospheric Chemistry and Physics 7 (21), 5675–5694.

IPCC, 1999. Aviation and the Global Atmosphere. Cambridge University Press, UK. Available at: http://www.grida.no/climate/ipcc/aviation/index.htm.

IPCC, 2001. Climate change 2001: the scientific basis. In: Houghton, J.T., Ding, Y., Griggs, D.J., Moguer, M., Van der Linden, P.J., Dai, L., Maskell, K., Johnson, C.A. (Eds.). Cambridge University Press.

IPCC/TEAP, 2005. Intergovernmental Panel on Climate Change (IPCC) and Technology and Economic Assessment Panel (TEAP). In: Metz, B., et al. (Eds.), Special

Report on Safeguarding the Ozone Layer and the Global Climate System: Issues Related to Hydrofluorocarbons and Perfluorocarbons. Cambridge University Press, UK, pp. 87–88.

IPCC, 2007. The Physical Science Basis. Contribution of Working Group I to the Fourth Assessment Report of the Intergovernmental Panel on Climate Change. Cambridge University Press, Cambridge, United Kingdom and New York, NY, USA.

IPCC, 2009. Meeting report of the expert meeting on the science of alternative metrics. In: Plattner, G.-K., Stocker, T.F., Midgley, P., Tignor, M. (Eds.), IPCC Working Group Technical Support Unit. University of Bern, Bern, Switzerland, 75 pp.

Isaksen, I.S.A., Zerefos, C., Kourtidis, K., Meleti, C., Dalsøren, S.B., Sundet, J.K., Zanis, P., Balis, D., 2005. Tropospheric ozone changes at unpolluted and semi-polluted regions induced by stratospheric ozone changes. Journal of Geophysical Research 110, DO2302. doi:10.1029/2004JD004618.

Isaksen, I.S.A., Dalsøren, S.B., Li, L., Wang, W.-C., 2009. Introduction to special section on 'East Asia Climate and Environment. Tellus 61 (4), 583–589. doi:10.1111/j.1600-0889.2009.00432.x.

Iversen, T., Joranger, E., 1995. Arctic air pollution and large scale atmospheric flows. Atmospheric Environment 19, 2099–2108.

Jacob, D.J., Winner, D.A., 2009. Effect of climate change on air quality. Atmospheric Environment 43, 51–63.

Jacobson, M.Z., 1999. Isolating nitrated and aromatic aerosols and nitrated aromatic gases as sources of ultraviolet light absorption. Journal of Geophysical Research 104 (D3), 3527–3542.

Jacobson, M.Z., 2001. Global direct radiative forcing due to multicomponent anthropogenic and natural aerosols. Journal of Geophysical Research 106 (D2), 1551–1568.

Jacobson, M.Z., 2002. Control of fossil fuel particulate black carbon and organic matter, possibly the most effective method of slowing global warming. Journal of Geophysical Research 107. doi:10.1029/2001JD001376.

Jacobson, M.Z., 2004. Climate response of fossil fuel and biofuel soot, accounting for soot's feedback to snow and sea ice albedo and emissivity. Journal of Geophysical Research 109, D21201. doi:10.1029/2004JD004945.

Jacobson, M.Z., Streets, D.G., 2009. Influence of future anthropogenic emissions on climate, natural emissions, and air quality. Journal of Geophysical Research 114, D08118. doi:10.1029/2008JD011476.

Jaegle, L., Martin, R.V., Chance, K., Steinberger, L., Kurosu, T.P., Jacob, D.J., Modi, A.I., Yoboue, V., Sigha-Nkamdjou, L., Galy-Lacaux, C., 2004. Satellite mapping of rain-induced nitric oxide emissions from soils. Journal of Geophysical Research – Atmospheres 109 (D21).

Johnson, B.T., Shine, K.T., Forster, P.M., 2004. The semi-direct aerosol effect: impact of absorbing aerosols on marine stratocumulus. Quarterly Journal of the Royal Meteorological Society 130, 1407–1422.

Johnson, C., Stevenson, D., Collins, W., Derwent, R., 2001. Role of climate feedback on methane and ozone studied with a coupled ocean-atmosphere-chemistry model. Geophysical Research Letters 28 (9), 1723–1726.

Jones, A., Haywood, J.M., Boucher, O., 2007. Aerosol forcing, climate response and climate sensitivity in the Hadley Centre Climate Model HadGEM2-AML. Journal of Geophysical Research 112, D20211. doi:10.1029/2007JD008688.

Jonson, J.E., Simpson, D., Fagerli, H., Solberg, S., 2006. Can we explain the trends in European ozone levels? Atmospheric Chemistry and Physics 6, 51–66.

Jorgenson, M.T., Shur, Y.L., Pullman, E.R., 2006. Abrupt increase in 353 permafrost degradation in Arctic Alaska. Geophysical Research Letters 33 (354), L02503. doi:10.1029/2005GL024960.

Joshi, M., Shine, K., Ponater, M., Stuber, N., Sausen, R., Li, L., 2003. A comparison of climate response to different radiative forcings in three general circulation models: towards an improved metric of climate change. Climate Dynamics 20 (7–8), 843–854.

Jöckel, P., Tost, H., Pozzer, A., Brühl, C., Buchholz, J., Ganzeveld, L., Hoor, P., Kerkweg, A., Lawrence, M.G., Sander, R., Steil, B., Stiller, G., Tanarhte, M., Taraborrelli, D., van Aardenne, J., Lelieveld, J., 2006. The atmospheric chemistry general circulation model ECHAM5/MESSy1: consistent simulation of ozone from the surface to the mesosphere. Atmospheric Chemistry and Physics 6, 5067–5104.

Kandlikar, M., 1995. The relative role of trace gas emissions in greenhouse abatement policies. Energy Policy 23 (10), 879–883.

Karlsdóttir, S., Isaksen, I.S.A., Myhre, G., Berntsen, T.K., 2000. Trend analysis of $O_3$ and CO in the period 1980–1996: A three-dimensional model study. Journal of Geophysical Research 105 (D23), 28907–28934.

Kaufman, Y.J., Tanre, D., Boucher, O., 2002. A satellite view of aerosols in the climate system. Nature 419 (6903), 215–223.

Kaufmann, R.K., Stern, D.I., 2002. Cointegration analysis of hemispheric temperature relations. Journal of Geophysical Research 107 (D2), 4012. doi:10.1029/2000JD000174.

Keating, T.J., West, J.J., Farrell, A.E., 2004. Prospects for international management of inter-continental air pollution transport. In: Stohl, A. (Ed.), Intercontinental Transport of Air Pollution. Springer, Berlin, pp. 295–320.

Kim, S.W., Heckel, A., McKeen, S.A., Frost, G.J., Hsie, E.-Y., Trainer, M.K., Richter, A., Burrows, J.P., Peckham, S.E., Grell, G.A., 2006. Satellite-observed US power plant $NO_x$ emission reductions and their impact on air quality. Geophysical Research Letters 33 (22).

Kim, B.-G., Miller, M.A., Schwartz, S.E., Liu, Y., Min, Q., 2008. The role of adiabaticity in the aerosol first indirect effect. Journal of Geophysical Research 113. doi:10.1029/2007JD008961.

Kinne, S., Schulz, M., Textor, C., Guibert, S., Balkanski, Y., Bauer, S.E., Berntsen, T., Berglen, T.F., Boucher, O., Chin, M., Collins, W., Dentener, F., Diehl, T., Easter, R., Feichter, J., Fillmore, D., Ghan, S., Ginoux, P., Gong, S., Grini, A., Hendricks, J., Herzog, M., Horowitz, L., Isaksen, I., Iversen, T., Kirkevåg, A., Kloster, S., Koch, D., Kristjansson, J.E., Krol, M., Lauer, A., Lamarque, J.F., Lesins, G., Liu, X., Lohmann, U., Montanaro, V., Myhre, G., Penner, J.E., Pitari, G., Reddy, S., Seland, O., Stier, P., Takemura, T., Tie, X., 2006. An AeroCom initial assessment – optical properties in aerosol component modules of global models. Atmospheric Chemistry and Physics 6, 1815–1834.

Kleeman, M.J., 2007. A preliminary assessment of the sensitivity of air quality in California to global change. Climatic Change 87, S273–S292.

Kleffmann, J., Gavriloaiei, T., Hofzumahaus, A., Holland, F., Koppmann, R., Rupp, L., Schlosser, E., Siese, M., Wahner, A., 2005. Daytime formation of nitrous acid: a major source of OH radicals in a forest. Geophysical Research Letters 32, L05818. doi:10.1029/2005GL022524.

Klimont, Z., Streets, D.G., 2007. Emissions inventories and projections for assessing hemispheric or intercontinental transport. In: Keating, T., Zuber, A. (Eds.), Hemispheric Transport of Air Pollution 2007. Atmospheric Pollution Studies No. 16, ECE/EB.AIR/94. United Nations, Geneva.

Klimont, Z., Cofala, J., Xing, J., Wei, Wei, Zhang, C., Wang, S., Kejun, J., Bhandari, P., Mathura, R., Purohit, P., Rafaj, P., Chambers, A., Amann, M., Hao, J., 2009. Projections of $SO_2$, $NO_x$, and carbonaceous aerosols emissions in Asia. Tellus B. doi:10.1111/j.1600-0889.2009.00428.x.

Knudsen, M.F., Riisager, P., 2009. Is there a link between Earth's magnetic field and low-latitude precipitation?. January 2009. Geology 37 (1), 71–74. doi:10.1130/G25238A.1.

Koch, D., Bond, T.C., Streets, D., Unger, N., van der Werf, G.R., 2007. Global impacts of aerosols from particular source regions and sectors. Journal of Geophysical Research 112, D02205. doi:10.1029/2005JD007024.

Konovalov, I.B., Beekmann, M., Richter, A., Burrows, J.P., 2006. Inverse modelling of the spatial distribution of $NO_x$ emissions on a continental scale using satellite data. Atmospheric Chemistry and Physics 6, 1747–1770.

Koren, I., Kaufman, Y.J., Remer, L.A., Martins, J.V., 2004. Measurement of the effect of Amazon smoke on inhibition of cloud formation. Science 303, 1342–1345.

Koren, I., Martins, J.V., Remer, L.A., Afargan, H., 2008. Smoke invigoration versus inhibition of clouds over the Amazon. Science 321, 946–949.

Korolev, A., 2007. Limitations of the Wegener–Bergeron–Findeisen mechanism in the evolution of mixed-phase clouds. Journal of Atmospheric Science 64, 3372–3375.

Kotamarthi, V.R., Wuebbles, D.J., Reck, R.A., 1999. Effects of non-methane hydrocarbons on lower stratospheric and upper tropospheric 2-D zonal average model chemical climatology. Journal Geophysical Research 104, 21537–21547.

Kristjánsson, J.E., 2002. Studies of the aerosol indirect effect from sulfate and black carbon aerosols. Journal of Geophysical Research 107. doi:10.1029/2001D000887.

Kristjánsson, J.E., Stjern, C., Stordal, F., Fjaeraa, A.M., Myhre, G., Jonasson, K., 2008. Cosmic rays and clouds – a reassessment using MODIS data. Atmospheric Chemistry and Physics 8, 7373–7387.

Krueger, A.J., 1989. The global distribution of total ozone – Toms satellite measurements. Planetary and Space Science 37 (12), 1555–1565.

Kulmala, M., Reissell, A., Sipila, M., Bonn, B., Ruuskanen, T.M., Lehtinen, K.E.J., Kerminen, V.-M., Strom, J., 2006. Deep convective clouds as aerosol production engines: role of insoluble organics. Journal of Geophysical Research 111, D17202. doi:10.1029/2005JD006963.

Kupiainen, K., Klimont, Z., 2007. Primary emissions of fine carbonaceous particles in Europe. Atmospheric Environment 41/10, 2156–2170. doi:10.1016/j.atmosenv.2006.10.066.

Kvalevåg, M.M., Myhre, G., 2007. Human impact on direct and diffuse solar radiation during the industrial era. Journal of Climate 20 (19), 4874–4883.

Labitzke, K., 1987. Sunspots, the QBO, and the stratospheric temperature in the North polar region. GRL 14, 535–537.

Labitzke, K., van Loon, H., 1988. Association between the 11-year solar cycle, the QBO, and the atmosphere, I. The troposphere and stratosphere on the northern hemisphere winter. Journal of Atmospheric Terrestrial Physics 50, 197–206.

Lacis, A., Wuebbles, D.J., Logan, J.A., 1990. Radiative forcing by changes in the vertical distribution of ozone. Journal of Geophysical Research 95, 9971–9981.

Laj, P., Klausen, J., Bilde, M., Plaβ-Duelmer, C., Pappalardo, G., Clerbaux, C., Baltensperger, U., Hjorth, J., Simpson, D., Reimann, S., Coheur, P.-F., Richter, A., De Mazière, M., Rudich, Y., McFiggans, G., Torseth, K., Wiedensohler, A., Morin, S., Schulz, M., Allan, J., Attié, J.- L., Barnes, I., Birmilli, W., Cammas, P., Dommen, J., Dorn, H.-P., Fowler, D., Fuzzi, J.- S., Glasius, M., Granier, C., Hermann, M., Isaksen, I., Kinne, S., Koren, I., Madonna, F., Maione, M., Massling, A., Moehler, O., Mona, L., Monks, P., Müller, D., Müller, T., Orphal, J., Peuch, V.-H., Stratmann, F., Tanré, D., Tyndall, G., Riziq, A. A., Van Roozendael, M., Villani, P., Wehner, B., Wex, H., Zardini, A. A., 2009. Measuring Atmospheric Composition Change, 5352–5415.

Lamarque, J.-F., Hess, P., Emmons, L., Buja, L., Washington, W., Granier, C., 2005. Tropospheric ozone evolution between 1890 and 1990. Journal of Geophysical Research 110, D08304. doi:10.1029/2004JD005537.

Langner, J., Bergstrom, R., Foltescu, V., 2005. Impact of climate change on surface ozone and deposition of sulphur and nitrogen in Europe. Atmospheric Environment 39, 1129–1141.

Latham, J., Rasch, P., Chen, C.-C., Kettles, L., Gadian, A., Gettelman, A., Morrison, H., Bower, K., Choularton, T., 2008. Global temperature stabilization via controlled albedo enhancement of low-level maritime clouds. Philosophical Transactions of the Royal Society A. doi:10.1098/rsta.2008.0137.

Laut, P., 2003. Solar activity and terrestrial climate: an analysis of some purported correlations. Journal of Atmospheric Solar Terrestrial Physics 65, 801–812.

Lawrence, D.M., Slater, A.G., 2005. A projection of severe near 361 surface permafrost degradation during the 21st century. Geophysical Research 362 Letters 32, L24401. doi:10.1029/2005GL025080.
Lean, J., Beer, J., Bradley, R., 1995. Reconstruction of solar irradiance since 1610-Implications for climate-change. Geophysical Research Letters 22, 3195–3198.
Lean J., 2004. Solar irradiance reconstruction. IGBP PAGES/World Data Center for Paleoclimatology, 2004-035, GBP PAGES/WDCA.
Lean, J.L., 2006. Comment on 'Estimated solar contribution to the global surface warming using the ACRIM TSI satellite composite' by N.Scafetta, B.J. West. Geophysical Research Letters 33, L15701. doi:10.1029/2005GL025342.
Lean, J.L., Rind, D.H., 2008. How natural and anthropogenic influences alter global and regional surface temperatures: 1889 to 2006. Geophysical Research Letters 35, L18701. doi:10.1029/2008GL034864.
Lee, D.S., Pitari, G., Grewe, V., Gierens, K., Penner, J.E., Petzold, A., Prather, M., Schumann, U., Bais, A., Berntsen, T., Iachetti, D., Lim, L.L., Sausen, R., 2009. Scientific assessment of the impacts of aviation on climate change and ozone depletion. Atmospheric Environment (Accepted).
Lefohn, A.S., Husar, J.D., Husar, R.B., 1999. Estimating historical anthropogenic global sulfur emission patterns for the period 1850–1990. Atmospheric Environment 33, 3435–3444.
Legrand, M., Hammer, C., De Angelis, M., Savarino, J., Delmas, R., Clausen, H., Johnsen, S.J., 1997. Sulfur-containing species (methanesulfonate and $SO_4$) over the last climatic cycle in the Greenland Ice Core Project (central Greenland) ice core. Journal of Geophysical Research 102 (C12), 26663–26,679.
Lelieveld, J., Dentener, F., 2000. What controls tropospheric ozone? Journal of Geophysical Research 105, 3531–3551.
Lelieveld, J., Peters, W., Dentener, F.J., Krol, M.C., 2002. Stability of tropospheric hydroxyl chemistry. Journal of Geophysical Research 107 (D23), 4715.
Lelieveld, J., van Aardenne, J., Fischer, H., de Reus, M., Williams, J., Winkler, P., 2004. Increasing ozone over the Atlantic ocean. Science 304, 1483–1487.
Lelieveld, J., Butler, T.M., Crowley, J.N., Dillon, T.J., Fischer, H., Ganzeveld, L., Harder, H., Lawrence, M.G., Martinez, M., Taraborrelli, D., Williams, J., 2008. Atmospheric oxidation capacity sustained by a tropical forest. Nature 452 (7188), 737–740.
Levelt, P.F., van den Oord, G.H.J., Dobber, M.R., Mälkki, A., Visser, H., de Vries, J., Stammes, P., Lundell, J.O.V., Saari, H., 2006. Science objectives of the Ozone monitoring instrument. IEEE Transactions on Geoscience and Remote Sensing 44 (5), 1199–1208.
Levin, Z., Cotton, W., 2007. Aerosol Pollution Impact on Precipitation: A Scientific Review. Report from the WMO/IUGG international Aerosol Precipitation Science Assessment Group (IAPSAG). World Meteorological Organization, Geneva, Switzerland.
Liao, H., Seinfeld, J.H., 2005. Global impacts of gas-phase chemistry–aerosol interactions on direct radiative forcing by anthropogenic aerosols and ozone. Journal of Geophysical Research 110, D18208.
Liao, H., Chen, W.-T., Seinfeld, J.H., 2006. Role of climate change in global predictions of future tropospheric ozone and aerosols. Journal of Geophysical Research 111, D12304. doi:10.1029/2005JD006852.
Liepert, B.G., 2002. Observed reductions of surface solar radiation at sites in the United States and worldwide from 1961 to 1990. Geophysical Research Letters 29. doi:10.1029/2002GL014910.
Liu, X.H., Penner, J.E., Das, B.Y., Bergmann, D., Rodriguez, J.M., Strahan, S., Wang, M., Feng, Y., 2007. Uncertainties in global aerosol simulations: assessment using three meteorological data sets. Journal of Geophysical Research 112 (D11).
Lockwoo, M., 2002. Long-term variations in the open solar flux and possible links to earth's climate, from solar min to max: half a solar cycle with SoHO. SP-508. ESA, 507–522.
Lockwood, M., Frölich, C., 2007. Recent oppositely directed trends in solar climate forcings and the global mean surface air temperature. Proceedings of the Royal Society A. doi:10.1098/rspa.2007.1880.
Logan, J.A., 1998. An analysis of ozonesonde data for the troposphere: recommendations for testing 3-d models and development of a gridded climatology for tropospheric ozone. Journal of Geophysical Research 10 (D13), 16115–16149.
Lohmann, U., 2002. Possible aerosol effects on ice clouds via contact nucleation. Journal of Atmospheric Science 59, 647–656.
Lohmann, U., Feichter, J., 2001. Can the direct and semi-direct aerosol effect compete with the indirect effect on a global scale. Geophysical Research Letters 28 (1), 159–161.
Lohmann, U., Diehl, K., 2006. Sensitivity studies of the importance of dust ice nuclei for the indirect aerosol effect on stratiform mixed-phase clouds. Journal of Atmospheric Science 63, 968–982.
Lohmann, U., 2008. Global anthropogenic aerosol effects on convective clouds in ECHAM5-HAM. Atmospheric Chemistry and Physics 8, 2115–2131.
Lubin, D., Vogelmann, A.M., 2006. A climatologically significant aerosol longwave indirect effect in the Arctic. Nature 439, 453–456.
Mahowald, N.M., Luo, C., 2003. A less dusty future? Geophysical Research Letters 30 (17), 1903. doi:10.1029/2003GL017880.
Manne, A.S., Richels, R.G., 2001. An alternative approach to establishing trade offs among greenhouse gases. Nature 410, 675–677.
Marsh, N.D., Svensmark, H., 2000. Low cloud properties influenced by cosmic rays. Physical Review Letters 85 (23), 5004–5007.
Martin, R.V., Fiore, A.M., Van Donkelaar, A., 2004. Space-based diagnosis of surface ozone sensitivity to anthropogenic emissions. Geophysical Research Letters 31, L06120. doi:10.1029/2004GL019416.
Martin, R.V., Sauvage, B., Folkins, I., Sioris, C.E., Boone, C., Bernath, P., Ziemke, J., 2007. Space-based constraints on the production of nitric oxide by lightning. Journal of Geophysical Research-Atmospheres 112, D09309. doi:10.1029/2006JD007831.
Matthes, S., Grewe, V., Sausen, R., Roelofs, G.-J., 2007. Global impact of road traffic emissions on tropospheric ozone. Atmospheric Chemistry and Physics 6, 1075–1089.
Matsueda, M., Mizuta, R., Kusunoki, S., 2009. Future change in wintertime atmospheric blocking simulated using a 20-km-mesh atmospheric global circulation model. Journal of Geophysical Research 114, D12114. doi:10.1029/2009JD011919.
McComiskey, A., Feingold, G., 2008. Quantifying error in the radiative forcing of the first aerosol indirect effect. Geophysical Research Letters 35. doi:10.1029/2007GL032667.
McConnell, J., Edwards, R., Kok, G.L., Flanner, M.G., Zender, C.S., Saltzman, E.S., Banta, J.R., Pasteris, D.R., Carter, M.M., Kahl, J.D.W., 2007. 20th-century industrial black carbon emissions altered Arctic climate forcing. Science 317, 1381–1384. doi:10.1126/science.1144856.
Meehl, G.A., Washington, W.M., Wigley, T.M.L., Arblaster, J.M., Dai, A., 2003. Solar and greenhouse gas forcing and climate response in the twentieth century. Journal of Climate 16426–444.
Menon, S., Hansen, J., Nazarenko, L., Luo, Y., 2002. Climate effects of black carbon aerosols in China and India. Science 297, 2250–2252.
Menon, S., Rotstayn, L., 2006. The radiative influence of aerosol effects on liquid-phase cumulus and stratiform clouds based on sensitivity studies with two climate models. Climate Dynamics 27, 345–356.
Mercado, L.M., Bellouin, N., Sitch, S., Boucher, O., Huntingford, C., Wild, M., Cox, P.M., 2009. Impact of changes in diffuse radiation on the global land carbon sink. Nature 458, 1014–1018.
Mickley, L.J., Murti, P.P., Jacob, D.J., Logan, J.A., Rind, D., Koch, D., 1999. Radiative forcing from tropospheric ozone calculated with a unified chemistry-climate model. Journal of Geophysical Research 104, 30. 153–30 172.
Miller, R.L., Schmidt, G.A., Shindell, D.T., 2006. Forced variations of annular modes in the 20th century Intergovernmental Panel on Climate Change Fourth Assessment Report models. Journal of Geophysical Research 111, D18101. doi:10.1029/2005JD006323.
Mishchenko, M.I., Geogdzhayev, I.V., Rossow, W.B., Cairns, B., Carlson, B.E., Lacis, A.A., Liu, L., Travis, L.D., 2007. Long-term satellite record reveals likely recent aerosol trend. Science 315, 1543.
Monks, P.S., Granier, C., Fuzzi, S., Stohl, A., Williams, M., Akimoto, H., Amman, M., Baklanov, A., Baltensperger, U., Bey, I., Blake, N., Blake, R.S., Carslaw, K., Cooper, O.R., Dentener, F., Fowler, D., Fragkou, E., Frost, G., Generoso, S., Ginoux, P., Grewe, V., Guenther, A., Hansson, H.C., Henne, S., Hjorth, J., Hofzumahaus, A., Huntrieser, H., Isaksen, I.S.A., Jenkin, M.E., Kaiser, J., Kanakidou, M., Klimont, Z., Kulmala, M., Laj, P., Lawrence, M.G., Lee, J.D., Liousse, C., Maione, M., McFiggans, G., Metzger, A., Mieville, A., Moussiopoulos, N., Orlando, J.J., O'Dowd, C., Palmer, P.I., Parrish, D., Petzold, A., Platt, U., Pöschl, U., Prévôt, A.S.H., Reeves, C.E., Reiman, S., Rudich, Y., Sellegri, K., Steinbrecher, R., Simpson, D., ten Brink, H., Theloke, J., van der Werf, G., Vautard, R., Vestreng, V., Vlachokostas, Ch., von-Glasow, R., 2009. Atmospheric Composition Change – Global and Regional Air Quality 43, 5268–5351.
Moussiopoulos, N., Isaksen, I.S.A. (Eds.), 2006. Proceedings of the Workshop on Model Benchmarking and Quality Assurance 29/30 May 2006. Greece, Thessaloniki. Available at: http://www.accent-network.org/farcry_accent/download.cfm?DownloadFile=4C5CBBCB-BCDC-BAD1-A23A2B54239B5545
Muller, J.F., Stavrakou, T., 2005. Inversion of CO and $NO_x$ emissions using the adjoint of the IMAGES model. Atmospheric Chemistry and Physics 5, 1157–1186.
Murphy, D.M., Fahey, D.W., 1994. An estimate of the flux of stratospheric reactive nitrogen and ozone into the troposphere. Journal of Geophysical Research 99 (D3), 5325–5332.
Myhre, G., Grini, A., Metzger, S., 2006. Modelling of nitrate and ammonium-containing aerosols in presence of sea salt. Atmospheric Chemistry and Physics 6, 4809–4821.
Myhre, G., Nilsen, J.S., Gulstad, L., Shine, K.P., Rognerud, B., Isaksen, I.S.A., 2007a. Radiative forcing due to stratospheric water vapour from $CH_4$ oxidation. Geophysical Research Letters 34 (1), L01807. doi:10.1029/2006GL027472.
Myhre, G., Stordal, F., Johnsrud, M., Kaufman, Y.J., Rosenfeld, D., Storelvmo, T., Kristjansson, J.E., Berntsen, T.K., Myhre, A., Isaksen, I.S.A., 2007b. Aerosol-cloud interaction inferred from MODIS satellite data and global aerosol models. Atmospheric Chemistry and Physics 7 (12), 3081–3101.
Myhre, G., Berglen, T.F., Johnsrud, M., Hoyle, C.R., Berntsen, T.K., Christopher, S.A., Fahey, D.W., Isaksen, I.S.A., Jones, T.A., Kahn, R.A., Loeb, N., Quinn, P., Remer, L., Schwarz, J.P., Yttri, K.E., 2009. Modelled radiative forcing of the direct aerosol effect with multi-observation evaluation. Atmospheric Chemistry and Physics 9, 1365–1392.
Myhre, G., 2009. Consistency between satellite-derived and modeled estimates of the direct aerosol effect. Science 325 (5937), 187–190. doi:10.1126/science.1174461.
Nakicenovic N., Davidson O., Davis G., Grubler A., Kram T., Rovere E.L.L., Metz B., Morita T., Pepper W., Pitcher H., Sankovski A., Shukla P., Swart R., Watson R., Dadi Z., 2000. Emissions Scenarios: A Special Report of Working Group III of the Intergovernmental Panel on Climate Change (Summary for Policy Makers), IPCC: 27.
Norris, J.R., Wild, M., 2007. Trends in aerosol radiative effects over Europe inferred from observed cloud cover, solar "dimming" and solar "brightening". Journal of Geophysical Research 112, D08214. doi:10.1029/2006JD007794.
Novelli, P.C., Masarie, K.A., Lang, P.M., 1998. Distributions and recent changes of carbon monoxide in the lower troposphere. Journal of Geophysical Research 103 (D15), 19015–19034.

Novelli, P.C., Masarie, K.A., Lang, P.M., Hall, B.D., Myers, R.C., Elkins, J.W., 2003. Reanalysis of tropospheric CO trends: effects of the 1997–1998 wildfires. Journal of Geophysical Research 108 (D15), 4464. doi:10.1029/2002JD003031.

Ohara, T., Akimoto, H., Kurokawa, J., Horii, N., Yamaji, K., Yan, X., Hayasaka, T., 2007. An Asian emission inventory of anthropogenic emission sources for the period 1980–2020. Atmospheric Chemistry and Physics 7, 4419–4444.

Ohmura, A., Lang, H., 1989. Secular variation of global radiation over Europe. In: Lenoble, J., Geleyn, J.F. (Eds.), Current Problems in Atmospheric Radiation. Deepak, Hampton, VA, pp. 98–301.

Ohmura, A., Dutton, E.G., Forgan, B., Frohlich, C., Gilgen, H., Hegner, H., Heimo, A., Konig-Langlo, G., McArthur, B., Muller, G., Philipona, R., Pinker, R., Whitlock, C.H., Dehne, K., Wild, M., 1998. Baseline Surface Radiation Network, a new precision radiometry for climate research. Bulletin of the American Meteorology Society 79, 2115–2136.

Olivier J., Peters J., Granier C., Pétron G., Müller J.F., Wallens S., 2003. Present and future surface emissions of atmospheric compounds, POET Report 2, EU Project EVK-1999–00011 2003.

Olsen, M.A., Douglass, A.R., Schoeberl, M.R., 2003. A comparison of Northern and Southern Hemisphere cross-tropopause ozone flux. Geophysical Research Letters 30 (7), 1412. doi:10.1029/2002GL016538.

Oltmans, S.J., Lefohn, A.S., Scheel, H.E., Harris, J.M., Levy II, H., Galbally, I.E., Brunke, E.-G., Meyer, C.P., Lathrop, J.A., Johnson, B.J., Shadwick, D.S., Cuevas, E., Schmidlin, F.J., Tarasick, D.W., Claude, H., Kerr, J.B., Uchino, O., Mohnen, V., 1998. Trends of ozone in the troposphere. Geophysical Research Letters 25, 139–142.

Oltmans, S.J., Lefohn, A.S., Harris, J.M., Galbally, I., Scheel, H.E., Bodeker, G., Brunke, E., Claude, H., Tarasick, D., Johnson, B.J., Simmonds, P., Shadwick, D., Anlauf, K., Hayden, K., Schmidlin, F., Fujimoto, T., Akagi, K., Meyer, C., Nichol, S., Davies, J., Redondas, A., Cuevas, E., 2006. Long-term changes in tropospheric ozone. Atmospheric Environment 40, 3156–3173.

O'Neill, B.C., 2000. The jury is still out on global warming potentials. Climatic Change 44, 427–443.

Ordóñez, C., Brunner, D., Staehelin, J., Hadjinicolaou, P., Pyle, J.A., Jonas, M., Wernli, H., Prévôt, A.S.H., 2007. Strong influence of lowermost stratospheric ozone on lower tropospheric background ozone changes over Europe. Geophysical Research Letters 34, L07805. doi:10.1029/2006GL029113.

Osterkamp, T.E., 2005. The recent warming of permafrost in Alaska. Global And Planetary Change 49, 187–202.

Palle, E., Montanes-Rodriguez, P., Goode, P.R., Koonin, S.E., Wild, M., Casadio, S., 2005. A multi-data comparison of shortwave climate forcing changes. Geophysical Research Letters 32 (21), L21702. doi:10.1029/2005GL023847.

Palmer, P.I., Jacob, D.J., Fiore, A.M., Martin, R.V., Chance, K., Kurosu, T.P., 2003. Mapping isoprene emissions over North America using formaldehyde column observations from space. Journal of Geophysical Research-Atmospheres 108 (D6).

Palmer, P.I., Abbot, D.S., Fu, T.M., Jacob, D.J., Chance, K., Kurosu, T.P., Guenther, A., Wiedinmyer, C., Stanton, J.C., Pilling, M.J., Pressley, S.N., Lamb, B., Sumner, A.L., 2006. Quantifying the seasonal and interannual variability of North American isoprene emissions using satellite observations of the formaldehyde column. Journal of Geophysical Research – Atmosphere 111 (D12). doi:10.1029/2005JD006689.

Pan, L.L., Wei, J.C., Kinnison, D.E., Garcia, R.R., Wuebbles, D.J., Brasseur, G.P., 2007. A set of diagnostics for evaluating chemistry–climate models in the extratropical tropopause region. Journal of Geophysical Research 112, D09316. doi:10.1029/2006JD007792.

Parrish, D.D., Millet, D.B., Goldstein, A.H., 2008. Increasing ozone concentrations in marine boundary layer air flow at the west coasts of North America and Europe. Atmospheric Chemistry and Physics Discussion 8, 13847–13901.

Penner, J.E., Bergmann, D.J., Walton, J.J., Kinnison, D., Prather, M.J., Rotman, D., Price, C., Pickering, K.E., Baughcum, S., 1998. An evaluation of upper tropospheric $NO_x$ with two models. Journal of Geophysical Research 103, 22097–22113.

Penner, J.E., Zhang, S.Y., Chuang, C.C., 2003. Soot and smoke aerosols may not warm climate. Journal of Geophysical Research 108 (21), 4657. doi:10.1029/2003JD003409.

Penner, J.E., Chen, Y., Wang, M., Liu, X., 2009. Possible influence of anthropogenic aerosols on cirrus clouds and anthropogenic forcing. Atmospheric Chemistry and Physics 9, 879–896.

Perlwitz, J., Pawson, S., Fogt, R.L., Nielsen, J.E., Neff, W.D., 2008. Impact of stratospheric ozone hole recovery on Antarctic climate. Geophysical Research Letters 35, L08714. doi:10.1029/2008GL033317.

Petron, G., Granier, C., Khattatov, B., Yudin, V., Lamarque, J.F., Emmons, L., Gille, J., Edwards, D.P., 2004. Monthly CO surface sources inventory based on the 2000–2001 MOPITT satellite data. Geophysical Research Letters 31, L21107. 21110.21029/22004GL020560.

Pierce, J.R., Adams, P.J., 2009. Can cosmic rays affect cloud condensation nuclei by altering new particle formation rates? Geophysical Research Letters 36, L09820. doi:10.1029/2009GL037946.

Pinker, R.T., Zhang, B., Dutton, E.G., 2005. Do satellites detect trends in surface solar radiation? Science 308, 850–854.

Pison, I., Bousquet, P., Chevallier, F., Szopa, S., Hauglustaine, D., 2009. Multi-species inversion of $CH_4$, CO and $H_2$ emissions from surface measurements. Atmospheric Chemistry and Physics 9, 5281–5297.

Posselt, R., Lohmann, U., 2008. Influence of Giant CCN on warm rain processes in the ECHAM5 GCM. Atmospheric Chemistry and Physics 8, 3769–3788.

Prather, M., Ehhalt, D., 2001. Chapter 4. Atmospheric Chemistry and Greenhouse Gases. In: Houghton, J.T., et al. (Eds.), Climate Change 2001: The Scientific Basis. Cambridge U. Press, Cambridge, pp. 239–287.

Prather, M., Gauss, M., Berntsen, T., Isaksen, I., Sundet, J., Bey, I., Brasseur, G., Dentener, F., Derwent, R., Stevenson, D., Grenfell, L., Hauglustaine, D., Horowitz, L., Jacob, D., Mickley, L., Lawrence, M., von Kuhlmann, R., Muller, J.-F., Pitari, G., Rogers, H., Johnson, M., Pyle, J., Law, K., van Weele, M., Wild, O., 2003. Fresh air in the 21st century? Geophysical Research Letters 30 (2), 1100. doi:10.1029/2002GL016285.

Pruppacher, H.R., Klett, J.D., 1997. Microphysics of Clouds and Precipitation, Second edition. Kluwer Academic, Norwell, Massachusetts.

Putaud, J.P., Raes, F., Van Dingenen, R., Bruggemann, E., Facchini, M.C., Decesari, S., Fuzzi, S., Gehrig, R., Hüglin, C., Laj, P., Lorbeer, G., Maenhaut, W., Mihalopoulos, N., Müller, K., Querol, X., Rodriguez, S., Schneider, J., Spindler, G., ten Brinkj, H., Tørseth, K., Wiedensohler, A., 2004. European aerosol phenomenology-2: chemical characteristics of particulate matter at kerbside, urban, rural and background sites in Europe. Atmospheric Environment 38 (16), 2579–2595.

Quaas, J., Boucher, O., Bellouin, N., Kinne, S., 2008. Satellite based estimate of the direct and indirect climate forcing. Journal of Geophysical Research. doi:10.1029/2007JD008962.

Quinn, P.K., Bates, T.S., 2005. Regional aerosol properties: Comparisons of boundary layer measurements from ACE 1, ACE 2, aerosols99, INDOEX, ACE Asia, TARFOX, and NEAQS. Journal of Geophysical Research 110 (D14), D14202.

Quinn, P.K., Shaw, G., Andrews, E., Dutton, E.G., Ruoho-Airola, T., Gong, S.T., 2007. Arctic haze: current trends and knowledge gaps. Tellus 59B, 99–114.

Quinn, P.K., Bates, T.S., Baum, E., Doubleday, N., Fiore, A.M., Flanner, M., Fridlind, A., Garrett, T.J., Koch, D., Menon, S., Shindell, D., Stohl, A., Warren, S.G., 2008. Short-lived pollutants in the Arctic: their climate impact and possible mitigation strategies. Atmospheric Chemistry and Physics 8, 1723–1735.

Racherla, P.N., Adams, P.J., 2006. Sensitivity of global tropospheric ozone and fine particulate matter concentrations to climate change. Journal of Geophysical Research 111, D24103. doi:10.1029/2005JD006939.

Ramanathan, V., Callis, L., Cess, R., Hansen, J., Isaksen, I.S.A., Kuhn, W., Lacis, A., Luther, F., Mahlman, J., Reck, R., Schlesinger, M., 1987. Climate–chemical interactions and effects of changing atmospheric trace gases. Review of Geophysics and Space Physics 25, 1441–1482.

Ramanathan, V., Crutzen, P.J., Kiehl, J.T., Rosenfeld, D., 2001. Atmosphere – Aerosols, climate, and the hydrological cycle. Science 294 (5549), 2119–2124.

Ramanathan, V., Ramana, M.V., Roberts, G., Kim, D., Corrigan, C., Ramana, M.V., Roberts, G., Kim, D., Corrigan, C., Chung, C., Winker, D., 2007. Warming trends in Asia amplified by brown cloud solar absorption. Nature 448 (7153) 575–U5.

Ramanathan, V., Carmichael, G., 2008. Global and regional climate changes due to black carbon. Nature Geoscience 1 (4), 221–227.

Ramaswamy, V., Bowen, M.M., 1994. Effect of changes in radiatively active species upon the lower stratospheric temperatures. Journal of Geophysical Research 99 (D9), 18909–18921.

Randel, W.J., Wu, F., Vomel, H., Nedoluha, G.E., Forster, P., 2006. Decreases in stratospheric water vapor after 2001: links to changes in the tropical tropopause and the Brewer-Dobson circulation. Journal of Geophysical Research 111, D12312. doi:10.1029/2005JD006744.

Rao, S., Riahi, K., Kupiainen, K., Klimont, Z., 2005. Long-term scenarios for black and organic carbon emissions. Environmental Sciences 2 (2–3), 205–216.

Rasch, P.J., Crutzen, P.J., Coleman, D.B., 2008. Exploring the geoengineering of climate using stratospheric sulfate aerosols: the role of particle size. Geophysical Research Letters 35, L02809. doi:10.1029/2007GL032179.

Reeve, N., Toumi, R., 1999. Lightning activity as an indicator of climate change. Quarterly Journal of the Royal Meteorological Society 125 (555), 893–903.

Riahi, K., Grübler, A., Nakicenovic, N., 2006. Scenarios of long-term socio-economic and environmental development under climate stabilization. Technological Forecasting and Social Change 74 (7), 887–935.

Richardson, I.G., Cliver, E.W., Cane, H.V., 2002. Long-term trends in interplanetary magnetic field strength and solar wind structure during the twentieth century. Journal of Geophysical Research 107. doi:10.1029/2001JA000507.

Richter, A., Eyring, V., Burrows, J.P., Bovensmann, H., Lauer, A., Sierk, B., Crutzen, P.J., 2004. Satellite measurements of $NO_2$ from international shipping emissions. Geophysical Research Letters 31, L23110. doi:10.1029/2004GL020822.

Richter, A., Burrows, J.P., Nüß, H., Granier, C., Niemeier, U., 2005. Increase in tropospheric nitrogen dioxide over China observed from space. Nature 437, 129–132.

Ritter, C., Notholt, J., Fisher, J., Rathke, C., 2005. Direct thermal radiative forcing of tropospheric aerosol in the Arctic measured by ground based infrared spectrometry. Geophysical Research Letters 32. doi:10.1029/2005GL024331.

Roelofs, G.-J., Lelieveld, J., 1995. Distribution and budget of $O_3$ in the troposphere calculated with a chemistry general circulation model. Journal of Geophysical Research 100 (D10), 20983–20998.

Rosenfeld, D., 1999. TRMM observed first direct evidence of smoke from forest fires inhibiting rainfall. Geophysical Research Letters 26, 3105–3108.

Rosenfeld, D., Woodley, W.L., 2000. Deep convective clouds with sustained supercooled liquid water down to −37.5 °C. Nature 405, 440–442.

Royal Society, 2008. Ground-level ozone in the 21st century: future trends, impacts and policy implications. Science Policy Report 15/08. Available at:: http://royalsociety.org/document.asp?tip=0&id=8039.

Rubin, J.I., Kean, A.J., Harley, R.A., Millet, D.B., Goldstein, A.H., 2006. Temperature dependence of volatile organic compound evaporative emissions from motor vehicles. Journal Geophysical Research 111, D03305. doi:10.1029/2005JD006458.

Salby, M., Callagan, P., 2000. Connection between the Solar Cycle and the QBO: the missing link. Journal of Climate 13, 328–338.

Salby, M., Callaghan, P., 2004. Evidence of the solar cycle in the general circulation of the stratosphere. Journal of Climate 17, 34–46.
Sanderson, M.G., Collins, W.J., Hemming, D.L., Betts, R.A., 2007. Stomatal conductance changes due to increasing carbon dioxide levels: projected impact on surface ozone levels. Tellus Series B 59 (3), 404. doi:10.1111/j.1600-0889.2007.00277.x.
Santer, B.D., Taylor, K.E., Wigley, T.M.L., Johns, T.C., Jones, P.D., Karoly, D.J., Mitchell, J.F.B., Oort, A.H., Penner, J.E., Ramaswamy, V., Schwarzkopf, M.D., Stouffer, R.J., Tett, S., 1996. A search for human influences on the thermal structure of the atmosphere. Nature 382, 39–46.
Santer, B.D., Wehner, F., Wigley, T.M.L., Sausen, R., Meehl, G.A., Taylor, K.E., Ammann, C., Arblaster, J., Washington, W.M., Boyle, J.S., Brüggemann, W., 2003a. Contributions of anthropogenic and natural forcing to recent tropopause height changes. Science 301, 479–483.
Santer, B.D., Sausen, R., Wigley, T.M.L., Boyle, J.S., AchutaRao, K., Doutriaux, C., Hansen, J.E., Meehl, G.A., Roeckner, E., Ruedy, R., Schmidt, G., Taylor, K.E., 2003b. Behavior of tropopause height and atmospheric temperature in models, reanalyses, and observations: decadal changes. ACL 1-1. Journal of Geophysics 108 (D1), 4002. doi:10.1029/2002JD002258.
Satheesh, S.K., Ramanathan, V., 2000. Large differences in tropical aerosol forcing at the top of the atmosphere and Earth's surface. Nature 405, 60–63.
Sausen, R., Santer, B.D., 2003. Use of changes in tropopause height to detect human influences on climate. Meteorologische Zeitschrift 12, 131–136.
Sausen, R., Isaksen, I., Grewe, V., Hauglestaine, D., Lee, D.S., Myhre, G., Kohler, M.O., Pitari, G., Schumann, U., Stordal, F., Zerefos, C., 2005. Aviation radiative forcing in 2000: an update on IPCC (1999). Meteorologische Zeitschrift 14, 555–561.
Scafetta, N., West, B.J., 2005. Estimated solar contribution to the global surface warming using the ACRIM TSI satellite composite. Geophysical Research Letters 32 doi:10.1029/2005GL023849.
Scherer, M., Vomel, H., Fueglistaler, S., Oltmans, S.J., Staehelin, J., 2008. Trends and variability of midlatitude stratospheric water vapour deduced from the re-evaluated Boulder balloon series and HALOE. Atmospheric Chemistry and Physics 8 (5), 1391–1402.
Schoeberl, M.R., Ziemke, J.R., Bojkov, B., Livesey, N., Duncan, B., Strahan, S., Froidevaux, L., Kulawik, S., Bhartia, P.K., Chandra, S., Levelt, P.F., Witte, J.C., Thompson, A.M., Cuevas, E., Redondas, A., Tarasick, D.W., Davies, J., Bodeker, G., Hansen, G., Johnson, B.J., Oltmans, S.J., Vömel, H., Allaart, M., Kelder, H., Newchurch, M., Godin-Beekmann, S., Ancellet, G., Claude, H., Andersen, S.B., Kyrö, E., Parrondos, M., Yela, M., Zablocki, G., Moore, D., Dier, H., von der Gathen, P., Viatte, P., Stübi, R., Calpini, B., Skrivankova, P., Dorokhov, V., de Backer, H., Schmidlin, F.J., Coetzee, G., Fujiwara, M., Thouret, V., Posny, F., Morris, G., Merrill, J., Leong, C.P., Koenig-Langlo, G., Joseph, E., 2007. A trajectory-based estimate of the tropospheric ozone column using the residual method. Journal of Geophysical Research-Atmospheres 112, D24S49. doi:10.1029/2007JD008773.
Schultz, M., Jacob, D.J., Wang, Y., Logan, J.A., Atlas, E.L., Blake, D.R., Blake, N.J., Bradshaw, J.D., Browell, E.V., Fenn, M.A., Flocke, F., Gregory, G.L., Heikes, B.G., Sachse, G.W., Sandholm, S.T., Shetter, R.E., Singh, H.B., Talbot, R.W., 1999. On the origin of tropospheric ozone and $NO_x$ over the tropical South Pacific. Journal of Geophysical Research 104, 5829–5843.
Schulz, M., Textor, C., Kinne, S., Balkanski, Y., Bauer, S., Berntsen, T., Berglen, T., Boucher, O., Dentener, F., Guibert, S., Isaksen, I.S.A., Iversen, T., Koch, D., Kirkevåg, A., Liu, X., Montanaro, V., Myhre, G., Penner, J.E., Pitari, G., Reddy, S., Seland, Ø., Stier, P., Takemura, T., 2006. Radiative forcing by aerosols as derived from the AeroCom present-day and pre-industrial simulations. Atmospheric Chemistry and Physics 6, 5225–5246.
Schumann, U., Huntrieser, H., 2007. The global lightning-induced nitrogen oxides source. Atmospheric Chemistry and Physics Discussions 7, 2623–2818.
Sharma, S., Lavoué, D., Cachier, H., Barrie, L.A., Gong, S.L., 2004. Long-term trends of the black carbon concentrations in the Canadian Arctic. Journal of Geophysical Research 109, D15203. doi:10.1029/2003JD004331.
Sharma, S., Andrews, E., Barrie, L.A., Ogren, J.A., Lavoué, D., 2006. Variations and sources of the equivalent black carbon in the high Arctic revealed by long-term observations at Alert and Barrow: 1989–2003. Journal of Geophysical Research 111, D14208. doi:10.1029/2005JD006581.
Sheehan, P.E., Bowman, F.K., 2001. Estimated effects of temperature on secondary organic aerosol concentrations. Environmental Science and Technology 35, 2129–2135.
Shindell, D., Rind, D., Balachandran, N., Lean, J., Lonergan, P., 1999. Solar cycle variability, ozone and climate. Science 284, 305–308.
Shindell, D.T., Schmidt, G.A., Miller, R.L., Rind, D., 2001. Northern Hemisphere winter climate response to greenhouse gas, ozone, solar, and volcanic forcing. Journal of Geophysical Research 106 (D7), 7193–7210.
Shindell, D.T., Faluvegi, G., Bell, N., 2003. Preindustrial-to-present day radiative forcing by tropospheric ozone from improved simulations with the GISS chemistry–climate GCM. Atmospheric Chemistry and Physics 3, 1675–1702.
Shindell, D.T., Walter, B.P., Faluvegi, G., 2004. Impacts of climate change on methane emissions from wetlands. Geophysical Research Letters 31, L21202. doi:10.1029/2004GL021009.
Shindell, D.T., Faluvegi, G., Bell, N., Schmidt, G.A., 2005. An emissions-based view of climate forcing by methane and tropospheric ozone. Geophysical Research Letters 32, L04803. doi:10.1029/2004GL021900.
Shindell, D.T., Faluvegi, G., Stevenson, D.S., Krol, M.C., Emmons, L.K., Lamarque, J.-F., Pétron, G., Dentener, F.J., Ellingsen, K., Schultz, M.G., Wild, O., Amann, M., Atherton, C.S., Bergmann, D.J., Bey, I., Butler, T., Cofala, J., Collins, W.J., Derwent, R.G., Doherty, R.M., Drevet, J., Eskes, H.J., Fiore, A.M., Gauss, M., Hauglustaine, D.A., Horowitz, L.W., Isaksen, I.S.A., Lawrence, M.G., Montanaro, V., Müller, J.-F., Pitari, G., Prather, M.J., Pyle, J.A., Rast, S., Rodriguez, J.M., Sanderson, M.G., Savage, N.H., Strahan, S.E., Sudo, K., Szopa, S., Unger, N., van Noije, T.P.C., Zeng, G., 2006. Multimodel simulations of carbon monoxide: comparison with observations and projected near-future changes. Journal of Geophysical Research 111, D19306. doi:10.1029/2006JD007100.
Shindell, D.T., Faluvegi, G., Bauer, S.E., Koch, D.M., Unger, N., Menon, S., Miller, R.L., Schmidt, G.A., Streets, D.G., 2007. Climate response to projected changes in short-lived species under an A1B scenario from 2000–2050 in the GISS climate model. Journal of Geophysical Research 112, D20103. doi:10.1029/2007JD008753.
Shindell, D., Lamarque, J.-F., Unger, N., Koch, D., Faluveg, G., Bauer, S., Teich, H., 2008a. Climate forcing and air quality change due to regional emissions reductions by economic sector. Atmospheric Chemistry and Physics Discussions 8, 11609–11642.
Shindell, D.T., Chin, M., Dentener, F., Doherty, R.M., Faluvegi, G., Fiore, A.M., Hess, P., Koch, D.M., MacKenzie, I.A., Sanderson, M.G., Schultz, M.G., Schulz, M., Stevenson, D.S., Teich, H., Textor, C., Wild, O., Bergmann, D.J., Bey, I., Bian, H., Cuvelier, C., Duncan, B.N., Folberth, G., Horowitz, L.W., Jonson, J., Kaminski, J.W., Marmer, E., Park, R., Pringle, K.J., Schroeder, S., Szopa, S., Takemura, T., Zeng, G., Keating, T.J., Zuber, A., 2008b. A multi-model assessment of pollution transport to the Arctic. Atmospheric Chemistry and Physics 8, 5353–5372.
Shine, K.P., Cook, J., Highwood, E.J., Joshi, M.M., 2003. An alternative to radiative forcing for estimating the relative importance of climate change mechanisms. Geophysical Research Letters 30 (20), 2047.
Shine, K.P., Fuglestvedt, J.S., Hailemariam, K., Stuber, N., 2005. Alternatives to the global warming potential for comparing climate impacts of emissions of greenhouse gases. Climatic Change 68, 281–302.
Shine, K.P., Berntsen, T.K., Fuglestvedt, J.S., Bieltvedt Skeie, R., Stuber, N., 2007. Comparing the climate effect of emissions of short- and long-lived climate agents. Philosophical Transactions of the Royal Society A 365, 1903–1914.
Simpson, D., Yttri, K.E., Klimont, Z., Kupiainen, K., Caseiro, A., Gelencsér, A., Pio, C., Puxbaum, H., Legrand, M., 2007. Modeling carbonaceous aerosol over Europe: analysis of the CARBOSOL and EMEP EC/OC campaigns. Journal of Geophysical Research 112, D23S14. doi:10.1029/2006JD008158.
Sirois, A., Barrie, L.A., 1999. Arctic lower tropospheric aerosol trends and composition at Alert, Canada: 1980–1995. Journal of Geophysical Research 104, 11599–511,618.
Sitch, S., Cox, P.M., Collins, W.J., Huntingford, C., 2007. Indirect radiative forcing of climate change through ozone effects on the land-carbon sink. Nature 448. doi:10.1038/nature06059.
Sloan, T., Wolfendale, A.W., 2008. Testing the proposed causal link between cosmic rays and cloud cover. Environmental Research Letters 3, 024001. doi:10.1088/1748-9326/3/2/024001.
Smith S.J., Conception E., Andres R., Lurz J., 2004. Historical Sulfur Dioxide Emissions 1850–2000: Methods and Results. PNNL Research Report, PNNL-14537, College Park, Maryland, US.
Smith, S.C., Lee, J.D., Bloss, W.J., Johnson, G.P., Ingham, T., Heard, D.E., 2006. Concentrations of OH and $HO_2$ radicals during NAMBLEX: measurements and steady state analysis. Atmospheric Chemistry and Physics 6, 1435–1453.
Soden, B.J., Wetherald, R.T., Stenchikov, G.L., Robock, A., 2002. Global cooling after the eruption of Mount Pinatubo: A test of climate feedback by water vapor. Science 296, 727–730.
Solanki, S.K., Usoskkin, I.G., Kromer, B., Schüssler, M., Beer, J., 2004. Unusual activity of the Sun during recent decades compared to the previous 11,000 years. Nature 431, 1084–1087.
Solberg, S., Hov, Ø., Søvde, A., Isaksen, I.S.A., Coddeville, P., De Backer, H., Forster, C., Orsolini, Y., Uhse, K., 2008. European surface ozone in the extreme summer 2003. Journal of Geophysical Research 113, D07307. doi:10.1029/2007JD009098.
Solberg, S., Derwent, R.G., Hov, O., Langner, J., Lindskog, A., 2005. European abatement of surface ozone in a global perspective. Ambio 34 (1), 47–53.
Sotiropoulou, R.-E.P., Nenes, A., Adams, P.J., Seinfeld, J.H., 2007. Cloud condensation nuclei prediction error from application of Köhler theory: importance for the aerosol indirect effect. Journal of Geophysical Research. doi:10.1029/2006JD007834.
Stanhill, G., Cohen, S., 2001. Global dimming: a review of the evidence for a widespread and significant reduction in global radiation. Agricultural and Forest Meteorology 107, 255–278.
Stavrakou, T., Müller, J.-F., Boersma, K.F., De Smedt, I., van der, A.R.J., 2008. Assessing the distribution and growth rates of $NO_x$ emission sources by inverting a 10-year record of $NO_2$ satellite columns. Geophysical Research Letters 35, L10801. doi:10.1029/2008GL033521.
Stavrakou, T., Müller, J.-F., De Smedt, I., Van Roozendael, M., van der Werf, G.R., Giglio, L., Guenther, A., 2009a. Global emissions of non-methane hydrocarbons deduced from SCIAMACHY formaldehyde columns through 2003–2006. Atmospheric Chemistry and Physics 9, 3663–3679.
Stavrakou, T., Müller, J.-F., De Smedt, I., Van Roozendael, M., Kanakidou, M., Vrekoussis, M., Wittrock, F., Richter, A., Burrows, J.P., 2009b. The continental source of glyoxal estimated by the synergistic use of spaceborne measurements and inverse modelling. Atmospheric Chemistry and Physics Discussions 9, 13593–13628.
Stern, D.I., 2005. Global sulfur emissions from 1850 to 2000. Chemosphere 58, 163–175.
Stevenson, D.S., Johnson, C.E., Collins, W.J., Derwent, R.G., Shine, K.P., Edwards, J.M., 1998. Evolution of tropospheric ozone radiative forcing. Geophysical Research Letters 25, 3819–3822.
Stevenson, D.S., Doherty, R.M., Sanderson, M.G., Johnson, C.E., Collins, W.J., Derwent, R.G., 2005. Impacts of climate change and variability on tropospheric ozone and its precursors. Faraday Discussions 130, 41–57. doi:10.1039/b417412g.

Stevenson, D.S., Dentener, F.J., Schultz, M.G., Ellingsen, K., van Noije, T.P.C., Wild, O., Zeng, G., Amann, M., Atherton, C.S., Bell, N., Bergmann, D.J., Bey, I., Butler, T., Cofala, J., Collins, W.J., Derwent, R.G., Doherty, R.M., Drevet, J., Eskes, H.J., Fiore, A.M., Gauss, M., Hauglustaine, D.A., Horowitz, L.W., Isaksen, I.S.A., Krol, M.C., Lamarque, J.-F., Lawrence, M.G., Montanaro, V., Müller, J.-F., Pitari, G., Prather, M.J., Pyle, J.A., Rast, S., Rodriguez, J.M., Sanderson, M.G., Savage, N.H., Shindell, D.T., Strahan, S.E., Sudo, K., Szopa, S., 2006. Multimodel ensemble simulations of present-day and near-future tropospheric ozone. Journal of Geophysical Research 111, D08301. doi:10.1029/2005JD006338.

Stohl, A., 2006. Characteristics of atmospheric transport into the Arctic troposphere. Journal of Geophysical Research 111, D11306. doi:10.1029/2005JD006888.

Storelvmo, T., Kristjánsson, J.E., Lohmann, U., Iversen, T., Kirkevåg, A., Seland, Ø., 2008a. Modeling the Wegener-Bergeron-Findeisen process – implications for aerosol indirect effects. Environmental Research Letters 3 (045001), 3214–3230.

Storelvmo, T., Kristjánsson, J.E., Lohmann, U., 2008b. Aerosol influence on mixed-phase clouds in CAM-Oslo. Journal of Atmospheric Science 60, 3214–3230.

Storelvmo, T., Lohmann, U., Bennartz, R., 2009. What governs the spread in shortwave forcings in the transient IPCC AR4 models. Geophysical Research Letters 36. doi:10.1029/2008GL036069 2008c.

Stott, P.A., Mitchell, J.F.B., Allen, M.R., Delworth, T.L., Gregory, J.M., Meehl, G.A., Santer, B.D., 2006. Observational constraints on past attributable warming and predictions of future global warming. Journal Climate 19, 3055–3069.

Strahan, S.E., Duncan, B.N., Hoor, P., 2007. Observationally derived transport diagnostics for the lowermost stratosphere and their application to the GMI chemistry and transport model. Atmospheric Chemistry and Physics 7, 2435–2445.

Streets, D.G., Bond, T.C., Carmichael, G.R., Fernandes, S.D., Fu, Q., He, D., Klimont, Z., Nelson, S.M., Tasi, N.Y., Wang, M.Q., Woo, J.-H., Yarber, K.F., 2003. An inventory of gaseous and primary aerosol emissions in Asia in the year 2000. Journal Geophysical Research 108 (D21), 8809. doi:10.1029/2002JD003093.

Streets, D.G., Bond, T.C., Lee, T., Jang, C., 2004. On the future of carbonaceous aerosol emissions. Journal of Geophysical Research 104, D24212. doi:10.1029/2004JD004902.

Streets, D.G., Zhang, Q., Wang, L., He, K., Hao, J., Wu, Y., Tang, Y., Carmichael, G.R., 2006a. Revisiting China's CO emissions after the Transport and Chemical Evolution over the Pacific (TRACE-P) mission: synthesis of inventories, atmospheric modeling, and observations. Journal of Geophysical Research 111, D14306.

Streets, D.G., Wu, Y., Chin, M., 2006b. Two-decadal aerosol trends as a likely explanation of the global dimming/brightening transition. Geophysical Research Letters 33. doi:10.1029/2006GL026471.

Stroeve, J., Holland, M.M., Meier, W., Scambos, T., Serreze, M.C., 2007. Arctic sea ice decline: faster than forecast. Geophysical Research Letters 402 (34), L09501. doi:10.1029/2007GL029703.

Stuber N., Myhre G., Highwood E.J., Radel G., Shine K.P. Idealised aerosol perturbations in two GCMs: towards an improved understanding of the semi-direct aerosol effect. Climate Dynamics, submitted for publication.

Sudo, K., Takahashi, M., Akimoto, H., 2003. Future changes in stratosphere-troposphere exchange and their impacts on future tropospheric ozone simulations. Geophysical Research Letters 30 (24), 2256. doi:10.1029/-2003GL018526.

Sudo, K., Akimoto, H., 2007. Global source attribution of tropospheric ozone: long-range transport from various source regions. Journal of Geophysical Research 112, D12302. doi:10.1029/2006JD007992.

Sun, H.L., Biedermann, L., Bond, T.C., 2007. Color of brown carbon: a model for ultraviolet and visible light absorption by organic carbon aerosol. Geophysical Research Letters 34 (17).

Szopa, S., Hauglustaine, D.A., Vautard, R., Menut, L., 2006. Future global tropospheric ozone changes and impact on European air quality. Geophysical Research Letters 33, L14805.

Søvde, O.A., Gauss, M., Isaksen, I.S.A., Pitari, G., Marizy, C., 2007. Aircraft pollution – a futuristic view. Atmospheric Chemistry and Physics 7 (13), 3621–3632.

Tagaris, E., Manomaiphiboon, K., Liao, K.-J., Leung, L.R., Woo, J.-H., He, S., Amar, P., Russell, A.G., 2007. Impacts of global climate change and emissions on regional ozone and fine particulate matter concentrations over the United States. Journal of Geophysical Research 112, D14312. doi:10.1029/2006JD008262.

Textor, C., Schulz, M., Guibert, S., Kinne, S., Balkanski, Y., Bauer, S., Berntsen, T., Berglen, T., Boucher, O., Chin, M., Dentener, F., Diehl, T., Easter, R., Feichter, H., Fillmore, D., Ghan, S., Ginoux, P., Gong, S., Grini, A., Hendricks, J., Horowitz, L., Huang, P., Isaksen, I., Iversen, T., Kloster, S., Koch, D., Kirkevåg, A., Kristjansson, J.E., Krol, M., Lauer, A., Lamarque, J.F., Liu, X., Montanaro, V., Myhre, G., Penner, J., Pitari, G., Reddy, S., Seland, Ø., Stier, P., Takemura, T., Tie, X., 2006. Analysis and quantification of the diversities of aerosol life cycles within AeroCom. Atmospheric Chemistry and Physics 6 (7), 1777–1813.

Textor, C., Schulz, M., Guibert, S., Kinne, S., Balkanski, Y., Bauer, S., Berntsen, T., Berglen, T., Boucher, O., Chin, M., Dentener, F., Diehl, T., Feichter, J., Fillmore, D., Ginoux, P., Gong, S., Grini, A., Hendricks, J., Horowitz, L., Huang, P., Isaksen, I.S.A., Iversen, T., Kloster, S., Koch, D., Kirkevåg, A., Kristjansson, J.E., Krol, M., Lauer, A., Lamarque, J.F., Liu, X., Montanaro, V., Myhre, G., Penner, J.E., Pitari, G., Reddy, M.S., Seland, Ø., Stier, P., Takemura, T., Tie, X., 2007. The effect of harmonized emissions on aerosol properties in global models – an AeroCom experiment. Atmospheric Chemistry and Physics 7 (17), 4489–4501.

Thompson, A.M., Stewart, R.W., Owens, M.A., Herwehe, J.A., 1989. Sensitivity of tropospheric oxidants to global chemical and climate change. Atmospheric Environment 23 (3), 519–532.

Tol, R.S.J., Berntsen, T.K., O'Neill, B.C., Fuglestvedt, J.S., Shine, K.P., Balkanski, Y., Makra, L., 2008. Metrics for Aggregating the Climate Effect of Different Emissions: A Unifying Framework, 257. ESRI Working Paper, ESRI, Dublin, Ireland.

Tsigaridis, K., Kanakidou, M., 2003. Global modelling of secondary organic aerosol in the troposphere: a sensitivity analysis. Atmospheric Chemistry and Physics 3, 1849–1869.

Tsigaridis, K., Krol, M., Dentener, F.J., Balkanski, Y., Lathière, J., Metzger, S., Hauglustaine, D.A., Kanakidou, M., 2006. Change in global aerosol composition since preindustrial times. Atmospheric Chemistry and Physics Discussions 6, 5585–5628.

Tsigaridis, K., Kanakidou, M., 2007. Secondary organic aerosol importance in the future Atmosphere. Atmospheric Environment 41 (22), 4682–4692.

Turquety, S., Logan, J.A., Jacob, D.J., Hudman, R.C., Leung, F.Y., Heald, C.L., Yantosca, R.M., Wu, S., Emmons, L.K., Edwards, D.P., Sachse, G.W., 2007. Inventory of boreal fire emissions for North America in 2004: importance of peat burning and pyroconvective injection. Journal of Geophysical Research 112, D12S03. doi:10.1029/2006JD007281.

Twomey, S., 1974. Pollution and the planetary albedo. Atmospheric Environment 8, 1251–1256.

Twomey, S., 1977. The influence of pollution on shortwave albedo of clouds. Journal of Atmospheric Science 34, 1149–1152.

Unger, N., Shindell, D.T., Koch, D.M., Amann, M., Cofala, J., Streets, D.G., 2006. Influences of man-made emissions and climate changes on tropospheric ozone, methane and sulfate at 2030 from a broad range of possible futures. Journal of Geophysical Research 111, D12313. doi:10.1029/2005JD006518.

Unger, N., Shindell, D.T., Koch, D.M., Streets, D.G., 2008. Air pollution radiative forcing from specific emissions sectors at 2030. Journal of Geophysical Research 113, D02306. doi:10.1029/2007JD008683.

van der Werf, G.R., Randerson, J.T., Giglio, L., Collatz, G.J., Kasibhatla, P.S., Arellano Jr., A.F., 2006. Interannual variability in global biomass burning emissions from 1997 to 2004. Atmospheric Chemistry and Physics 6, 3423–3441.

Van Loon, M., Vautard, R., Schaap, M., Bergström, R., Bessagnet, B., Brandt, J., Builtjes, P.J.H., Christensen, J.H., Cuvelier, C., Graff, A., Jonson, J.E., Krol, M., Langner, J., Roberts, P., Rouil, L., Stern, R., Tarrasón, L., Thunis, P., Vignati, E., White, L., Wind, P., 2006. Evaluation of long-term ozone simulations from seven regional air quality models and their ensemble average. Atmospheric Environment 41 (10), 2083–2097.

van Noije, T.P.C., Eskes, H.J., van Weele, M., van Velthoven, P.F.J., 2004. Implications of the enhanced Brewer-Dobson circulation in European Centre for Medium-Range Weather Forecasts reanalysis ERA-40 for the stratosphere-troposphere exchange of ozone in global chemistry-transport models. J. Geophys. Res. 109, D19308. doi:10.1029/2004JD004586.

van Aardenne J.A., Dentener F., Olivier J.G.J., Peters J.A.W.H., Ganzeveld L.N., 2005. The EDGAR 3.2 Fast Track 2000 dataset (32FT2000), Bilthoven, Edgard Consortium.

Vautard, R., Van Loon, M., Schaap, M., Bergström, R., Bessagnet, B., Brandt, J., Builtjes, P.J.H., Christensen, J.H., Cuvelier, C., Graff, A., Jonson, J.E., Krol, M., Langner, J., Roberts, P., Rouil, L., Stern, R., Tarrasón, L., Thunis, P., Vignati, E., White, L., Wind, P., 2006. Is regional air quality model diversity representative of uncertainty for ozone simulation? Geophysical Research Letters 33, L24818. 1029/2006GL27610.

Verheggen, B., Cozic, J., Weingartner, E., Bower, K., Mertes, S., Connoly, P., Gallagher, M., Flynn, M., Choularton, T., Baltensberger, U., 2007. Aerosol portioning between the interstitial and the condensed phase in mixed-phase clouds. Journal of Geophysical Research 112. doi:10.1029/2007JD008714.

Vestreng V., Rigler E., Adams M., Kindborn K., Pacyna J.M., Denier van der Gon H., Reis S., Travnikov O., 2006. Inventory Review 2006, Emission Data reported to the LRTAP Convention and NEC Directive: stage 1, 2 and 3 review, and evaluation of inventories of HMs and POPs. MSC-W Technical Report 1/2006, 1504-6179.

Vingarzan, R., 2004. A review of surface ozone background levels and trends. Atmospheric Environment 38, 201–401.

Walter, B.P., Heimann, M., Matthews, E., 2001. Modeling modern methane emissions from natural wetlands 2. Interannual variations 1982–1993. Journal of Geophysical Research 106, 34207–34219.

Walter, B.P., Zimov, S.A., Chanton, J.P., Verbyla, D., Chapin, F.S., 2006a. Methane bubbling from Siberian thaw lakes as a positive feedback to climate warming. Nature 443, 71–75.

Walter, K.M., Zimov, S.A., Chanton, J.P., Verbyla, D., Chapin, F.S., 2006b. Methane bubbling from Siberian thaw lakes as a positive feedback to climate warming. Nature 443, 71–75. doi:10.1038/nature05040.

Wang, Y.-M., Lean, J.L., Sheeley, N.R., 2005. Modeling the Sun's magnetic field and irradiance since 1713. Astrophysics Journal 625, 522–538.

Wang, Y.H., Jacob, D.J., 1998. Anthropogenic forcing on tropospheric ozone and OH since preindustrial times. Journal of Geophysical Research 103, 123–131.

Wang, Y.X., McElroy, M.B., Martin, R.V., Streets, D.G., Zhang, Q., Fu, T.M.A., 2007. Seasonal variability of NOx emissions over east China constrained by satellite observations: implications for combustion and microbial sources. Journal of Geophysical Research 112, D06301. doi:10.1029/2006JD007538.

Wang, C., 2005. A modeling study of the response of tropical deep convection to the increase of cloud condensation nuclei concentration: 1. dynamics and microphysics. Journal of Geophysical Research 110 (D6), D21211.

Wang, W.-C., Sze, N.D., 1980. Coupled effects of atmospheric $N_2O$ and $O_3$ on the Earth's climate. Nature 286, 589–590. doi:10.1038/286589a0.

Wania, R., 2007. Modelling Northern Peatland Land Surface Processes, Vegetation Dynamics and Methane Emissions. PhD thesis. University of Bristol, UK. November 2007.

Warren, S.G., Wiscombe, W.J., 1980. A model for the spectral albedo of snow. II: snow containing atmospheric aerosols. Journal of Atmospheric Science 37, 2734–2745.

Wild, M., Ohmura, A., Gilgen, H., Rosenfeld, D., 2004. On the consistency of trends in radiation and temperature records and implications for the global hydrological cycle. Geophysical Research Letters 31, L11201. doi:10.1029/2003GL019188.

Wild, M., Gilgen, H., Roesch, A., Ohmura, A., Long, C.N., Dutton, E.G., Forgan, B., Kallis, A., Russak, V., Tsvetkov, A., 2005. From dimming to brightening: decadal changes in surface solar radiation. Science 308, 847–850.

Wild, O., 2007. Modelling the global tropospheric ozone budget: exploring the variability in current models. Atmospheric Chemistry and Physics 7, 2643–2660.

Wild, M., Ohmura, A., Makowski, K., 2007. Impact of global dimming and brightening on global warming. Geophysical Research Letters 34, L04702. doi:10.1029/2006GL028031.

Wild, M., 2009. Global dimming and brightening: a review. Journal of Geophysical Research 114, D00D16. doi:10.1029/2008JD011470.

Wittrock, F., Richter, A., Oetjen, H., Burrows, J.P., Kanakidou, M., Myriokefalitakis, S., Volkamer, R., Beirle, S., Platt, U., Wagner, T., 2006. Simultaneous global observations of glyoxal and formaldehyde from space. Geophysical Research Letters 33 (16). doi:10.1029/2006GL026310.

Wong, S., Wang, W.-C., Isaksen, I.S.A., Berntsen, T.K., Sundet, J.K., 2004. A global climate-chemistry model study of present-day tropospheric chemistry and radiative forcing from changes in tropospheric $O_3$ since the preindustrial period. Journal of Geophysical Research 109, D11309. doi:10.1029/2003JD003998.

Worden, H.M., Bowman, K.W., Worden, J.R., Eldering, A., Beer, R., 2008. Satellite measurements of the clear-sky greenhouse effect from tropospheric ozone. Nature Geoscience 1, 305–308.

Wu, S., Mickley, L.J., Jacob, D.J., Rind, D., Streets, D.G., 2008a. Effects of 2000–2050 changes in global tropospheric ozone and the policy-relevant background surface ozone in the United States. Journal of Geophysical Research 113, D18312. doi:10.1029/2007JD009639.

Wu, S., Mickley, L.J., Leibensperger, E.M., Jacob, D.J., Rind, D., Streets, D.G., 2008b. Effects of 2000–2050 global change on ozone air quality in the United States. Journal of Geophysical Research 113, D06302. doi:10.1029/2007JD008917.

Yamaji, K., Toshimasa, O., Itsushi, U., Jun-ichi, K., Pakpong, P., Hajime, A., 2008. Future prediction of surface ozone over east Asia using models-3 community multiscale air quality modeling system and regional emission inventory in Asia. Journal of Geophysical Research 113, D08306. doi:10.1029/2007JD008663.

Yienger, J., Galanter, M., Holloway, T., Phadnis, M., Guttikunda, S., Carmichael, G., Moxim, W., Levy II, H., 2000. The episodic nature of air pollution transport from Asia to North America. Journal of Geophysical Research 105 (D22), 26931–26945.

Young, L.-H., Benson, D.R., Montanaro, W.M., Lee, S.-H., Pan, L.L., Rogers, D.C., Jensen, J., Stith, J.L., Davis, C.A., Campos, T.L., Bowman, K.P., Cooper, W.A., Lait, L.R., 2007. Enhanced new particle formation observed in the northern midlatitude tropopause region. Journal of Geophysical Research 112, D10218. doi:10.1029/2006JD00810.

Zeng, G., Pyle, J.A., 2003. Changes in tropospheric ozone between 2000 and 2100 modeled in a chemistry-climate model. Geophysical Research Letters 30 (7), 1392. doi:10.1029/2002GL016708.

Zhang, L.M., Michelangeli, D.V., Taylor, P.A., 2006. Influence of aerosol concentration on precipitation formation in low-level stratiform clouds. Journal Atmospheric Science 37, 203–217.

Zhang, Q., Streets, D.G., He, K., Wang, Y., Richter, A., Burrows, J.P., Uno, I., Jang, C.J., Chen, D., Yao, Z., Lei, Y., 2007. $NO_x$ emission trends for China, 1995-2004: the view from the ground and the view from space. Journal of Geophysical Research 112, D22306.

Zhang, L., Jacob, D.J., Boersma, K.F., Jaffe, D.A., Olson, J.R., Bowman, K.W., Worden, J.R., Thompson, A.M., Avery, M.A., Cohen, R.C., Dibb, J.E., Flock, F.M., Fuelberg, H.E., Huey, L.G., McMillan, W.W., Singh, H.B., Weinheimer, A.J., 2009. Transpacific transport of ozone pollution and the effect of recent Asian emission increases on air quality in North America: an integrated analysis using satellite, aircraft, ozonesonde, and surface observations. Atmospheric Chemistry and Physics 8, 6117–6136.

Zimov, S.A., Schuur, E.A.G., Chapin III, F.S., 2006. Permafrost and the global carbon budget. Science 312, 1612–1613.